2017

Persistent Inward Currents Play a Role in Muscle Dysfunction Seen in Myotonia Congenita

Ahmed Alaa Hawash
Wright State University

PERSISTENT INWARD CURRENTS PLAY A ROLE IN MUSCLE DYSFUNCTION

SEEN IN MYOTONIA CONGENITA

A Dissertation submitted in partial fulfillment of
requirements for the degree of
<u>Doctor of Philosophy</u>

By

AHMED ALAA HAWASH
B.S. New York Institute of Technology, 2012

2017
Wright State University

WRIGHT STATE UNIVERSITY

GRADUATE SCHOOL

June 1 2017

I HEREBY RECOMMEND THAT THE DISSERTATION PREPARED UNDER MY
SUPERVISION BY <u>Ahmed Alaa Hawash ENTITLED Persistent Inward Currents Play a
Role in Muscle Dysfunction Seen in Myotonia Congenita</u> BE ACCEPTED IN PARTIAL
FULFUILLMENT OF THE REQUIREMENTS FOR THE DEGREE OF Doctor of
Philosophy.

_____
Mark Rich, M.D.,Ph.D.
Dissertation Director

_____
Mill W. Miller, Ph.D.
Director, Biomedical Sciences Ph.D. Program

_____
Robert E. W. Fyffe, Ph.D.
Vice President for Research and
Dean of the Graduate School

Committee on Final Examination

_____
Mark Rich, M.D., Ph.D.

_____
Andrew Voss, Ph.D.

_____
Dan Halm, Ph.D.

_____
Lynn Hartzler, Ph.D.

_____
Christopher Wyatt, Ph.D.

iii

ABSTRACT

Hawash, Ahmed Alaa. Ph.D., Biomedical Sciences Ph.D. Program, Wright State University, 2017. Persistent Inward Currents Play a Role in Muscle Dysfunction Seen in Myotonia Congenita.

Myotonia congenita is a rare skeletal muscle channelopathy caused by a reduced chloride channel (ClC-1) current, which results in debilitating muscle hyperexcitability, prolonged contractions, and transient episodes of weakness.

The excitatory events that trigger myotonic action potentials in the absence of stabilizing ClC-1 current are not fully understood. My *in vitro* intracellular recordings from a mouse homozygous knockout of ClC-1 revealed a slow after-depolarization (AfD) that triggers myotonic action potentials. The AfD is well-explained by a tetrododoxin-sensitive and voltage-dependent Na^+ persistent inward current (NaPIC). Notably, this NaPIC undergoes slow inactivation over seconds, thus providing the first mechanistic explanation for the end of myotonic runs. Highlighting the significance of this mechanism, we show that ranolazine and elevated serum divalent cations eliminate myotonia by inhibiting AfD and NaPIC.

The electrophysiological events responsible for the transient weakness are not well understood either. My *in vitro* intracellular recordings revealed a novel behavior, in which the muscle is functionally inexcitable for seconds to minutes. This hanging behavior, as I refer to it, is likely to be responsible for periods of weakness described by

patients and is explained by another persistent inward current. Partial pharmacological

block of this other PIC decreases the hanging behavior in myotonic muscle.

This work significantly changes our understanding of the mechanisms underlying

myotonia and transient weakness seen in myotonia congenita and reveals a novel and

highly effective therapeutic target.

Table of Contents

List of Figures

List of Tables

Acknowledgments

I would like to thank the Wright State University Boonshoft School of Medicine and the Graduate School, specifically the Biomedical Sciences Ph.D. program, for giving me this opportunity.

None of the work in this dissertation would have been possible without the help, support, and mentorship of several individuals. I would like to especially thank Dr. Mark M. Rich for the continued mentorship, patience, generosity, optimism, humor and support. You have been invaluable to my education, professional, and personal development over the years. During the Medical Neuroscience course, I could not see myself joining your lab in a million years. But after three years of working with you, I am certain I made the right choice. It has been an honor to work and learn from you and I look forward to continuing to work with you through the coming years. I would also like to thank all current and previous lab members of the Rich Lab (Rich Gang) including Dr. Xueyong Wang, Dr. Qingbo Wang, newly-minted Dr. Kevin Novak and Dr. Jacob Vincent, and Lori Goss for making lab life tolerable and for all of their time and input during lab discussions. I would like to thank Dr. Andrew Voss and his lab members for taking me into his lab and allowing me to add a whole new dimension to my project. I would like to thank my committee members for their dedication, time, and mentorship as I have progressed through this process. I would also like to thank my close friends who made these years enjoyable while still fruitful. Lastly and most importantly, I would like to thank my family, specifically my parents. Thank you for spending the time on the phone, listening to me complain on and on about failed experiments and uncertainty about decisions. Without your unwavering support, none of this would be conceivable.

This work is dedicated to my late grandmother, Nagafa Eldoky, who longed for the day

she would get to call me Dr. Hawash. I love you.

Chapter I: Purpose & Aims

Purpose

Myotonia congenita is an uncommon inherited skeletal muscle disease, with a prevalence of about 1:100,000, caused by a loss of chloride conductance. However, through the understanding of the electrophysiological consequences of the CLC-1 loss-of-function mutation caused by this disease, we can further understand the interplay of ionic currents that result in the production of myotonia, or involuntary firing of action potentials by the muscle.

Through recognizing the ionic currents and their dynamics in producing myotonia, we can then begin to target specific channel kinetic states using available pharmacological agents, alleviating some of the symptoms myotonia congenita patients complain of.

Hypothesis: The activity of persistent inward currents, in addition to K buildup in the T-tubules, produces dysfunctions seen in myotonia congenita muscles.

Specific Aims

Specific Aim I:

Hypothesis: A persistent inward current plays a central role in triggering myotonic bursts, producing muscle stiffness in myotonia congenita patients.

Adrian and Bryant concluded that K buildup in the T-tubules is largely responsible for myotonic firing of myotonia congenita muscle, mentioning the need for an additional depolarizing current to produce myotonia (Adrian and Bryant 1974; Adrian and Marshall 1976). Using current clamp and voltage clamp recordings of myotonic muscle, we will determine the presence of such an ionic current that would contribute to the production of myotonia and test whether or not its presence is a requirement for myotonic firing. We expect to identify a persistent current that is central to the production of myotonia, making it a pharmacological target for the elimination of muscle stiffness seen in patients.

Specific Aim II:

Hypothesis: A persistent inward current is responsible for novel behaviors seen in myotonia congenita muscle that may explain symptoms of transient weakness in myotonia congenita patients.

A common complaint of myotonia congenita patients is intermittent bouts of muscle weakness, following episodes of stiffness. Preliminary current clamp records in myotonia congenita show a behavior that may very well correlate with the aforementioned weakness. Through further investigation of current clamp records and voltage clamp

records, we aim to determine the ionic currents and their interactions in producing this novel behavior seen in myotonic muscle. We expect to identify another persistent current that is responsible for this novel behavior. Furthermore, we will attempt to target this current to abolish this behavior.

Chapter II: Background

Skeletal Muscle Contraction

Skeletal muscle differs from other excitable tissues in that the electrical signal is translated into a mechanical force that can be seen grossly (Huxley 1958). Skeletal muscle fibers rapidly convert an electrical signal (action potential) into a mechanical contraction. One nerve stimulus induces one action potential which is converted into one contraction.

The signal for contraction to begin is a quick increase in the $[Ca]_i$ in the vicinity of myosin and actin filaments (Ashley and Ridgway 1968). $[Ca]_i$ acts as a secondary messenger, translating the electrical signal (action potential) into a mechanical contraction. This phenomenon is known as excitation-contraction (E-C) coupling (Frank 1958; Sandow 1965). This occurs over two phases: (1)Depolarization of the T-tubules, activating the dihydropyridine receptor (DHPR) ($Ca_V1.1$) and (2)Ca release from the sarcoplasmic reticulum through a physical interaction of the DHPR and the ryanodine receptor (RYR1)(Desmedt and Hainaut 1977; Wagenknecht, Grassucci et al. 1989). Action potentials propagate along the sarcolemma and down the T-tubules (Gonzalez-Serratos 1971; Bastian and Nakajima 1974). Ca is released from the SR through the RYRs, and diffuses throughout the myoplasm (Suarez-Isla, Orozco et al. 1986). Ca is

then sequestered using binding proteins like troponin C, SERCA, and calmodulin, bringing the myoplasmic $[Ca]_i$ back to resting levels.

Whereas normal muscle responds with a single action potential in response to a single stimulus, myotonic muscle will respond to the same stimulus with runs of action potentials, causing a sustained contraction.

Skeletal Muscle Channelopathies

Ion channelopathies of the skeletal muscle are numerous and include a wide variety of phenotypes ranging from changes in excitability to disruption of E-C coupling (Cannon 2006). Mutations of ion channels range from coding deficits leading to the absence of functional channels in the plasma membrane to aberrant gating properties of the mutated channel. These channel defects predispose patients to acute attacks of stiffness or transient attacks of paralysis (Cannon 2015) These disorders are very rare (1:100,000).

The neuromuscular junction (NMJ) is a synapse wherein the postsynaptic end-plate potential (EPP) elicited by a single motoneuron impulse exceeds the threshold for generation of an action potential (AP) in the muscle fiber (Strickholm 1974). Coupling of the EPP to the generation and propagation of an AP throughout the muscle fiber is essential to achieve rapid and spatially uniform contraction. The APs travel both longitudinally along the surface membrane sarcolemma and radially inward along the T-tubules where depolarization induces the conformational change of $Ca_V1.1$ channels that activates RYRs (the Ca channel of the SR) (Gonzalez-Serratos 1971; Bastian and Nakajima 1974; Suarez-Isla, Orozco et al. 1986).

Myotonia

Myotonia is the delayed relaxation of a muscle or prolonged contraction after brief electrical stimulation or mechanical stimulation (as in percussion myotonia), and is most often due to a channelopathy causing an increased excitability in the muscle (Adrian and Bryant 1974; Jurkat-Rott and Lehmann-Horn 2005). Myotonia, as a behavior, can be seen in multiple disorders. These can be largely split into 2 categories based on the presence or absence of degenerative findings in the skeletal muscle. Dystrophic myotonias, as seen in Myotonic Dystrophy, show "denervation-like" findings on microscopy including increases in fiber size variation, central nucleation, nuclear clumps, and fiber atrophy (Schoser, Schneider-Gold et al. 2004). In contrast, non-dystrophic myotonias, as seen in Myotonia Congenita, do not show similar histological findings.

Myotonia congenita is a disease, strictly of the skeletal muscle, caused by a loss-of-function mutation in CLCN1 gene, encoding the CLC-1 chloride channel found in the sarcolemma (Kubisch, Schmidt-Rose et al. 1998). Patients often complain of "muscle stiffness" and have difficulty in relaxation of muscle after extended use.

This disease is diagnosed by familial history with an accompaniment of symptoms. A needle electromyogram (EMG) is a classical diagnostic tool for myotonia congenita (Fournier, Arzel et al. 2004; Colding-Jorgensen 2005). Myotonia is seen very uniquely through EMG, showing sustained bursts of muscle after-discharges that persist for seconds to minutes after the end of a voluntary contraction (Heatwole, Statland et al. 2013) The amplitude and frequency of these bursts wax and wane, producing a classical "dive-bomber" sound (Fournier, Arzel et al. 2004; Colding-Jorgensen 2005; Heatwole, Statland et al. 2013).

The earliest evidence that myotonic bursting is indeed caused by a defect in the skeletal muscle, independent of motoneurons input, was shown in myotonic goat muscle in 1939 (Brown & Harvey 1939). Further evidence was shown by selective curare block of the NMJ with sustained myotonic firing (Lanari 1946). As curare eliminates muscle excitation from the NMJ, it proved that the muscle itself was the origin of the spontaneous firing of action potentials. These myotonic bursts vary in amplitude and frequency, but are sufficient to produce sustained contraction by SR Ca release, leading to muscle stiffness in the patient (Colding-Jorgensen 2005).

Non-dystrophic Myotonia: Myotonia congenita

The most common non-dystrophic myotonias are caused by chloride channel mutations and sodium channel mutations.

The first evidence of myotonia being caused by a decrease in resting chloride conductance were shown by Lipicky in 1966, in which myotonic muscle was shown to have a large input resistance, as compared to untreated WT muscle (Lipicky and Bryant 1966). Myotonic behavior can be introduced acutely to WT muscle by reversible block of the CLC-1 chloride channel with 9-AC. This was found in conjunction with a decrease in the rheobase current, the amount of injected current required to fire a single action potential (Lipicky and Bryant 1966; Lipicky, Bryant et al. 1971).

Genetic causation of myotonia congenita has been further confirmed with the identification of loss-of-fucntion mutations in the *CLCN1* gene, which encodes for the CLC-1 channel, in mice, humans, dogs, and goats (Steinmeyer, Klocke et al. 1991; Koch,

Steinmeyer et al. 1992; Beck, Fahlke et al. 1996; Rhodes, Vite et al. 1999). There are over 60 distinct mutations identified that result in loss-of-function changes, leading to myotonia congenita (Pusch 2002). The range of *CLCN1* mutations include missense, nonsense, insertions, deletions, and splice mutations (Matthews, Fialho et al. 2010). There is no clear correlation between genotype and phenotype for the various mutation types.

Clinical Features of Myotonia Congenita

Myotonia congenita can follow an autosomal dominant (Thomsen's disease) or autosomal recessive (Becker's disease) inheritance pattern (Heine, George et al. 1994; Steinmeyer, Lorenz et al. 1994). Thomsen's disease was first described in the 1870s by Dr. Thomsen, who suffered from the disease himself. Becker's disease was first identified in 1966, even though it is far more common than Thomsen's disease. These two present very similarly, except for the presentation of transient weakness, which typically presents only in the autosomal recessive form (Deymeer, Cakirkaya et al. 1998). Prognosis for both Thomsen's and Becker's patients are favorable with a normal life expectancy (Gutmann and Phillips 1991).

Myotonia congenita patients develop muscle stiffness, early on in childhood. In response to this involuntary firing, many patients exhibit muscle hypertrophy and a bodybuilding appearance, even as a child. Intensity of stiffness seems to correlate with suddenness of voluntary movements and is often followed a period of transient weakness (Ricker, Haass et al. 1978; Drost, Blok et al. 2001). The pattern of affected muscles varies from patient

to patient. The severity of muscle stiffness also varies based on several factors including emotion, temperature, exercise, and pregnancy (Gutmann and Phillips 1991; Lacomis, Gonzales et al. 1999; Colding-Jorgensen 2005). Patients report accompanying pain with myotonia (Trip, Drost et al. 2006).

Relief of muscle stiffness is seen with repeated use of muscle. This compensatory behavior is almost universal among myotonia congenita patients. Low-level use of a muscle group before full use will alleviate stiffness and involuntary contraction. This is known as the warmup phenomenon (Trivedi, Bundy et al. 2013; Novak, Norman et al. 2015).

Myotonia congenita patients are generally advised to make lifestyle modifications and avoid triggering activities, as these differ greatly from person to person (Colding-Jorgensen 2005). Instead of sudden, forceful movements, patients are advised to gradually increase muscle exertion in an attempt to warm up the muscle. The use-dependent Na channel blocker, mexiletine, is somewhat effective at reducing the severity of myotonia (Statland, Bundy et al. 2012; Desaphy, Gramegna et al. 2013; Trivedi, Bundy et al. 2013). Ranolazine, a slow inactivator of the Na channel, has been shown to reduce myotonia as well, although no clinical data is available yet (Novak, Norman et al. 2015). There are currently no drugs available that act directly on the chloride channel. As gene therapy to introduce normal ClC-1 channels is not available, targeting and modulating other genetically normal channels is the approach currently being taken.

CLC-1 Role in Muscle Excitability

The CLC-1 channel is encoded by the *CLCN1* gene, located on Chromosome 7q35. CLC-1 is almost exclusively expressed in skeletal muscle, with minimal expression in the kidneys, liver, and smooth muscle (Steinmeyer, Ortland et al. 1991). There is no concensus on the precise localization (sarcolemma vs T-tubule) of the channel. Some have found it to localize to the sarcolemma only (Lueck, Rossi et al. 2010) while others have called into question this conclusion based on the imaging methodologies used (Lamb, Murphy et al. 2011) . Neonatal mice show low CLC-1 mRNA levels and chloride currents and increase to adult levels over 20 days (Klocke, Steinmeyer et al. 1994; Lueck, Lungu et al. 2007).

The CLC-1 channel is a homodimeric, double-pored chloride channel. Each of these pores is comprised of two protopores that gate independently but can also be gated by a common gate (Pusch, Steinmeyer et al. 1994; Fahlke, Knittle et al. 1997; Saviane, Conti et al. 1999; Dutzler, Campbell et al. 2002). Open probability at normal resting potentials is ~20% and increases with further depolarization. Open probability also increase with external chloride (Pusch, Steinmeyer et al. 1994). Gating is also modified by pH and ATP (Rychkov, Pusch et al. 1996; Tseng, Bennetts et al. 2007).

In stark contrast to other excitable tissues, the resting membrane conductance in muscle is about 70-80% due to chloride conductance (Hodgkin and Horowicz 1959; Palade and Barchi 1977). The Cl current in resting fibers, however is minimal, as the Cl equilibrium potential is near the resting membrane potential, providing minimal driving force for Cl. In skeletal muscle, the main functions of the Cl conductance are:

1. Regulate muscle excitability and act as a "voltage clamp." The large chloride conductance acts as an electrical buffer to keep the membrane potential at its resting values.

2. In addition to K efflux, a Cl influx contributes to repolarization from an action potential in skeletal muscle (Cannon 2015). .

3. Counteract the depolarizing effect of K accumulation in the muscle's T-tubule system. With a Cl current, each impulse depolarizes the fiber by 0.1 mV. Without a Cl current, that increases to 1 mV. (Adrian and Bryant 1974; Adrian and Marshall 1976; Cannon 2006)

A reduction of Cl conductance by 50% does not cause myotonia (Chen, Niggeweg et al. 1997). The presumption is that the remaining functional Cl channels generate enough of a Cl current to offset the K buildup in the T-tubules. A reduction of at least 70% Cl conductance is necessary to produce myotonia, explaining why heterozygotes of the autosomal recessive disease (Becker's Disease) show no symptoms (Adrian and Marshall 1976; Furman and Barchi 1978).

Current Understanding of Mechanism Underlying Myotonia

The working hypothesis of the mechanism underlying myotonic bursting was introduced by Adrian and Bryant. They stated that an activity-dependent accumulation of K ions in the extracellular T-tubular system is the source of the depolarization needed for sustained myotonic firing (Adrian and Bryant 1974). With each individual action potential's repolarization phase, K effluxes into the extracellular compartment through both the

surface membrane and the T-tubular membrane. Passive diffusion is not fast enough to equilibrate the K accumulated in the T-tubules, due to its long, narrow geometry (Fraser, Huang et al. 2011). The high surface area/volume ratio of the T-tubules results in an increase of the local $[K]_o$ in the T-tubule by 0.4mM with each individual action potential (Adrian and Marshall 1976; Cannon, Brown et al. 1993; Wallinga, Meijer et al. 1999). Normally, K will efflux during repolarization both in WT muscle as well as ClC muscle. But with a loss in chloride current, K currents become vital to repolarization. In the absence of a Cl current, the depolarization induced by K buildup would be unopposed.

This K buildup in the T-tubules of CLCN1[adr-mto2J] muscle produces an after-depolarization from resting potential, thought to be large enough to reach action potential threshold and induce myotonic firing. This is an additive effect, depolarizing the fiber by ~1mV per action potential (Adrian and Bryant 1974). This value increases with higher-frequency firing, as less and less time is available for passive diffusion. This hypothesis is supported by data showing that detubulation, the elimination of the T-tubular system through osmotic shock, prevents afterdepolarization and abolishes myotonic firing entirely (Adrian and Bryant 1974; Cannon, Brown et al. 1993).

Warmup Phenomenon

Repetitive activity in patients with myotonia congenita induces a reduction in muscle stiffness. This is known as the warmup phenomenon (Birnberger, Rudel et al. 1975; Horlings, Drost et al. 2009). The mechanism behind warmup has perplexed the field for years. Understanding the mechanism underlying warmup could be instrumental in

treatment of myotonia congenita. Changes in membrane potential and slow inactivation of the fast Na channels have been proposed as mechanisms (Van Beekvelt, Drost et al. 2006; Lossin and George 2008; Lossin 2013).

A classical test used to demonstrate the warmup phenomenon is the step-climbing test. After five consecutive attempts of climbing a flight of steps, patients will take a significantly shorter time to complete the task once more than when compared directly after a rest period (Rudel, Ricker et al. 1988).

Novak and Rich have shown, through in vivo testing, that our CLCN1[adr-mto2J] mice exhibit warmup. Righting reflex time decreases with repeated testing. Also shown was induction of warmup in in vitro CLCN1[adr-mto2J] muscle (Novak, Norman et al. 2015). Current clamp recordings showed that muscle was warmed up after inducing 5,000 action potential was no longer myotonic. After allowing the muscle to rest for minutes afterwards, the warmup was relieved and the muscle returned to its original myotonic state. They concluded that warmup was acting through the slow inactivation of sodium channels, proposing Na channel slow inactivators as a potential treatment for myotonia congenita patients.

Persistent Inward Currents

Motoneurons have the ability to sustain steady, repetitive firing in response to prolonged inputs (Granit, Kernell et al. 1963; Kernell 1965). The transformation of steady depolarization into repetitive firing is thought to be achieved by persistent inward currents (PICs). Motoneurons have been shown to possess large PICs that could increase

firing rate and prolong firing after cessation of an input (Schwindt and Crill 1977; Schwindt and Crill 1980; Schwindt and Crill 1982). The PIC is a depolarizing inward current that activates for as long as the membrane potential stays depolarized. It is not susceptible to voltage-dependent fast inactivation, and so it continues to pass an inward current long after the fast Na currents have inactivated. This mechanism comes into play when sustained firing is needed. PICs have a voltage-dependence of activation, distinguishing them from ion channels that are always open, as seen in the leak channels or the channels that lack a strong voltage-dependence.

In spinal motoneurons, there are two recognized PICs: Persistent Na (Hsiao, Del Negro et al. 1998; Lee and Heckman 2001; Li and Bennett 2003) and low voltage-activated L-Type Ca (Schwindt and Crill 1980; Hounsgaard and Kiehn 1985; Hounsgaard and Kiehn 1993).

The NaPIC activates quickly at subthreshold potentials, helping depolarize the cell to threshold, and has partial time-dependent inactivation (Hsiao, Del Negro et al. 1998; Li and Bennett 2003). It plays an essential role in the initiation of action potentials during rhythmic firing. This subthreshold NaPIC is hypothesized to pass through the same fast Na channels that are responsible for action potentials. A small percentage of these channels (1-3%) enter a non-inactivating or persistent conductive state (Alzheimer, Schwindt et al. 1993). The NaPIC plays an essential role in intitiating spikes during repetitive firing (Lee and Heckman 2001; Kuo, Lee et al. 2003; Harvey, Li et al. 2006; Theiss, Kuo et al. 2007). Modulation of this current by serotenergic and noradrenergic agonists and antagonists changes neuronal excitability. This PIC has been shown to be blocked by riluzole and phenytoin, although the mechanisms are not clearly delineated as

these drugs have numerous off-target effects (Lampl, Schwindt et al. 1998; Zeng, Powers et al. 2005; Harvey, Li et al. 2006; Theiss, Kuo et al. 2007).

The CaPIC activation potentials are more variable. It has very slow activation and deactivation kinetics and little to no time-dependent inactivation (Hounsgaard and Kiehn 1989; Perrier, Alaburda et al. 2002; Li and Bennett 2003). This PIC passes through the L-Type Ca channel. Repeated depolarization of the membrane potential allows for the activation of the CaPIC. The CaPIC tends to increase in amplitude with repeated activation and may underlie the hysteresis seen in PIC activation and deactivation potentials. PICs classically exhibit onset-offset or activation-deactivation hysteresis, in which they are deactivated at more negative potentials than they are activated (Schwindt and Crill 1980). This is known as "warm up" – not to be confused with the warmup phenomenon seen in myotonia congenita muscle (Svirskis and Hounsgaard 1997; Lee and Heckman 1998; Li and Bennett 2003; Elbasiouny, Bennett et al. 2005; Elbasiouny, Bennett et al. 2006; Li and Bennett 2007). Warmup of the CaPIC is thought to come about by additional L-Type Ca channel openings due to an increased intracellular Ca concentration caused by the repeated depolarizations (Dolphin 1996; Perrier, Mejia-Gervacio et al. 2000).

PICs are difficult to recognize, as they are relatively small and necessary for function. PICs were only described when blockers of other voltage-gated channels were used to unmask the PIC.

Motoneurons exhibit a phenomenon known as bistability due to the presence of PICs. A short pulse of excitatory input may produce self-sustained firing, which could be terminated with an inhibitory input (Heckman, Johnson et al. 2008). When blocking the

firing, the membrane potential can be seen to be held at a plateau, pointing to the steady depolarization caused by the activation of the PIC. This is needed for sustained firing and has been implicated in postural motoneuron firing, where steady firing must be sustained for long periods of time (Hounsgaard, Hultborn et al. 1988).

Slow Inactivation of Voltage-Dependent Channels

Slow inactivation is believed to be a distinct process, independent of fast inactivation. When a muscle fiber is depolarized for seconds or minutes, Na channels enter a slow inactivation state, which can only be relieved by long periods of repolarizations (Adelman and Palti 1969; Adelman and Palti 1969; Chandler and Meves 1970; Khodorov, Vornovitskii et al. 1974; Fox 1976; Khodorov, Vornovitskii et al. 1976; Khodorov 1981; Almers, Stanfield et al. 1983). This process is thought to involve multiple channel states.

Different parts of the channel are responsible for fast and slow inactivation. Evidence for this is shown in treatments that remove fast inactivation still leave channels susceptible to slow inactivation. These were named N-type and C-type inactivation in Shaker K channels (Hoshi, Zagotta et al. 1991). Fast inactivation occurs via an intracellular N-terminus inactivation gate, obstructing the inner pore (Hille 1978). C-Type slow inactivation closes a gate at the extracellular end of the pore, the selectivity filter (Hille 1978). The outermost end of the selectivity filter rearranges during slow inactivation of Na channels (Balser, Nuss et al. 1996; Townsend and Horn 1997)

Chapter III: General Methods

Using in vitro electrophysiology recordings, this proposal will investigate the mechanism(s) underlying behaviors leading to muscle dysfunction in myotonia congenita. The general methods used are described in detail below.

Mice

All animal procedures used were performed in accordance with the policies of the Institutional Animal Care and Use Committee of Wright State University. The great majority of experiments were performed using a colony of CLCN1$^{adr-mto2J}$ mice, which have a null mutation in the *CLCN1* gene, representative of myotonia congenita. The mice were obtained from Jackson Laboratory (Bar Harbor, ME) and a breeding colony was established. Myotonia was confirmed visually via the myotonic appearance of the animals as previously described (Hoppe, Lehmann-Horn et al. 2013). Asymptomatic WT and heterozygous littermates were used as controls. As unaffected littermates have previously been shown not to have myotonia or alterations in macroscopic chloride currents, we did not make an effort to distinguish them from wild-type mice (Mehrke 1988, Reininghaus 1988). Mice were used from 2 months to 6 months of age, irrespective of sex.

Mouse cages contained corn cob bedding and environmental enrichment. Mice were supplied with moistened chow paste (Irradiated Rodent Diet; Harlan Teklad 2918) and water ad libitum. Environmental conditions were maintained with a 12-h day/night cycle and constant temperature (21–23 °C). The behavior and physical condition of the mice

are tested daily for weight loss and priapism.

Electrophysiology

Current Clamp

Prior to removal of muscle for recording, mice were euthanized via CO_2 inhalation followed by cervical dislocation. For current clamp recordings, both *extensor digitorum longus* muscles were dissected out tendon to tendon. Experiments were done on the first muscle while the second muscle was maintained in oxygenated solution. Records from the second muscle began within 3 hours of dissection. Muscles were maintained and recorded from at 21-23 ^{o}C. Electrical properties of the muscle have been shown to be stable for 6 hours in vitro (Novak 2015). The recording chamber was continuously perfused with 40mL of recirculating Ringer solution.

To prevent muscle contraction and allow for stable electrical recordings, muscles were loaded with 50μM BTS (Tokyo Chemical Industry, Tokyo, Japan) for 45 minutes prior to recording. BTS was dissolved in DMSO and added to the perfusate. Maximal DMSO concentration was kept under 0.15%, which has been found not to affect resting membrane properties of skeletal muscle (Pedersen 2009).

Staining and impaling of muscle fibers was performed as previously described (Novak 2015). Briefly, muscles were stained for 3 minutes with 10μM 4-(4-diethylaminostyrl)-N-methylpyridinium iodide (Molecular Probes, Eugene, OR) and imaged with an upright epifluorescence microscope (Leica DMR, Bannockburn, IL). Muscle fibers were impaled with 2 sharp microelectrodes filled with 3M KCl solution containing 1mM sulforhodamine to visualize the electrodes with epifluorescence. Electrode resistances

were ~20 MΩ on average. Capacitance compensation was optimized prior to recording.

Fibers with resting potentials more depolarized than -70mV were excluded from analysis.

Action potential voltage-threshold was defined as the voltage at which dV/dt was equal to

10 mV/ms.

The recording chamber was continually perfused with:

Ringer solution containing (in mM): 118 NaCl, 3.5 KCl, 2 $CaCl_2$, 0.7 $MgSO_4$, 26.2

$NaHCO_3$, 1.7 NaH_2PO_4, 5.5 glucose, and pH 7.3-7.4 with 95% O_2 and 5% CO_2.

Modified Ringer solution for high divalent experiments containing (in mM): 118 NaCl,

3.5 KCl, 5 $CaCl_2$, 2 $MgSO_4$, 26.2 $NaHCO_3$, 1.7 NaH_2PO_4, 5.5 glucose, and pH 7.3-7.4

with 95% O_2 and 5% CO_2.

Drugs (in mM):

0.4 9-AC

0.01 Nifedipine

0.02 Bay-K

0.01 Retigabine

Voltage Clamp

Flexor digitorum brevis and *interosseous* muscle fibers were used rather than extensor

digitorum longus as these muscles contain shorter fibers which allow for better space

clamp and voltage control. Isolation of fibers and recordings were performed as

previously shown (Waters, Varuzhanyan et al. 2013). Briefly, muscles were surgically

removed, pinned to Sylgard-bottomed Petri dishes, and enzymatically dissociated at 37

°C under mild agitation for ~1 h using 1,000 U/mL of collagenase type IV (Worthington

Biochemical). Collagenase was dissolved in the extracellular solution used for recordings (below). Mechanical dissociation was completed using mild trituration in buffer with no collagenase. The fibers were allowed to recover at 21–23 °C for 1 h before being used for electrical measurements.

Fibers were visualized using an Olympus BX51WI microscope, and images were acquired with a CCD camera (ST-7XMEI-C1, Santa Barbara Instruments). Electrical properties were measured under standard current and voltage clamp conditions at 21–23 °C using two aluminosilicate intracellular microelectrodes (part 30-0110, Harvard Apparatus) an Axoclamp 900A amplifier, a Digidata 1440a digitizer, and pCLAMP 10 data acquisition and analysis software (Molecular Devices). The voltage-sensing electrode was connected with an Axoclamp HSx1 headstage. The current-passing electrode was connected with an Axoclamp HSx10 headstage that was modified to have a 2-MΩ output resistor (HSx5). Both the current-passing and voltage-sensing electrodes were filled with the same solutions (below). Data were acquired at 20 kHz. Current and voltage records were low-pass filtered with the internal Axoclamp 900A filters at 1 kHz. The voltage clamp command signal was low-pass filtered with an external Warner LFP-8 at 1 kHz. Filtering the voltage clamp records at 2 or 4 kHz produced no difference in measurements of peak current, conductance, or capacitance.

The internal (electrode) and extracellular solutions are listed below. The average electrode resistance was 15.0 MΩ. After impalement, 20 minutes of hyperpolarizing current injection was allowed for equilibration of the electrode solution with the sarcoplasm before data acquisition. 30mM EGTA was used in the internal solutions to prevent contractions.

Physiological Solutions

Internal solution (in mM) was as follows: 75 aspartate, 30 EGTA, 15 Ca(OH)2, 5 MgCl2, 5 ATP di-Na, 5 phosphocreatine di-Na, 5 glutathione, 20 MOPS, and pH 7.2 with KOH.

Extracellular solution (in mM) was as follows: 144 NaCl, 4 KCl, 1.2 CaCl2, 0.6 MgCl2, 5 glucose, 1 NaH2PO4, 10 MOPS, and pH 7.4 with NaOH.

K-Free Solutions

Internal solution (in mM) was as follows: 75 aspartate, 30 EGTA, 15 Ca(OH)2, 5 MgCl2, 5 ATP di-Na, 5 phosphocreatine di-Na, 5 glutathione, 20 MOPS, and pH 7.2 with CsOH.

Extracellular solution (in mM) was as follows: 144 NaCl, 4 CsCl, 1.2 CaCl2, 0.6 MgCl2, 5 glucose, 1 NaH2PO4, 10 MOPS, 0.05 BaCl2 and pH 7.4 with NaOH.

K-Free Solutions with Increased Extracellular Divalents

Internal solution (in mM) was as follows: 75 aspartate, 30 EGTA, 15 Ca(OH)2, 5 MgCl2, 5 ATP di-Na, 5 phosphocreatine di-Na, 5 glutathione, 20 MOPS, and pH 7.2 with CsOH.

Extracellular solution (in mM) was as follows: 144 NaCl, 4 CsCl, 5 CaCl2, 2 MgCl2, 5 glucose, 1 NaH2PO4, 10 MOPS, 0.05 BaCl2 and pH 7.4 with NaOH.

Drugs (in mM):

0.4 9-AC

0.02 Nifedipine

0.001 TTX

0.1 3,4-DAP

0.01 Ouabain

0.02 Bay-K

0.1 Verapamil

Statistical Analyses

Differences between two data sets were analyzed using Student's (unpaired) two-tailed *t*-test, assuming unequal variance (Sigmaplot 13.0). For comparisons within the same fiber or myotonic runs, paired two-tailed *t*-tests were used. All data are presented as means $\pm$ SEM. $p < 0.05$ was considered to be significant. Sample sizes were chosen based on the lab's previous experiences in the calculation of experimental variability. The numbers of animals and fibers used are described in the corresponding figure legends and text. No blinding was used for the animal groups as ClCn1$^{adr-mto2J}$ mice are easily identifiable from their unaffected littermates phenotypically. This was not significant issue for analysis of voltage clamp and current clamp data as analysis is largely automated and thus not susceptible to subjective bias.

Chapter IV: Specific Aim I

Presence of a Na Persistent Current Playing a Central Role in Myotonic Firing

The overall objective of Specific Aim I is to establish the presence of a Na persistent inward current in myotonic muscle and describe its role in myotonic firing.

Introduction

Myotonia congenita is a member of a group of inherited skeletal muscle diseases known as the non-dystrophic myotonias (Lehmann-Horn, Jurkat-Rott et al. 2008; Trivedi, Cannon et al. 2014; Cannon 2015) and results from a loss-of-function in the muscle chloride channel (ClC-1) (Lipicky, Bryant et al. 1971; Steinmeyer, Klocke et al. 1991; Koch, Steinmeyer et al. 1992). The debilitating slowed muscle relaxation patients with myotonia congenita experience following voluntary contraction is caused by involuntary firing of action potentials (myotonia). Although it is well established that a decrease in ClC-1 conductance causes muscle hyperexcitability, the excitatory events that trigger myotonic action potentials (APs) are not fully understood. Because of this, the mainstay of therapy remains avoiding activities that trigger myotonia (Cannon 2015), which can include running, walking, or other daily activities. Alternatively, drugs that block Na^+ channels, such as mexiletine, are used to reduce excitability (Lehmann-Horn, Jurkat-Rott

et al. 2008; Trivedi, Cannon et al. 2014; Cannon 2015). However, many patients suffer side

effects or incomplete symptom resolution. Thus, there is a need to advance our

understanding of the currents which trigger myotonia if we are to develop improved

therapies.

The currently accepted explanation for the generation of myotonia is that K^+ exits the

fiber during voluntary APs and accumulates in the transverse tubules (t-tubules). T-

tubules are narrow invaginations of the surface membrane that are needed to conduct APs

into the middle of muscle fibers (Peachey 1975). The resulting K^+ build-up depolarizes

the resting membrane potential (Adrian and Bryant 1974; Adrian and Marshall 1976;

Wallinga, Meijer et al. 1999; Fraser, Huang et al. 2011) and is thought to open voltage-

gated Na^+ channels that trigger the involuntary APs causing myotonia (Burge and Hanna

2012; Skov, Riisager et al. 2013). Normally, ClC-1-mediated chloride currents, which

account for 70%-80% of resting muscle membrane conductance, offset the depolarizing

influence of K^+ accumulation and prevent myotonia (Adrian and Bryant 1974; Palade and

Barchi 1977; Steinmeyer, Klocke et al. 1991; Steinmeyer, Ortland et al. 1991).

One shortcoming of only considering t-tubular K+ buildup is that this model does not

clearly explain the cessation of myotonia after a time-course of seconds. Notably, we are

not the first to question K^+ build-up as the sole explanation for myotonia: In one of Dr.

Adrian's seminal papers on myotonia, he noted that "in the absence of a surface chloride

conductance tubular potassium accumulation could certainly contribute to the instability

of the membrane; but it is clear that potassium accumulation is not the only reason for the instability of myotonic muscle fibres" (Adrian and Marshall 1976). However, in the 40 years since this statement was published, no additional contributor to the generation of myotonia has been identified.

In neurons, repetitive firing is maintained by persistent inward currents (PICs), which are activated by long depolarizations and mediated by Na^+ (NaPIC) or Ca^{2+} (Harvey, Li et al. 2006; Heckman, Johnson et al. 2008; Powers, Nardelli et al. 2008; Heckman and Enoka 2012). A NaPIC has also been described in wild type skeletal muscle (Gage, Lamb et al. 1989). However, since its discovery in 1989, little attention has been paid to the muscle NaPIC and its function remains unknown. We hypothesized that the NaPIC in skeletal muscle plays a central role in triggering pathologic repetitive firing during myotonia. Indeed, in this report we show that the activation and inhibition of skeletal muscle NaPIC can explain both the onset and termination of myotonic APs. Moreover, we demonstrate that the inhibition of NaPIC prevents myotonic APs. Our findings lead to a new understanding of muscle hyperexcitability in myotonia congenita, explain the time-course for cessation of myotonic firing, and reveal a novel target for more effective therapies.

Results

The current accepted mechanism underlying myotonic firing is based on K buildup in the T-tubules, in addition to a lowered threshold (presumptively in response to the major loss in leak conductance).

I proposed an alternate hypothesis – one that includes the K buildup phenomenon but also accounts for an additional depolarizing event that was previously unaccounted for.

K⁺ buildup cannot be solely responsible for the depolarization needed for myotonic

firing.

Upon closer examination of a current clamp recording of myotonia, as seen in Figure 1.1, one can tell that K^+ buildup in the T-tubules does not fully explain the myotonic behavior for several reasons:

i. The variation in time and slope of the *afterdepolarization* phase cannot be explained by K buildup in the T-tubule system. The slow and steady depolarization of the membrane potential towards firing threshold is referred to as the afterdepolarization (AfD) phase. Throughout the myotonic run seen in Figure 1.1, the AfD lengthens in time and decrease in slope.

The slope of the afterdepolarization phase decreases as the number of myotonic action potentials increase. This is further demonstrated in Figure 1.6.

K buildup should be similar between action potentials, as in each individual action potential should allow for similar amounts of K flow into the T-tubules and cause similar amounts of depolarization. In fact, the depolarization caused by the K buildup of a single action potential was measured by Adrian and Bryant and found to be ~1 mV per action potential in EDL muscle (Adrian and Bryant 1974). It should be a consistent depolarization independent of the myotonic run. This behavior

led me to hypothesize that an additional source of depolarization must be

at least partially responsible for the afterdepolarization phase.

ii. The membrane potential at which K channel conductance is maximal is a

good estimate of the upper limit of E_K. E_K can only be more

hyperpolarized than this membrane potential. On Figure 1.1, the red arrow

points to the end of the repolarization (Max Repol.) phase of the action

potential, known to be the time at which relative K channel conductance is

maximal. If relative K channel conductance is maximal and there are no

other major leak currents at play (Cl current is absent in myotonic

muscle), then this membrane potential is close to E_K. The depolarization

(moving away from E_K) seen after the red arrow leads up to the myotonic

action potential.

iii. One can then safely assume that another depolarizing current is likely at

play during the myotonic run. This current turns off with delay as the

myotonic run goes on. This can especially be seen at the very end of the

myotonic run. The AfD (minimal at this point) depolarizes the fiber in an

attempt to reach firing threshold but it ultimately fails to do so and the

fiber returns towards its original resting membrane potential.

Details of myotonic firing

Intracellular recordings of myotonic APs were performed under current clamp conditions

in the extensor digitorum longus (EDL) muscle, a standard muscle used for this

procedure that can be removed with little perturbation and thus closely approximates *in vivo* conditions.

Evoked APs were triggered with 200ms step current pulses that depolarized the membrane potential by 15 to 25mV (Fig. 1.1). Following the evoked APs, I recorded trains of involuntary (myotonic) APs that were quite variable in length, lasting from 0.1 to 100 seconds. During the myotonic APs, the average maximum repolarization (Max Repol) was 16.2 ± 1.3mV (n = 51 fibers, 12 mice) more depolarized than the original resting potential (prior to current injection) and did not return to resting level until hundreds of ms or > 1s after the myotonic APs (Fig 1.1). This steady depolarization could be interpreted as K^+ buildup in the t-tubules.

The average AP threshold, defined as the voltage at which the AP rate of rise (dV/dt) was 10mV/ms, was 13.3 ± 0.5mV more depolarized than the Max Repol. After reaching the Max Repol between APs, the membrane potential would gradually depolarize over 20 to 50 ms until the AP threshold was reached. No explanation for the AfD has yet been proposed. During myotonia, the rate of AfD gradually decreased during the run of myotonia from 320.7 ± 20.9mV/sec at the first myotonic AP to 141.9 ± 8.9mV/sec by the last myotonic AP (Fig 1.1, n=51 fibers, 12 mice, p<.01).

Opening of K^+ channels eliminates myotonia.

Opening the K channels pharmacologically should increase extracellular K flow into the extracellular T-tubule. This should then increase the magnitude of depolarization caused by the K buildup following each individual AP. If K buildup alone was responsible for myotonia, then opening more K channels should exacerbate the myotonia.

There has been some evidence showing that opening K channels pharmacologically eliminates myotonia in acutely myotonic muscle treated with 9-AC (Su, Zei et al. 2012). I hypothesized that treating ClC muscle with the same drugs would yield the same result – elimination of myotonia.

Retigabine, an FDA-approved drug for treatment of epilepsy, is a KCNQ channel opener (Large, Sokal et al. 2012; Grunnet, Strobaek et al. 2014). KCNQ channels have been shown to localize to the T-tubular membrane in skeletal muscle (Iannotti, Panza et al. 2010). Figure 1.2 shows that myotonia is eliminated by 10 μM retigabine. Opening the KCNQ channels should exacerbate K buildup in the T-tubules, but it eliminates myotonia altogether.

Depolarizing event contributing to myotonic firing

My current clamp data strongly suggests that the AfD triggers myotonic APs and that the decreasing slope of the AfD is responsible for the termination of myotonia. To determine what underlies the AfD, we applied slow depolarization under well-controlled voltage clamp conditions. Before executing my planned voltage clamp studies, I delineated the characteristics of a depolarizing current that would play a role in the production of myotonic firing through the AfD. They are as follows:

    i.   Voltage-dependence: A depolarizing current involved in the production of myotonic firing would need to be able to depolarize the muscle fiber from the Max Repol. towards firing threshold. The fiber repolarizes and rests briefly between myotonic action potentials at voltages of -60 to -70 mV. From this

membrane potential, the fiber goes through its AfD, which this current would be at least partially responsible for.

ii.   Amplitude: Based on current clamp records, this AfD is 13.3 ± 0.5 mV. Through this, one can estimate the current density amplitude needed for this amount of depolarization. Input resistance of the EDL muscle was measured to be 0.9 ± 0.12 MΩ at RMP (prior to current injection). So, a current of ~14.8 nA would be needed for the AfD.

iii.   Kinetics: Of most interest was the kinetics that a depolarizing current must have to play a role in myotonia production. A myotonic run may run from <1 second to minutes. Even the shortest of myotonic runs require a current that can be repeatedly activated for seconds to minutes without inactivating.

Characteristics of Na$^+$ persistent inward current in muscle from ClC mice

In motor neurons, repetitive firing is triggered by persistent inward currents (PICs), which are carried by both Na$^+$ and Ca$^+$ channels (Harvey, Li et al. 2006; Heckman, Johnson et al. 2008; Powers, Nardelli et al. 2008; Heckman and Enoka 2012). A NaPIC has been described previously in skeletal muscle (Gage, Lamb et al. 1989); this NaPIC lacked fast inactivation and activated between −80 and −70mV, such that it would convert a steady depolarization from K$^+$ buildup into myotonia. In motor neurons, PICs are commonly measured by applying slow ramp depolarizations to inhibit channels with fast inactivation. To determine if PICs could contribute to the myotonic AfD, I applied slow ramp depolarization to dissociated flexor digitorum brevis (FDB) fibers. Because of their small size (400-500μm length x~40μm diameter), we were able to control whole FDB

fibers under voltage clamp. During ramp depolarizations at a rate of 10mV/sec in a normal K^+ solution with 20μM nifedipine to block $Ca_v1.1$ channels (Fig. 1.3A), we recorded an inward deflection in current consistent with the activation of a PIC in ClC FDB fibers (Fig 1.3B&C). This current activated at -73.7 ± 1.1 mV and was maximal at -34.7 ± 2.1 mV with a current density of -8.0 ± 1.6 nA/nF (n=3 mice, 21 fibers).

To determine whether this apparent PIC was due to a channel activation or a K^+ channel closing during ramp depolarization, I repeated recordings in K-free solutions that also contained 0.1mM 3,4-diaminopyridine and 50μM Ba^{2+} in the external solution to block K_v channels and Kir channels, respectively (Alagem, Dvir et al. 2001; Cheong, Dedman et al. 2001). Under these conditions, the apparent PIC was reduced by ~80% (Fig 1.3D), suggesting that the closing of a K^+ channel is a major contributor to the recorded current. The PIC that remained in the K^+-free conditions activated at -71.4 ± 0.78 mV, was maximal at -42.1 ± 2.0 mV, had a -1.4 ± 0.2 nA/nF maximum current density. Although the current is small, the depolarization caused by NaPIC would drive the closing of inwardly rectifying K^+ (Kir) channels (Standen and Stanfield 1980; Struyk and Cannon 2008) causing a further depolarization in a small positive feedback cycle. Thus, NaPIC could be a key depolarizing trigger that drives myotonia.

We also performed voltage-clamp ramp depolarizations on FDB fibers from unaffected wild-type siblings of ClC mice (WT) in K-free solutions. We used 400μM 9-anthracenecarboxylic acid to block ClC-1, an established method of pharmacologically inducing myotonia (Palade and Barchi 1977). In the WT FDB fibers, we recorded a NaPIC that activated at -73.3 ± 0.8 mV, was maximal at -51.1 ± 1.8mV, and had a -0.9 ± 0.2nA/nF maximum current density. The NaPIC in both ClC and WT fibers had

characteristics similar to that reported previously for NaPIC in skeletal muscle (Gage, Lamb et al. 1989).

To identify the channel through which this PIC passes, I attempted to block the PIC pharmacologically. After trial of multiple drugs, including nifedipine and verapamil, targeting a range of ion channels known to depolarize the skeletal muscle, tetrodotoxin (TTX) was the only drug to successfully block the PIC. This confirmed that the PIC, recorded in K-free conditions, does indeed pass through a TTX-sensitive channel. The current is likely mediated by Na^+ channels since it was eliminated by application of $1\mu M$ TTX (n=4 mice, 23 fibers) (Fig. 1.3D). It is very likely that the PIC passes through $Na_V1.4$, the same channel that is responsible for the fast Na current that depolarizes the fiber during an action potential. This finding is in line with findings in the motoneurons, as the NaPIC in motoneurons is thought to pass through $Na_V1.6$, the same channel responsible for the fast Na current (Brocard, Plantier et al. 2016).

Attempts to characterize this PIC using classical rectangular pulses for longer time periods were unsuccessful. The PIC was too difficult to discriminate out of the background currents, even with pharmacological block.

PIC is susceptible to slow inactivation

Slow inactivation is a property exhibited by some voltage-dependent ion channels, including Na channels (Adelman and Palti 1969; Almers, Stanfield et al. 1983). Longer depolarizations (on the order of seconds) lead to the slow inactivation of these channels and consequently require long periods of repolarization to relieve this inactivation.

As described earlier, the rate of AfD gradually declines during myotonia (Fig 1.1), suggesting that the underlying current slowly inactivates over hundreds of ms to seconds and lacks fast inactivation (which occurs over ms). The previous study which identified NaPIC in muscle (Gage, Lamb et al. 1989) did not determine whether the current inactivated over seconds. To examine slow inactivation, we modified our ramp protocols to slowly return to the baseline holding potential before repeating the slow depolarization, resembling a symmetrical saw-tooth pattern (Fig. 1.4). The mean current density of NaPIC on the descending ramp was reduced by 86% in ClC FDB fibers (–1.4 ± 0.2nA/nF on ascending ramp vs. –0.2 ± 0.1nA/nF on descending ramp, n = 20 fibers; 6 mice, p < .01). Slow inactivation was relieved by the hyperpolarization at the end of the descending ramp, as the mean NaPIC during the subsequent ascending ramp was –1.3 ± 0.2 nA/nF.

During the initial depolarizing phase of the ramp, the PIC activates at –71.4 ± 0.78mV and peaks at –42.1 ± 2.0mV, but then decreases in amplitude again before reaching -10 mV. This could possibly mean that the current has lost its driving force by this point. But earlier data showing TTX sensitivity points to the notion that this PIC passes through a Na channel. Our calculated equilibrium potential for Na is ~+50mV. So, the loss in driving force may account for slight decreases in the current amplitude, but the main cause of this decrease is likely caused by a decrease in conductance. Because the PIC isn't susceptible to fast inactivation, the cause of this decreased conductance is likely to be slow inactivation.

These data suggest that, while NaPIC lacks fast inactivation, it undergoes a reversible slow inactivation that could contribute to the reduction in the rate of the AfD during runs

of myotonia. These findings suggested that slow inactivation of NaPIC underlies the termination of myotonic firing.

Warmup abolishes myotonic firing and may be acting through the slow inactivation of PIC.

The warmup phenomenon has been described in myotonia congenita patients. Upon repeated use of a muscle group, the muscle acts normally and is no longer myotonic. Essentially, warmup is myotonic muscle acting normally after repetitive, high-frequency firing of muscle, on the order of minutes. However, it is not understood how warmup affects the state of the myotonic muscle.

The warmup phenomenon is demonstrated in Fig 1.5. Current clamp recordings show that, upon 200ms of depolarizing current injection, a CLCN1$^{adr-mto2J}$ muscle will exhibit myotonic firing. 5,000 APs are then triggered at a rate of 50Hz to induce warmup. The 200ms depolarizing current injection is then applied once again to induce myotonia. But the muscle, at this time, is "warmed up," and fires no myotonic action potentials. As time elapses from the "warmup" period, one can see that the afterdepolarization following the 200ms pulse gradually increases in size. This signifies the progressive relief of warmup and the muscle nearing a myotonic state. As time passes, this afterdepolarization is finally large enough to reach action potential threshold and fire myotonic action potentials.

If indeed this novel PIC is a requirement for myotonic firing, it is possible that "warming up" a muscle will act on the PIC. To test this, I attempted similar ramp voltage protocols

as those seen in Figure 1.3 prior to and after 5,000 induced "action potentials." These "action potentials" were done under voltage clamp as an instantaneous depolarization from -85mV to 0mV for 2ms at 50Hz. I expected to find a decrease in the PIC amplitude after this pseudo-warmup protocol. If the fiber was still intact and behaved properly, expected an increase in PIC amplitude towards its original size after a 5-minute rest period at -85mV. Unfortunately, my several attempts at this set of experiments were not successful. With such a harsh protocol, muscle fibers could not make it through the records. This is further discussed in the Discussion section.

Reduction in the rate of AfD is responsible for termination of myotonia

In a NaPIC model of myotonia, slow inactivation of NaPIC during a run of myotonia will cause a gradual decrease in the rate of the AfD. Furthermore, if inhibition of NaPIC underlies the termination of myotonia, the rate of the AfD should be at its minimum prior to termination of myotonia. This was the case. Before the first myotonic AP, the average AfD slope was 320.7 ± 20.9mV/sec; after the last myotonic AP, the average AfD slope was 141.9 ± 8.9 mV/s, its lowest value (51/51 fibers, 12 mice). Figure 1.6 shows a plot of the rate of the AfD during myotonia from a representative fiber. These data suggest that slow inactivation of NaPIC plays a central role in the termination of myotonia.

We also examined whether slow inactivation of the transient Na^+ current contributed to resolution of myotonia, as has recently been proposed (Lossin 2013; Novak, Norman et al. 2015). If the transient Na^+ channel availability decreases, the AP peak and dV/dt will decrease, whereas the AP threshold increases. By these measures a decrease in transient Na^+ channel availability only occurred in 13.7% of fibers prior to termination of

myotonia, there was no change in 27.5% of fibers, and an increase in 58.8% of fibers (Fig 1.6). The lack of correlation between transient Na channel availability and termination of myotonia argues strongly that inactivation of transient Na^+ currents does not play a central role in termination of myotonia. Another possibility is the resolution of t-tubular K^+ buildup. However, arguing against this idea is that the maximal repolarization following each myotonic AP did not correlate with termination of myotonia (Fig 1.6). The only parameter that closely correlated with termination of myotonia was reduction in the slope of the AfD.

Treatments that eliminate myotonia reduce NaPIC

The tight correlation between AfD rate and termination of myotonia, suggests that pharmacologically inhibiting NaPIC would prevent myotonia. We studied the mechanism of action of two different manipulations that eliminate myotonia (Fig 1.7A). The first was the Drug ranolazine, which was previously demonstrated to be effective in treating myotonia (Novak, Norman et al. 2015). With no exposure to ranolazine, myotonia was detected in 100% of ClC EDL fibers (n = 217 fibers, 28 mice); in the presence of 50μM ranolazine, 0% of ClC EDL fibers exhibited myotonia (Fig 1.7A, n=35 fibers, 4 mice). The second treatment we studied was elevated extracellular Ca^{2+} and Mg^{2+}, which has been shown to prevent myotonia (Skov, Riisager et al. 2013; Skov, De Paoli et al. 2015). We recorded from ClC EDL muscle in the presence of physiological (1.5mM Ca^{2+} and 1.4mM Mg^{2+}) and elevated (5mM Ca^{2+} and 2mM Mg^{2+}) extracellular divalent cation concentrations. Myotonia was detected in only 8.33% of fibers in the presence of high divalent cations (4 of 48 fibers, 4 mice, Fig 1.7A).

We next studied whether both treatments reduced NaPIC. Voltage clamp recordings in the presence of 50μM ranolazine revealed an 80% reduction in NaPIC current density (n =20 fibers, 3 mice, Fig 1.7B&C). When NaPIC was recorded in the presence of elevated extracellular divalent cations, the current density was reduced by 55% (n=25 fibers, 3 mice, Fig 1.7B). Thus, both ranolazine and the elevation of extracellular divalent cations eliminate myotonia and reduce NaPIC. The differences between control and treatment groups were statistically significant as determined by one-way ANOVA.

If NaPIC plays a central role in triggering the AfD, elimination of myotonia by both treatments should be paralleled by reduction in the rate of the AfD. The rate of the AfD in the presence of 50μM ranolazine was 54.7 ± 8.6mV/s, a value much lower than the rate of the AfD in untreated muscle just prior to termination of myotonia (141.9 ± 8.9mV/s). Elevation of divalent cation reduced the rate of the AfD to 38.1 ± 5.3mV/sec. These data are consistent with the possibility that a reduction of NaPIC causes a reduction in AfD and this is the mechanism underlying the efficacy of both treatments against myotonia.

That NaPIC and AfD are key determining factors in the onset and termination of myotonia is a dramatic shift from current views on myotonia. Hitherto, it was thought that treatments eliminate myotonia via effects on transient Na^+ channels that lead to elevation of AP threshold (Desaphy, Carbonara et al. 2014; Cannon 2015). Moreover, the previous model did not address termination of myotonia. To assess the previous model, we compared the AP threshold to the AfD in our ranolazine and high divalent records. If treatments eliminate myotonia by raising AP threshold and not altering AfD, the AfD following treatment should reach the pre-treatment AP threshold, but not trigger myotonia. The AP threshold of the first myotonic AP measured in ClC muscle was –48.9

± 0.8mV (n=51 fibers, 12 mice, Fig 1.7C). The peak of the AfD following a 200ms

stimulation in the presence of 50μM ranolazine averaged −62.1 ± 0.9mV (n=35 fibers, 4

mice, Fig 1.7C), a value significantly more negative than the pre-treatment AP threshold.

In the presence of elevated extracellular divalent cation, the peak voltage reached by the

AfD averaged −59.9 ± 0.8mV (n=4 mice, 42 fibers, Fig 1.7C). Thus, while both

treatments elevate AP threshold, in neither case does this appear to be the mechanism by

which they eliminate myotonia. In contrast, the onset, termination, and treatment of

myotonia can be understood by considering AfD and NaPIC.

Discussion

A new model of myotonic muscle hyperexcitability

In both the autosomal dominant (Thomsen) and recessive (Becker) forms of myotonia

congenita, loss of function mutations in the ClC-1 gene (*CLCN1*) cause muscle

hyperexcitability (Lehmann-Horn, Jurkat-Rott et al. 2008; Trivedi, Cannon et al. 2014;

Cannon 2015). However, it has remained unclear what excitatory events triggers

myotonic APs in the absence of the stabilizing ClC-1 current. Prior to this study, the only

excitatory factor implicated in the generation of involuntary action potentials (APs) in

myotonia congenita was a steady membrane depolarization from K^+ build-up in t-tubules

(Adrian and Bryant 1974; Adrian and Marshall 1976; Wallinga, Meijer et al. 1999;

Fraser, Huang et al. 2011) that activated the transient Na^+ channels responsible for APs

(Burge and Hanna 2012; Skov, Riisager et al. 2013). It was posited over four decades ago

that some additional factor was necessary to account for the spontaneous firing of APs

during myotonia (Adrian and Marshall 1976); but, until now, no such factor had been identified. While closely examining action potentials in the Clcn1[adr-mto2J] (ClC) mouse model of myotonia congenita, we observed two possible contributors to the depolarization that brings fibers to threshold during runs of myotonic APs: 1) a blunted repolarization between action potentials, presumably from K^+ build-up, and 2) a slow depolarization after each myotonic AP, which we termed the after-depolarization (AfD). We found that the onset of myotonia is accompanied by a steep AfD slope and the termination of myotonia follows a decrease in the AfD slope. Moreover, effective treatments reduced the AfD rate. No other action potential characteristic predicted the presence or end of myotonia. We further posited that a current, unmasked in the absence of ClC-1, underlay the AfD. A persistent inward Na^+ current (NaPIC) previously identified in wild type (WT) skeletal muscle (Gage, Lamb et al. 1989) exhibited characteristics that could generate the AfD. We found a NaPIC in muscle from ClC mice and WT siblings with properties similar to those initially described by Gage et al. Notably, the voltage dependent activation and very slow inactivation describe an excitatory current that would drive the closure of Kir channels and explain the AfD. Based on characteristics of the NaPIC, we present a modified model of the generation of myotonia in Fig 1.8.

In both models, the absence of a stabilizing chloride current through ClC-1 unmasks the depolarizing events. This occurs because the equilibrium potential for chloride is at or near the resting membrane potential (RMP) in skeletal muscle (–80 to –90mV) (Adrian and Bryant 1974; Palade and Barchi 1977). In the K^+ buildup model (Fig. 1.8, Left panel) the only depolarizing event is K^+ buildup in t-tubules, which is sufficient to drive the

membrane to the AP threshold. The role of K^+ buildup in myotonia is established from experiments showing that de-tubulation of muscle fibers eliminated myotonia (Adrian and Bryant 1974; Adrian and Marshall 1976). Arguing against this model fully explaining myotonia, we show that the average maximum repolarization between myotonic APs, which is driven primarily by the E_K, is 13mV more negative than the AP threshold. This strongly suggests that K^+ buildup alone could not trigger myotonia.

In the NaPIC model presented here, t-tubular K^+ buildup provides the initial depolarizing event, which explains the steady depolarization during myotonia. The maximum repolarization between APs reflects the magnitude of this depolarizing effect. Since the membrane potential remains subthreshold without an additional depolarizing event, the membrane potential would return to resting values. However, K^+ buildup is sufficient to activate NaPIC. In response to NaPIC, the membrane potential begins to depolarize past the maximum repolarization to generate the after-depolarization (AfD). Although NaPIC is small, we propose that the resulting depolarization will begin to close inwardly rectifying K^+ (Kir) channels. The steep voltage-dependence of Kir channels is such that they close at potentials slightly depolarized relative to the K^+ equilibrium potential (Standen and Stanfield 1980; Struyk and Cannon 2008).

In fact, the difference in amplitude seen between PICs recorded in physiological solutions versus K-free solutions can be accounted for by the closing of Kir channels. This would mimic a PIC activation and increase the apparent PIC amplitude. My model suggests that a possible approach to MC treatment may be using a K channel opener, as demostarted in the retigabine findings. This is unexpected as outward K flow into the T-tubule has been seen as the main culprit behind myotonic firing.

NaPIC in WT muscle

Our demonstration that NaPIC is present in WT muscle leads to the idea that the excitatory currents triggering myotonia are simply unmasked by the absence of ClC-1. Importantly, it also implies that NaPIC has a role in normal muscle function. One role of PICs in neurons is to convert steady depolarizations caused by the asynchronous firing of many weak synaptic inputs into repetitive spiking (Harvey, Li et al. 2006; Heckman, Johnson et al. 2008; Powers, Nardelli et al. 2008; Heckman and Enoka 2012). However, since skeletal muscle fibers receive only one synaptic input, there is no need for a PIC to convert multiple asynchronous synaptic firings into repetitive muscle APs. The normal function of NaPIC in muscle might be to improve the fidelity of neuromuscular transmission during periods of intense stimulation: in addition to enabling repetitive firing, PICs in neuronal dendrites serve as amplifiers for weak synaptic inputs (Lee and Heckman 2000; Heckman and Enoka 2012). During intense exertion, the neuromuscular junction is stimulated at rapid rates, resulting in depression of the endplate potential, such that synaptic transmission might fail (Rich 2006). The NaPIC in muscle could thus amplify subthreshold endplate potentials during strenuous activity.

Molecular identity of NaPIC

That NaPIC is sensitive to low doses of tetrodotoxin in ClC and WT muscle suggests that NaPIC is mediated by a standard skeletal muscle Na^+ channel that drives the AP rising phase, namely $Na_v1.4$ (Yang, Sladky et al. 1991). It is likely that NaPIC derives from small subset of $Na_v1.4$ channels that are in a different conformation. This understanding

41

is based on recordings from frog skeletal muscle, as well as rat and cat neurons, that single Na^+ channels shift modes between a normal, fast-inactivating mode and a mode lacking fast inactivation (Patlak and Ortiz 1986; Alzheimer, Schwindt et al. 1993). For simplicity, we refer to the currents through the $Na_v1.4$ channels that lack fast inactivation as NaPIC and the currents through the normal fast-inactivating $Na_v1.4$ channels as the transient Na^+ currents. We hypothesize that some Na^+ channel mutations that trigger myotonia do so by promoting the channel conformation that generates PIC. Mechanisms that have been identified in neurons as promoting NaPIC include cleavage by calpain and association of Na^+ channels with calmodulin (Brocard, Plantier et al. 2016; Yan, Wang et al. 2017).

We note that the NaPIC present in ClC muscle is distinct from the pathological persistent inward currents arising from mutations in Na^+ or Ca^+ channels that trigger periodic paralysis (Cannon 2015). NaPIC is too small to cause depolarization sufficient to cause muscle inexcitability and paralysis. Also, as it inactivates over seconds and could thus not cause the sustained depolarization that underlies periodic paralysis

NaPIC Models

The modeling of the functional behavior of ion channels has usually been based on the assumption of channel homogeneity – that every channel of the same subtype and isoform behaves similarly. However, single-channel electrical recordings have shown that this is not the case and is an oversimplication. I suggest that a subpopulation of the genetically normal $Na_v1.4$ channels are in an alternate mode, with altered kinetics, making them responsible for the NaPIC.

Na channels in muscle have been shown to function in several different modes. Open-time distributions of single Na channels involved in the bursting behavior seen in the Sartorius muscle of frogs were studied by Patlak. Although 80% of all bursts consisted of similar open-times. He concluded that the gating kinetics of individual Na channels are heterogenous (Patlak, Ortiz et al. 1986).

There are numerous possible explanations for the functional heterogeneity seen in these channels. Post-transcriptional modifications may result in slightly different sub-populations of these channels, leading to a permanent heterogeneity, as seen in the expression of TTX-sensitive and TTX-insensitive Na channels in denervated or developing muscle (Sherman and Catterall 1985). Another possibility is enzymatic degradation that could be introduced via the experimental setup. Cleavage of the Na channel by calpain has been shown to increase NaPIC in the spinal cord after injury. Although there are many reasons for a rise in intracellular Ca that can activate a calpain cleavage, experimental manipulation may be partially responsible for that.

Another explanation may be a phenomenon known as mode shifting (Hess, Lansman et al. 1984). Mode shifting can be due to reversible chemical modifications or slow changes in the protein conformation of the channel.

Yet another explanation is induced changes in the rate constants of Na channel modes. Inactivation is usually recognized as an inactivation form the open-state or Osi. Osi brings a channel form an aO-state (activation-gate and inactivation-gate open) to an aOI-state (activation-gate open, inactivation-gate closed) channel. The rate constant for the forward reaction is designated κ, while the rate constant for the reverse reaction is

designated λ. Normally, κ is much larger than λ (Armstrong 2006). A mild reduction in κ in a subset of the Na channels can also account for the presence of a NaPIC.

I suggest that the underlying mechanism for generation of NaPIC is a transient dysfunction in the inactivation gate of genetically normal $Na_V1.4$ channels.

Treating ClC-1 disorders by targeting NaPIC

Our model of NaPIC in myotonia reveals an attractive target for developing novel therapies with minimized side effects. Previously, the only ion channel target available for treatment was the transient Na^+ current responsible for the AP. Blocking this critical current poses serious difficulties, such as how to provide sufficient relief from involuntary APs while minimizing interference with voluntary APs, which can produce weakness and paralysis. Highlighting the importance of NaPIC to myotonia, we demonstrate that highly effective treatments for myotonia act against NaPIC. Prior to our study, treatment with ranolazine and elevation of extracellular divalent cations were thought to eliminate myotonia by different mechanisms. As we had not yet identified NaPIC, we proposed that ranolazine was eliminating myotonia by enhancing slow inactivation of transient Na^+ currents (Novak, Norman et al. 2015). Elevation of extracellular divalent cations was suggested to eliminate myotonia by a rightward shift in the voltage dependence of transient Na^+ activation, such that the AP threshold shifted to more depolarized potentials (Skov, Riisager et al. 2013; Skov, De Paoli et al. 2015). In the current study, we found that both ranolazine and elevated divalent cations eliminate myotonia primarily by inhibiting NaPIC, which is paralleled by a reduction in the rate of

AfD such that the threshold for triggering myotonic APs was not reached. Thus, while both ranolazine and elevation of extracellular divalent cations may raise AP threshold, this does not appear to be the mechanism underlying their efficacy against myotonia. These findings lead to the conclusion that targeting NaPIC is the most effective method of preventing myotonia.

Clinical Trial – Ranolazine as MC treatment

Arnold, W. D., Kline, D., Sanderson, A., Hawash, A. A., Bartlett, A., Novak, K. R., Rich, M. M., Kissel, J. T. (2017). "Open label trial for the treatment of myotonia congenita." Journal of Neurology. In press.

An open label, pilot study was designed to determine whether ranolazine could improve signs and symptoms of myotonia and muscle stiffness in patients with myotonia congenita (MC). Thirteen participants were assessed at baseline, 2, 4, and 5 weeks. Ranolazine was started after baseline assessment (500mg twice daily), increased as tolerated after week 2 (1000mg twice daily), and maintained until week 4. Outcomes included change from baseline to week 4 in self-reported severity of symptoms (stiffness, weakness, and pain), timed-up-and-go (TUG), hand grip and eyelid myotonia, and myotonia on electromyography (EMG).

Severity of stiffness, weakness, and pain symptoms were graded by participants (0-9, with 9 being the most severe) similar to a previously used symptom diary (Statland, Bundy et al. 2012). Hand grip myotonia was assessed by timing hand opening with a stopwatch following tight hand closure for 5 seconds.   Five consecutive trials were

performed. Eyelid myotonia was tested in a similar manner. A single trial of the Timed-up-and-go (TUG) was performed (Podsiadlo and Richardson 1991).

EMG myotonia was assessed in the tibialis anterior (TA) and abductor digiti minimi (ADM) muscles at baseline and Week 4. Presence or absence of myotonia following 15 needle movements (EMG frequency) and the duration of the longest sustained myotonic run (EMG duration) were quantified in each muscle.

Results show improvement in clinical and EMG assessments of myotonia. Assessment of EMG myotonia frequency has been used as an outcome in anti-myotonia trials (Statland, Bundy et al. 2012). We quantified EMG frequency and duration of myotonia, and interestingly, ranolazine showed an effect on duration but not frequency.

Mexiletine is the current treatment of choice in MC(Kwieciński, Ryniewicz et al. 1992; Statland, Bundy et al. 2012; Trivedi, Cannon et al. 2014). While this study does not allow comparison of ranolazine to mexiletine, having an alternative to mexiletine may be beneficial. An advantage of ranolazine is that mexiletine can easily completely block sodium current and induce loss of muscle excitability and weakness(Courtney 1981; Desaphy, Carbonara et al. 2014). Ranolazine does not directly block the sodium current, but instead enhances slow inactivation (Novak, Norman et al. 2015). As the voltage dependence of $Na_v1.4$ slow inactivation is shallow, ranolazine is unlikely to completely eliminate sodium current and thus may be less prone to cause muscle weakness(Rich and Pinter 2003; El-Bizri, Kahlig et al. 2011).

The findings, shown in Table 1.1, suggest that ranolazine is well tolerated over a period of four weeks and has possible benefit in MC suggesting the need for investigation in a randomized, controlled trial. The method by which ranolazine is acting on patient

symptoms can be explained directly by my earlier data showing ranolazine's effect on the
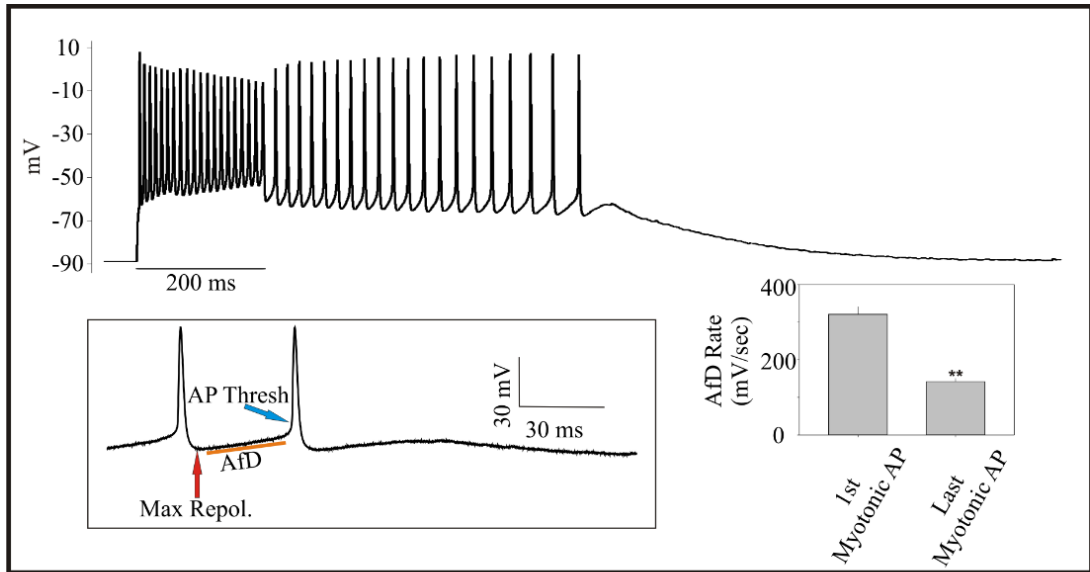
NaPIC.

Fig. 1.1: Myotonic firing in muscle from ClC mice due to both a steady depolarization and an after-depolarization.

Shown is the response of a ClC muscle fiber to a 200ms injection of stimulating current. The fiber fires multiple APs for the duration of the current injection, a normal behavior; then also continues to fire APs after the cessation of current injection (myotonia). Contributors to myotonic firing of APs include a steady depolarization and an after-depolarization (AfD) occurring between APs. The AfD occurs over 20-50ms and brings the fiber to threshold. The inset shows the final two APs of the run of myotonia on an expanded timescale. Max Repol.= the maximal repolarization following each AP; Threshold = AP threshold ($dV/dt = 10mV/ms$). An AfD is present following the last myotonic AP, but is too small to bring the fiber to threshold. Following the final AfD, there is a resolution of the steady depolarization as the fiber gradually returns to its resting membrane potential. Shown on the lower right is the mean value of the first and last AfD slopes (n=51 fibers, 12 mice, ** indicates $p<.01$ based on fiber variability).
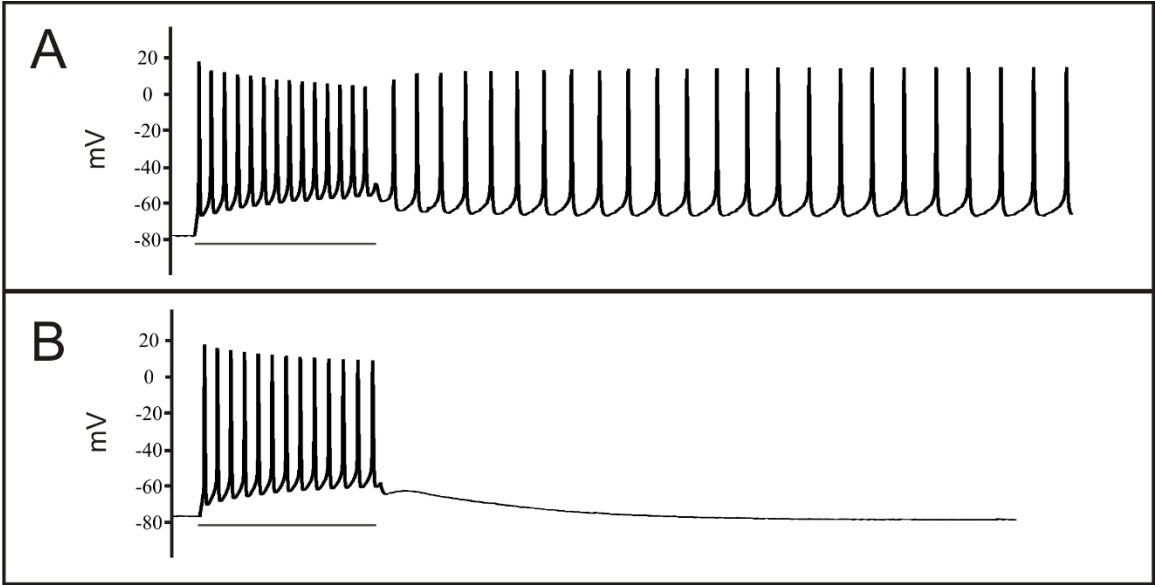
Fig 1.2: Myotonia is eliminated upon addition of 10 µM retigabine

(A) CLCN1$^{adr-mto2J}$ muscle is injected with a depolarizing current for 200 milliseconds, resulting in the firing of multiple action potentials for the duration of the injection, a normal behavior. The fiber continues to fire action potentials after the cessation of current injection (myotonia). **(B)** Upon addition of 10 µM retigabine, a KCNQ channel opener, the same fiber shows no myotonic firing with the preservation of firing during the current stimulus.

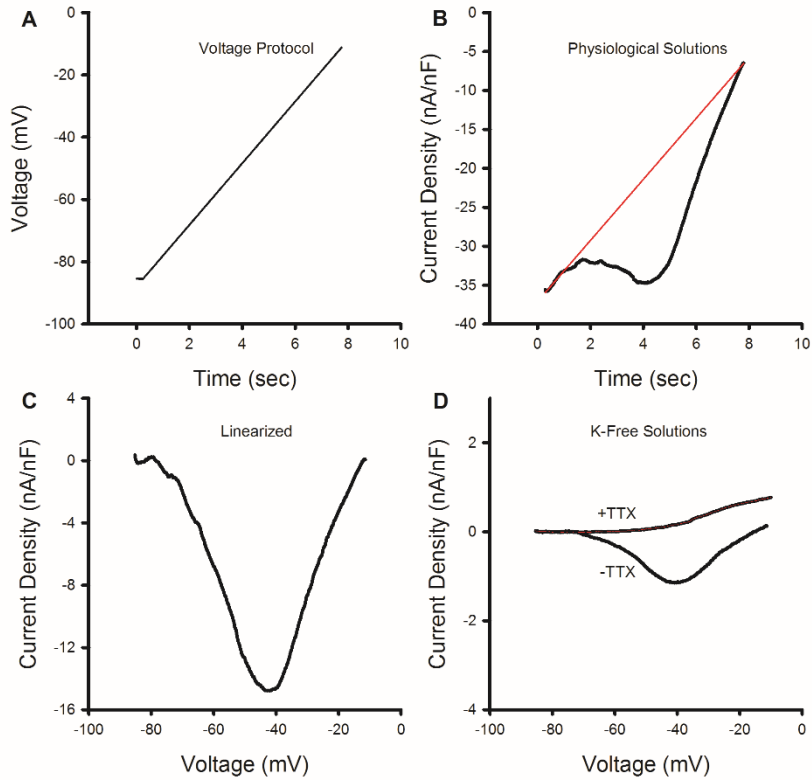n = 6 mice, 67 fibers. $p < .001$ based on fiber variability

Fig. 1.3: Characterization of a TTX-Sensitive Persistent Inward Current in ClC muscle.

(A) The voltage protocol used to identify PICs. From a holding potential of –85mV, fibers were depolarized to –10mV at a rate of 10mV/sec. **(B)** The current trace generated by the ramp depolarization in normal K^+ solution with 20µM nifedipine. A fit line (red) is drawn using the first 0.5 seconds of the raw trace, representing the leak current. Deviations from the leak current/fit line in the negative direction are consistent with activation of a PIC. n=3 mice, 21 fibers) **(C)** Shown is a trace generated by subtracting the leak trace shown in B and plotting against voltage. **(D)** Plot of leak-subtracted PIC in K-free solutions (-TTX). The PIC was blocked by the addition of 1µM TTX to the external solution (+TTX). (n=4 mice, 23 fibers)
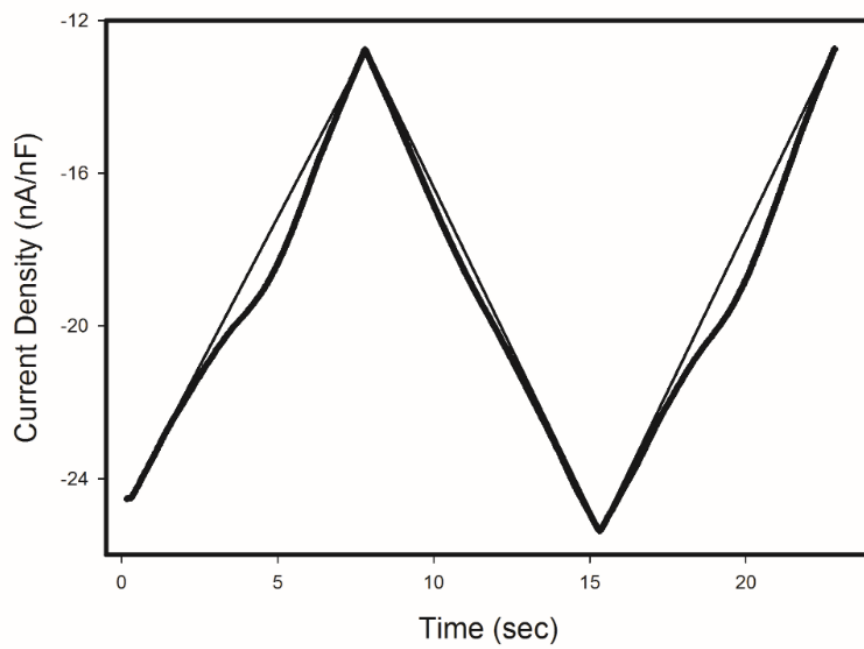
Fig. 1.4: Current recorded during a voltage-clamp ramp protocol with repeated slow depolarization

Current recorded during a voltage-clamp ramp protocol in which the fiber was slowly depolarized from a holding potential of –85mV to –10mV, repolarized to –85mV, and again depolarized to –10mV. The larger PIC during the depolarizing ramps than the repolarizing ramp shows that the muscle NaPIC undergoes slow inactivation. The recording was performed in K^+-free solutions. The fit lines for linear leak currents are superimposed on all three ramps.
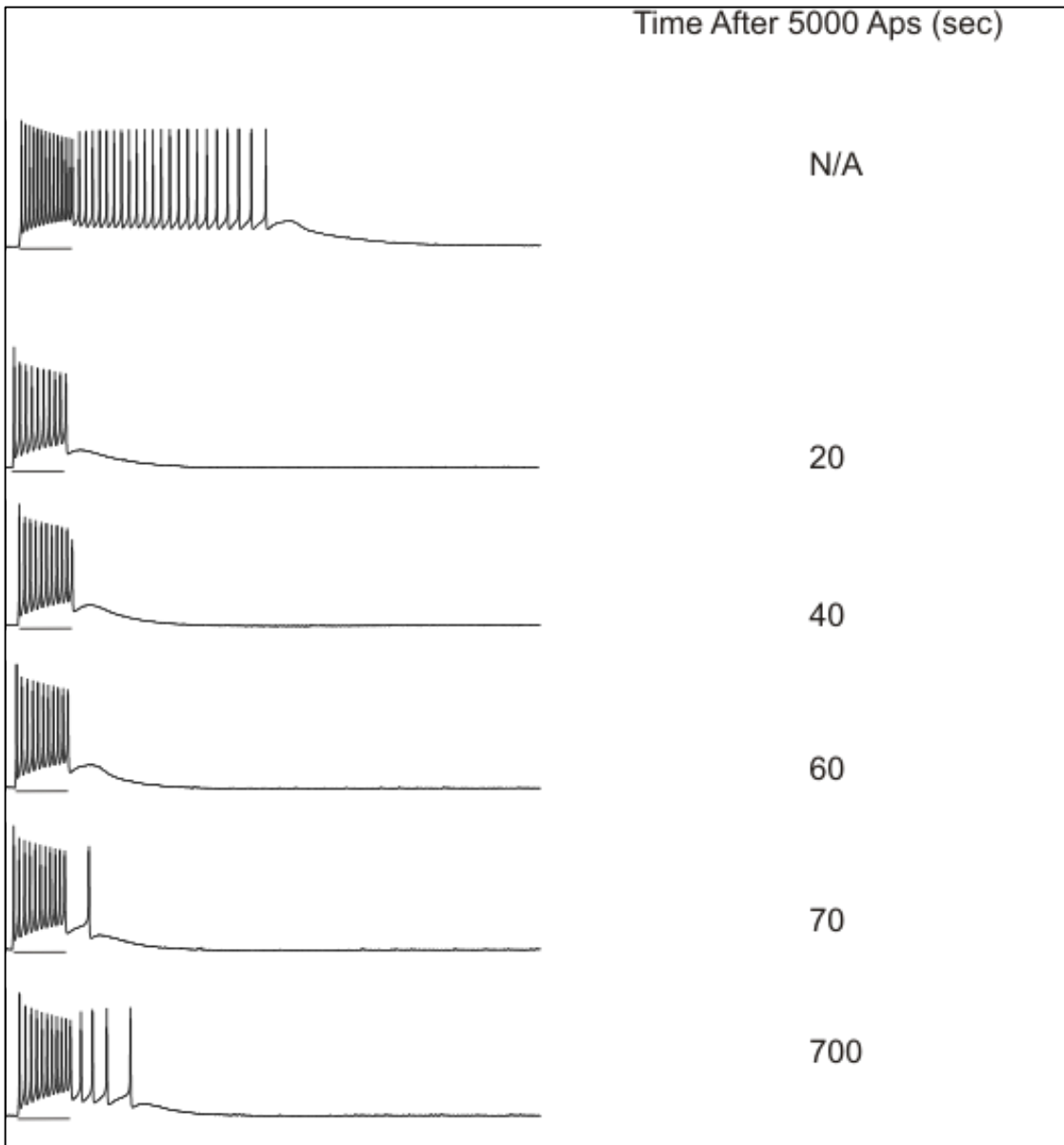
n = 20 fibers; 6 mice, p < .01, paired t-test

Time After 5000 Aps (sec)

N/A

20

40

60

70

700

Fig 1.5: Warmup eliminates myotonia temporarily.

Shown, in the top trace, is the response to a CLCN1$^{adr-mto2J}$ muscle fiber to a 200ms of depolarizing current injection. At the end of the current pulse, the fiber continues to fire myotonic action potentials.

5,000 APs are then triggered at a rate of 50Hz to induce warmup. The 200ms depolarizing current injection is then applied immediately to induce myotonia. But the muscle is warmed up and fires no myotonic action potentials.

As time elapses after the 5,000 APs, the afterdepolarization following the 200ms pulse gradually increases in size and rate, signifying the progressive relief of warmup and the muscle returning towards its original myotonic state. As more time passes, this afterdepolarization is finally large enough to reach action potential threshold and fire myotonic action potentials.
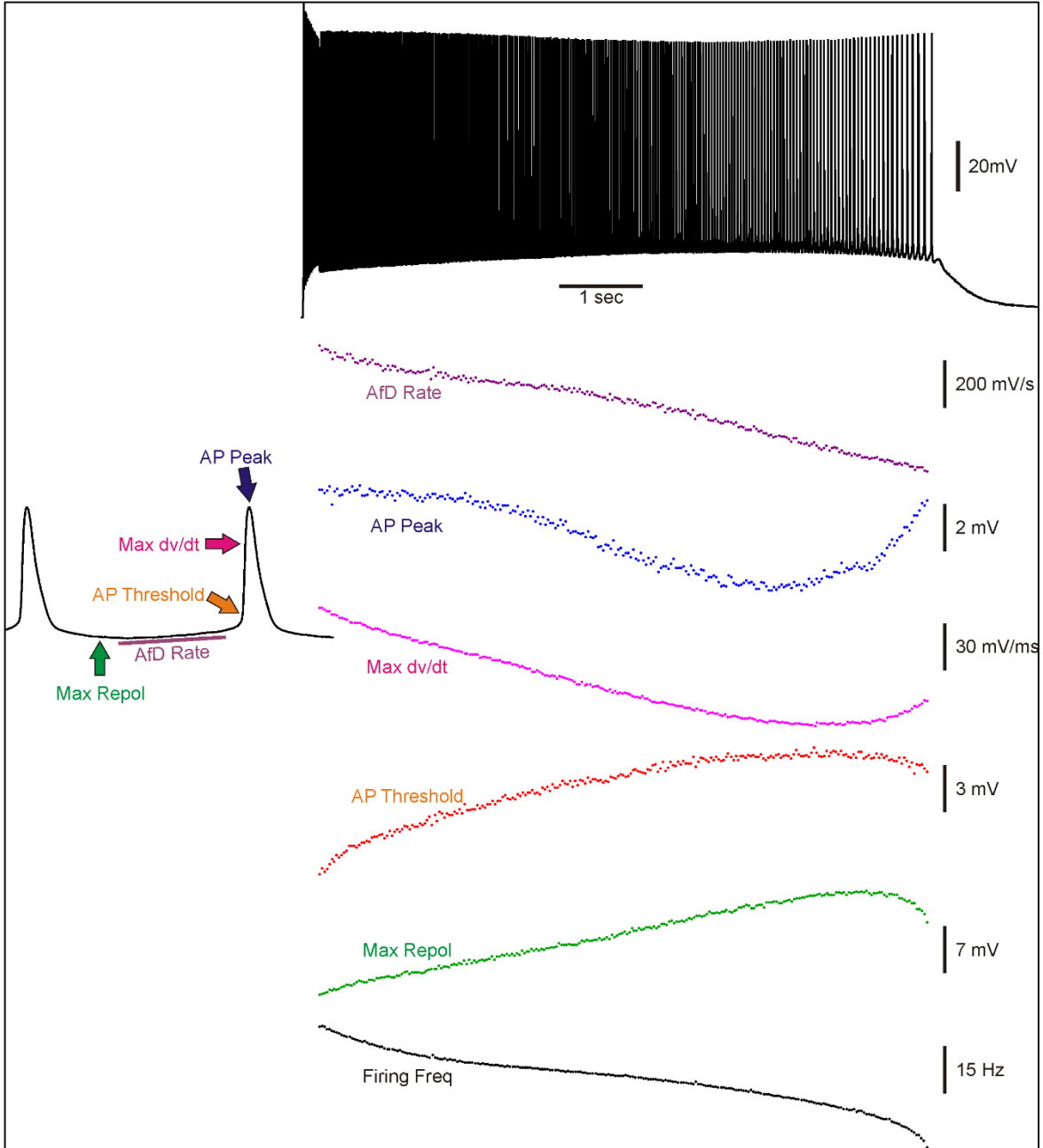
Fig. 1.6: Changes in AP parameters during a myotonic run.

Shown at the top is a 10-second run of myotonia triggered by a 200 ms stimulation. On the lower left is a blow-up of two APs from the middle of the myotonic run to demonstrate the AP parameters measured. On the lower right is a plot of the values of the various parameters, time-matched to the run of myotonia shown above. Termination of myotonia correlates with a reduction in the slope of the after-depolarization. AfD = after depolarization, AP peak = AP peak; Max dV/dt = the maximal rate of rise of the AP; AP thresh = AP threshold; Max Repol = the maximal repolarization reached between APs.
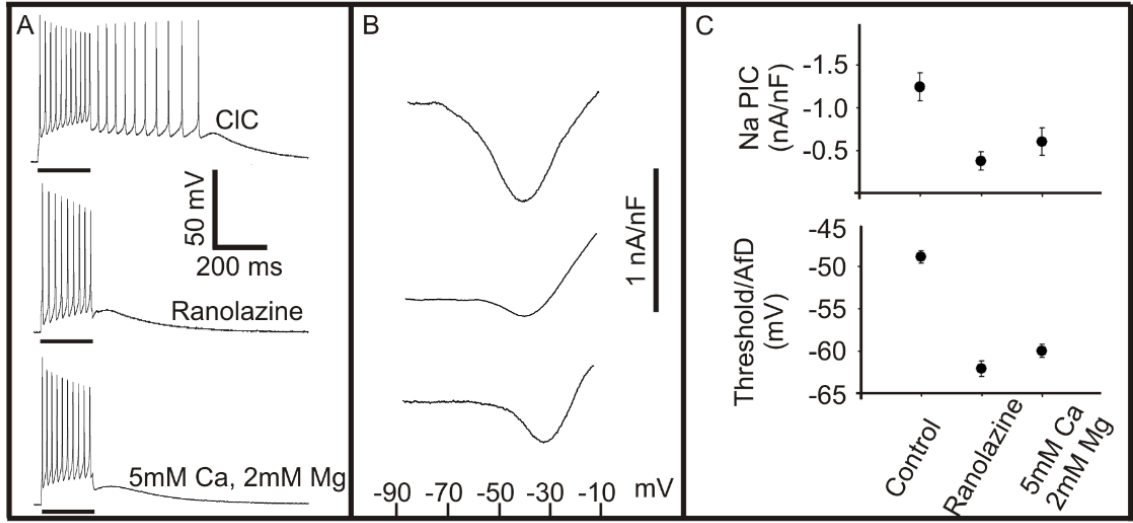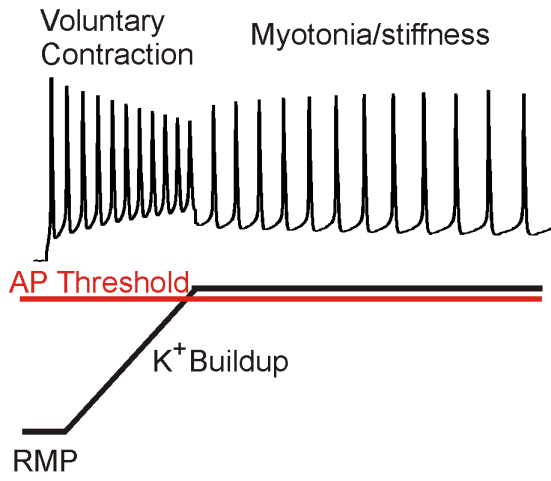
Fig. 1.7: Elimination of myotonia and parallel reduction of NaPIC by ranolazine, and divalent cation-treated ClC muscle.

(A) In untreated ClC muscle (top), myotonia is triggered with a 200ms depolarizing current pulse, whereas, 50μM ranolazine treatment (middle) and high extracellular divalent solutions (bottom) eliminate myotonia. **(B)** Representative NaPIC traces evoked by slow-depolarizing voltage ramps (similar to those shown in Fig. 2D) for untreated (top), ranolazine (middle), and elevated cation (bottom) groups. NaPIC current density is reduced by both ranolazine and elevated extracellular divalent concentration. **(C)** Top plot: ClC muscle (untreated) shows a maximal PIC current density of -1.25 ± 0.17nA/nF (n=23 fibers, 4 mice) vs. treatment with 50μM ranolazine (maximal PIC current density is reduced to -0.38 ± 0.11nA/nF; n = 20 fibers, 3 mice); and vs. elevated cation solutions (maximal PIC current density is decreased to -0.61 ± 0.16nA/nF; n = 25 fibers, 3 mice). Lower plot: Mean threshold of the first AP of a myotonic run of APs in ClC muscle (control) compared to the peak AfD following treatment with ranolazine and high divalent solution. Both treatments that eliminate myotonia cause the AfD to fail to reach the threshold at which myotonic firing is triggered in untreated, control muscle.

The differences between control and treatment groups were statistically significant as determined by one-way ANOVA.

K$^+$ buildup model

Voluntary Contraction   Myotonia/stiffness

AP Threshold

K$^+$ Buildup

RMP

NaPIC / K$^+$ buildup model

Voluntary Contraction   Myotonia/stiffness

AP Threshold
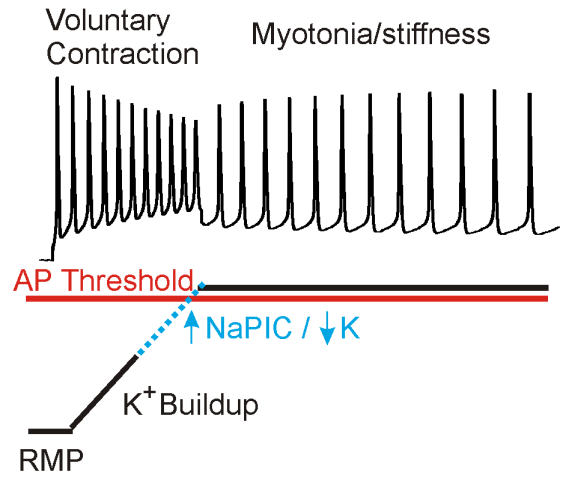
↑NaPIC / ↓K

K$^+$ Buildup

RMP

Fig. 1.8: A new model of generation of myotonia.

In the K^+ buildup model on the left, myotonia is triggered solely by a steady depolarization caused by K^+ buildup in t-tubules, which is sufficient to depolarize the membrane to the AP threshold and trigger myotonia. In the NaPIC and K^+ buildup model on the right, K^+ build-up is insufficient to trigger myotonia in isolation; but rather depolarizes the membrane sufficiently to activate NaPIC, which then contributes to the final depolarization that triggers myotonic APs.

Variable	Visit	N	Raw Mean / Median	Standard Deviation / Quartiles	Comparison to Baseline	95% Confidence Interval	p-value
Self-Reported Stiffness (0-9, 9=worst)	Baseline	13	5.46	2.18	0		
	Week 2	13	3.46	2.37	-2	(-3.42, -0.58)	0.0073
	Week 4	**12**	**2.08**	**1.73**	**-3.53**	**(-4.99, -2.07)**	**<0.0001**
	Week 5	13	6	2.45	0.54	(-0.89, 1.96)	0.4476
Self-reported Weakness (0-9, 9=worst)	Baseline	13	4.15	2.67	0		
	Week 2	13	3.23	2.45	-0.92	(-2.03, 0.19)	0.1005
	Week 4	**12**	**2.5**	**2.15**	**-1.81**	**(-2.95, -0.67)**	**0.0028**
	Week 5	13	5.08	2.6	0.92	(-0.19, 2.03)	0.1005
Self-reported Pain (0-9, 9=worst)	Baseline	13	4.08	3.01	0		
	Week 2	13	2.92	2.66	-1.15	(-2.42, 0.11)	0.0732
	Week 4	**12**	**2.42**	**2.61**	**-1.73**	**(-3.03, -0.43)**	**0.0107**
	Week 5	13	3.92	3.01	-0.15	(-1.42, 1.11)	0.8069
Hand Grip Opening Time (seconds)	Baseline	13	2.16	1.53	1		
	Week 2	13	1.75	0.47	0.91	(0.74, 1.13)	0.4045
	Week 4	**12**	**1.45**	**0.37**	**0.76**	**(0.61, 0.93)**	**0.0109**
	Week 5	13	1.91	0.89	0.94	(0.76, 1.16)	0.5928
Eyelid Opening Time (seconds)	Baseline	13	1.94	1.50	1		
	Week 2	13	1.81	0.90	1.000	(0.75, 1.32)	0.9919
	Week 4	**12**	**1.40**	**0.57**	**0.811**	**(0.60, 1.08)**	**0.1459**
	Week 5	13	1.73	0.66	0.980	(0.73, 1.30)	0.8747

Timed Up and Go (seconds)[b]	Baseline	12	9.99	3.36	1		
	Week 2	12	9.08	1.78	0.942	(0.84, 1.04)	0.2147
	Week 4	**11**	**8.68**	**1.59**	**0.887**	**(0.80, 0.99)**	**0.0318**
	Week 5	12	9.86	3.25	0.99	(0.90, 1.11)	0.8895
EMG Duration ADM[b] (microseconds)	Baseline	11	10082.73	13932.3	1		
	Week 4	**11**	**8582.55**	**14121.37**	**0.48**	**(0.35, 0.66)**	**0.0008**
EMG Duration TA[b] (microseconds)	Baseline	11	7159.09	7022.78	1		
	Week 4	**11**	**6288.27**	**6881.83**	**0.48**	**(0.29, 0.78)**	**0.0088**
EMG Frequency ADM[c] (0-15 insertions)	Baseline	13	13	(8, 15)	0		
	Week 4	**12**	**13**	**(2.5, 14)**	**1**	**(0, 3)**	**0.125**
EMG Frequency TA[c] (0-15 insertions)	Baseline	13	12	(6, 14)	0		
	Week 4	**12**	**11.5**	**(4, 14.5)**	**0.5**	**(-1, 3)**	**1**

Table 1.1: Results of symptom diary, clinical measures of muscle stiffness and mobility, and electrophysiology

Chapter V: Specific Aim II

Presence of a Ca Current Playing a Role in Producing Symptoms of Transient Weakness

The overall objective of Specific Aim II is to establish the presence of a Ca persistent inward current in myotonic muscle and describe its potential role in patient symptomology.

Introduction

Myotonia congenita patients complain of transient bouts of muscle weakness brought on by sudden movement after rest (Ferradini, Cassone et al. 2017). It appears after repetitive muscle contractions and improves with further contractions (Ricker, Haass et al. 1978). They are described to last seconds to minutes following episodes of muscle stiffness. It is known to be associated with a transient drop in compound muscle action potential amplitude, likely due to muscle inexcitability. Some patients report that transient weakness (in specific muscle groups) was a greater impediment than the stiffness (Rudel, Ricker et al. 1988). This weakness is not caused by failure of neuromuscular transmission (Ricker and Meinck 1972). Compound muscle action potentials (CMAPs) were shown to

fade with repetitive nerve stimulation. Decreases in muscle force measurements were also shown (Ricker, Meinch et al. 1973).

MC patients have been shown to be unable to sustain maximal muscle contraction for long periods of time. Isometric force measurements show maximal force on initial voluntary contraction, but a drop to a plateau afterwards (Rudel, Ricker et al. 1988).

An unanswered question is why patients experience transient weakness when myotonia congenita is believed to be a disease of muscle hyperexcitability. This novel behavior points to long periods of hypoexcitability and changes the view of this disease from one of strictly hyperexcitability to a constant flux between hyperexcitability and hypoexcitability, corresponding to patient symptoms of muscle stiffness and transient weakness.

Results

During current clamp recordings in Clcn1$^{adr-mto2J}$ (ClC) muscle, I discovered a novel behavior, not described in myotonic muscle before. In fact, this behavior was very reminiscent of behaviors seen in periodic paralysis, a skeletal muscle channelopathy caused by mutations in $Na_V1.4$ or $Ca_V1.1$. This incidental finding, seen during recordings of myotonic runs, was of great interest to me as the paralytic episodes seen in periodic paralysis have similarities to the weakness experienced by myotonia congenita patients.

This novel "hang" state, as I refer to it, lasts seconds to minutes. Spontaneous behaviors like this with no external stimulus led me to hypothesize that this behavior may be explained in part by the activation of a PIC. This PIC would not be the same NaPIC as

that described in the previous chapter. Although this current would have to be persistent (able to consistently pass current for extended time periods without inactivation), it would have a different voltage-dependence and amplitude than the NaPIC to play a role in this hanging behavior.

A novel source of depolarization would be needed to induce this "hang" state. A PIC would fit this requirement. I aimed to identify and characterize the current by using the following methods:

I. *To identify the characteristics of this depolarizing event,* I acquired current clamp recordings from myotonic muscle demonstrating the hang state and analyzed them.

II. *To identify the presence of a novel inward current that may play a role in "hanging",* I acquired voltage clamp recordings from myotonic muscle using a variety of protocols.

Discovery of the "hang" state in Clcn1$^{adr-mto2J}$ (ClC) muscle

Current clamp recordings were taken in ClC EDL muscle with protocols to induce myotonia. Specifically, 200 milliseconds of depolarizing current was injected into a muscle fiber, eliciting a myotonic run. Often, a myotonic run would lead into a hang state, as shown in Figure 2.1. Following a run of myotonia, the fiber spontaneously goes into a depolarized state or hang, rather than repolarizing towards the original resting membrane potential as seen in Figure 1. What determines whether a myotonic run will end as shown in Figure 1 or as shown in Figure 2.1 will be discussed later. **93.4%** exhibit

this hanging behavior following a myotonic run at least once while recording **(n=20 mice, 152 fibers)**. Myotonic fibers hang for **125.5 ± 10.1 seconds (n= 20 mice, 61 fibers)** before the spontaneous repolarization to RMP**.** The consistency of this finding in ClC muscle confirmed that this a reproducible, physiological behavior of the myotonic muscle, rather than irreversible damage caused by muscle damage due to muscle movement during the myotonic run. Further confirmation of this as a reproducible behavior, and not an artifact of damage is the return to the original resting membrane potential. If fibers were damaged due to the muscle movement, we would not see a return to resting membrane potential.

Figure 2.1 shows a rapid depolarization over a few myotonic action potentials to this depolarized hang state of **-26.4 ± 0.4 mV (n= 20 mice, 78 fibers)**. What this means for the individual muscle fiber is an absolute loss of excitability. At -26.4 mV, the transient $Na_V1.4$ channels responsible for initiating an action potential are almost completely inactivated and are unable to pass current (Rich and Pinter 2003; Novak, Nardelli et al. 2009). Figure 2.2 shows attempts to demonstrate this inexcitability by injecting larger and larger depolarizing currents during the hang state in an attempt to initiate an action potential, with no success. What is seen is a graded passive response of the membrane (depolarization proportional to current injected). A fiber in this hang state will not fire an action potential regardless of the strength of a synaptic input from the motoneuron innervating the muscle fiber. The muscle fiber is functionally paralyzed during this hang state. This finding led me to hypothesize that this novel behavior in myotonic muscle may be responsible for the episodes of transient weakness described by patients.

Another focus of Figure 2.1 is the demonstration of the repolarization from the hang state back towards RMP. This particular trace shows a spontaneous repolarization over the span of a few milliseconds. Prior to this repolarization or "pop-back", however, one can see a much slower repolarization during the hang state at a rate of **0.24 ± 0.1 mV/sec (n= 20 mice, 61 fibers)**. It is, as though, there is a slow repolarization of a few mV over seconds or minutes till the rapid pop-back over a few milliseconds. This pop-back only occurs at certain membrane potentials - always more hyperpolarized than the initial hanging potential. This value was measured to be **-38.9 ± 0.6 mV (n= 20 mice, 61 fibers)**. The initial hanging potential and the potential at which the fiber spontaneously repolarizes were compared via paired t-test and the difference was found to be statistically significant (p<0.001).

The repolarization can also be induced by a hyperpolarizing current injection. But the same rule applies. The membrane potential must be hyperpolarized with respect to the initial hang state membrane potential before it can be induced to pop back. If it has not yet reached that potential, a negative current pulse, regardless of amplitude (tested up to -100nA), will not induce a pop-back. This forced repolarization from the hang state is demonstrated in Figures 2.3 and 2.4. (n= 6 mice, 8 fibers)

Variations in the hang state

Of great interest is the variation in the pattern of events leading to the hang state and its resolution. Figure 2.5 shows five variations of myotonic runs leading into a hang state.

Hang states from ClC muscle differs in patterns of depolarization and repolarization. The rate of depolarization that triggers the hang state is not conserved, with periods of slow and rapid depolarization.

Typically, a fiber will begin to oscillate at some point during the hang state leading into a sudden repolarization towards RMP. The oscillations increase in amplitude with time and eventually lead into a spontaneous repolarization. These increasingly larger oscillations prior to spontaneous repolarization is consistent within each fiber

These variations tell me that the characteristics of the current underlying entry, duration, and resolution of the hang state can be modulated and may change due to several reasons.

The determinant of whether a myotonic run ends in a hang is the average membrane potentials achieved by the myotonic run.

Figure 2.6 shows two myotonic runs recorded from the same fiber minutes apart from each other.

Comparisons of myotonic runs ending in a hang state versus those ending in a conventional repolarization to the original RMP further reinforce that there is something fundamentally different about the myotonic runs. My focus was on measurements of the average membrane potential over the last second of the myotonic run. To account for any confounding factors that might differ between fibers, these analyses were done using a paired t-test (pairing of two myotonic runs in the same fiber). The two compared events had similar RMPs prior to 200ms current injection of similar magnitudes. Paired t-test revealed a significant difference in the average membrane potential of the last second of

the myotonic run (p < .001). Average membrane potential during the final second of

firing for conventionally ending myotonic runs was **-55.1 ± 1.5 mV** (n= 8 mice, 26 fibers)

while average membrane potential for myotonic runs ending in a hang was **-37.9 ± 1.2**

mV (n= 8 mice, 26 fibers). Paired t-tests revealed that this was a significant difference

(p<.001).

I hypothesized that the reason myotonic runs that do depolarize into a hang state do so

because the average membrane potential reaches the activation potential for a current that

is responsible for the hang state. On the other hand, if the average membrane potential is

not depolarized enough to activate this current (either a myotonic run is too short or fires

at too low a frequency), the fiber will repolarize towards RMP after the last myotonic AP

rather than go into a hang state.

Hang state is caused by the activation of an inward current.

The first question to address when attempting to understand the mechanism behind the

hang state is the nature of the depolarization. To depolarize the membrane potential, an

activated outward current may close or an inactive inward current may be activated. To

distinguish the two, I measured input resistance. Input resistance gives a good estimate of

the cumulative ion channel conductance of the fiber. Once steady-state is reached during

an input resistance pulse, one can assume that no voltage-dependent currents are opening

or closing during the pulse.

Figure 2.3 also shows responses to constant current injection – measurements of input

resistance both during the hang state and after repolarization to the RMP. Measurements

were only included in the data set if steady-state was achieved during the input resistance pulse, ensuring that no voltage-dependent channels were opened or closed during the measurement. Input resistance during the hang state was decreased during the hang state when compared to RMP.

Input resistance during the hang state was **0.50 ± 0.06 MΩ** while input resistance at RMP was **0.90 ± 0.12 MΩ** (n= 4 mice, 13 fibers). A paired t-test revealed a significant difference in the input resistance (p < .01). This finding led me to hypothesize that a channel is open during the hang state that is not open at RMP. This channel is likely to also be responsible for entry into the hang state.

Depolarizing current plays a role in inducing the "hang" state.

With the previous observations, I concluded that a depolarizing current is likely playing a central role in inducing the hang state. Upon closer inspection of the current clamp recording, as seen in Figure 2.1, one can get an idea of the characteristics of a depolarizing current that would be responsible for a hang state.

i. Voltage-dependence: A depolarizing current involved in the hang state would need to activate at a mean membrane potential that triggers the hang state. Based on Figure 2.6, the fiber's average membrane potential depolarizes slowly over seconds during a myotonic run, till it is depolarized to a potential able to activate this current. Only then can the fiber enter the hang state. The membrane potential at which the sudden repolarization takes place suggest a voltage at which many of these channels are closing.

74

ii. Amplitude: A depolarizing current involved in the hang state would need to be able to depolarize the muscle fiber from the maximal repolarization during a myotonic run towards the hanging start potential of -26.4 mV. The amplitude of this current must be relatively large, as compared to the NaPIC described in the previous chapter.

iii. Kinetics: The slow kinetics of activation and apparent lack of fast inactivation were pointing me in the direction of a PIC once again. The hang state varies in duration before spontaneous repolarization, but lasts **125.5 ± 10.1 seconds (n= 20 mice, 61 fibers)** on average. For a depolarizing current of this magnitude to not inactivate and continue to pass current for that long a period, it would likely be resistant to fast inactivation and have very slow kinetics. This led me to search for another PIC, aside from the NaPIC described earlier.

Presence of another persistent inward current in myotonic skeletal muscle.

Similar voltage clamp ramp protocols were used to characterize this PIC as those used in the previous chapter. The major differences are in the membrane potentials used. Ramp protocols were used, depolarizing from -85mV to +20mV at a rate of 10mV/sec. Based on the characteristics of the hang seen in the current clamp records, this PIC will have a larger amplitude and more depolarized voltage of activation than the previously described NaPIC.

During voltage clamp ramp protocols, one can first see the activation of the NaPIC studied earlier followed by the activation of a larger PIC that activates at a more

depolarized potential. Figure 2.7 shows this larger PIC clearly. Based on ramp protocols, this PIC activates at a membrane potential of **-18.3 ± 1.8 mV** and reaches its maximum at **24.2 nA/nF** at **-2.8 ± 1.5 mV (n= 12 mice, 32 fibers)**.

Rectangular voltage clamp protocols were also used in the study of this PIC, as it was large enough to clearly distinguish from the background currents. This is shown in Figure 2.8. Based on rectangular protocols, this PIC has a maximal amplitude of **30.5 ± 5.4 nA/nF** at **-5 mV (n= 7 mice, 15 fibers)**.

With a current density of this magnitude and voltage-dependence, this PIC is likely responsible for the depolarization leading to the hang state.

This PIC likely passes through the L-Type Ca Channel.

Voltage clamp PIC recordings showed the following results:

    i.   Nifedipine (20 µM): Nifedipine is a dihydropyridine blocker, used clinically for hypertension and angina. It is known to block L-Type Ca channels, including $Ca_V1.1$ (Jorquera, Altamirano et al. 2013). At 20 µM concentration, nifedipine largely blocks the PIC of interest as shown in Figure 2.9.

    ii.   Verapamil (100 µM): Verapamil is a non-dihydropyridine blocker, used clinically as an anti-arrhymtic agent. It is also known to block L-Type Ca channels, including $Ca_V1.1$ (Striessnig, Bolz et al. 2010). At 100 µM concentration, verapamil largely blocks the PIC of interest as shown in Figure 2.10.

iii. Bay-K (20 µM): Bay-K is an L-Type Ca channel activator, including

$Ca_V1.1$ (Jorquera, Altamirano et al. 2013). It acts by increasing the open

probability over a certain voltage range and increasing open time (Hadley

and Hume 1988). At 20 µM concentration, Bay-K enhances the PIC of

interest as shown in Figure 2.11.

Based largely on the pharmacological findings, this PIC passes through the L-Type Ca

channel. Specifically, this PIC likely passes through the $Ca_V1.1$ channel, as it is the main

L-Type Ca channel in the skeletal muscle, playing a necessary role in the excitation-

contraction coupling (Catterall 2011).

Nifedipine decreases the frequency of the hanging behavior

After recognizing that this PIC appears to pass through the L-Type Ca channel and is

susceptible to nifedipine as a blocker, I decided to check on the effect of nifedipine on the

hanging behavior directly. This would show a more direct relationship between the

properties of this PIC and the effect it has on myotonic muscle. I have previously

demonstrated that myotonic muscle goes into the hang state frequently and for long

durations.

Upon treatment with 10µM nifedipine, the frequency of hanging was decreased from

93.4% (n=20 mice, 152 fibers) to **25.0% (n=3 mice, 24 fibers)**. This finding provides a

clear link between the Ca PIC and the hanging behavior.

Wild-Type muscle exhibits similar behaviors and currents.

Wild-type muscle, made acutely myotonic by 9-AC treatment, taken from asymptomatic littermates of the CLCN1$^{adr-mto2J}$ mice, exhibit similar hanging behavior after myotonic runs, as shown in Figure 2.12. The most significant difference between CLCN1$^{adr-mto2J}$ muscle and WT muscle treated with 9-AC is the length of the hang period.

The hang state of myotonic WT muscle is briefer in duration than that of CLCN1$^{adr-mto2J}$ muscle, never exceeding 5 seconds before the sudden repolarization towards RMP. On average, myotonic WT muscle hangs for of **1.1 ± 0.1 sec (n=5 mice, 26 fibers)**. In stark contrast, CLCN1$^{adr-mto2J}$ muscle hangs for **125.5 ± 10.1 seconds (n= 20 mice, 61 fibers)**.

This difference in hang duration is likely related to the slope with which the hang repolarizes before it pops back towards RMP. Analyses show that the hang of WT muscle has a sharper slope and repolarizes during the hang more quickly at a rate of **10.8 ± 1.1 mV/sec (n=5 mice, 26 fibers)**. This would mean that the fiber is reaching that critical membrane potential for the sudden repolarization towards RMP more quickly, ending the hang phase. ClC myotonic muscle shows a much slower repolarization during the hang state at a rate of **0.24 ± 0.1 mV/sec (n= 20 mice, 61 fibers)**.

<u>Discussion</u>

Myotonia congenita patients often complain of transient bouts of muscle weakness, especially with movement after a resting period. The mechanism by which this dysfunction comes about is not understood. The specificity of the weakness after sudden

movement is very interesting. Sudden movement, especially after rest, will lead to a myotonia in ClC muscle as the muscle is not "warmed up."

Similarities to Periodic Paralysis

Myotonia congenita patients, specifically those with the autosomal recessive type, often complain of transient episodes of weakness. This complaint has similarities to a major complaint made by patients who suffer from a different skeletal muscle channelopathy called periodic paralysis. Episodic muscle weakness is a hallmark clinical sign for periodic paralysis (Statland and Barohn 2013; Al-Ghamdi, Darras et al. 2017).

Periodic paralysis is a disease of the skeletal muscle, causing transient episodes of muscle weakness/paralysis when triggered. This disease is very rare in the US. There are many subtypes of periodic paralysis but they all share a commonality of transient, triggered episodes. The subtypes are classified using various criteria, most commonly by episode trigger.

Periodic paralysis is further broken down depending on the causative mutation. The causative mutations are all ones of ion channels of the skeletal muscle. Periodic paralysis can be caused by mutations in the L-Type Ca channel ($Ca_V1.1$), the voltage-gated Na channel ($Na_V1.4$), the potassium inward-rectifier channel (Kir 2.1), and others. The most common mutation seen in patients is the R528H missense mutation of the $Ca_V1.1$ channel, responsible for about 30% of Periodic paralysis cases (Cannon 2010; George 2012; Wu, Mi et al. 2012; Cannon 2015). Specifically, this mutation produces a gating

pore, that allows for a substantial depolarizing gating pore current (Wu, Mi et al. 2012). This current is large enough to keep the membrane potential of a muscle fiber inexcitable (by Na channel inactivation) for minutes to hours, until the initiating trigger (most commonly decreased serum K levels) is alleviated.

A key difference between the two periods of inexcitability must be a property of the underlying channel kinetics, specifically slow inactivation. In periodic paralysis, the underlying current likely lacks slow inactivation, as an episode of weakness can last hours until the initiating trigger is resolved. In myotonia congenita, periods of weakness generally last much shorter periods, on the order of minutes. The reason for this is that the CaPIC, implicated in triggering the hang state, exhibits slow inactivation, making the attacks much shorter.

Discovery of the hang state in ClC muscle gives us great insight into the complaint of weakness among MC patients. Indeed, ClC fibers stay depolarized for extended periods of time, leaving the fast Na channels in an inactivated state just as periodic paralysis muscle fibers do. Reductions in CMAP amplitudes have also been demonstrated in both models, further pointing to similarities in the end behaviors of these diseases with differing depolarizing events leading to this state.

Activation and Inactivation of the CaPIC

I have concluded that the fate of a myotonic run (whether or not it would end in a hang state) was determined by the average membrane potential during the myotonic run. CaPICs in neurons are known to activate very slowly and then persist. A quick

depolarization to the activation potentials needed for CaPIC activation alone is not enough to activate the PIC. It needs to be an prolonged period of depolarization (Hounsgaard and Kiehn 1989; Alaburda, Perrier et al. 2002). Therefore, I conclude that the CaPIC is activating in response to the depolarized average membrane potential. When the average membrane potential is equal to or greater than the activation threshold for the PIC, the CaPIC will activate and begin to pass current, depolarizing the cell further and further till it reaches a new steady-state membrane potential – the hang.

The CaPIC must also be susceptible to some sort of inactivation which would explain the end of the hang state. Its identification on ramp protocols and persistence during rectangular protocols mean that it does not fast inactivate but both protocols show that it does slow inactivate. More experiments should be done to explore the exact kinetics of the slow inactivation via rectangular protocols, but my recordings show that it is on the order of seconds, not milliseconds. This likely plays a role in the slow repolarization during the hang and the sudden repolarization that ends the hang.

Discrepancies between CaPIC and Hanging Behavior

I have implicated the CaPIC as the major component in triggering the hang state. Upon closer investigation, however, one may notice two discrepancies. The first is that the CaPIC's activation potential does not necessarily match that of the starting hang potential. The second is that CaPIC slow inactivates over seconds (although more should be done to confirm this) while the hang in myotonic muscle lasts for over a minute on average. One reason for this mismatch is the difference in muscles used for current clamp

and voltage clamp experiments. The EDL is a much larger and more robust muscle than the smaller, more fragile FDB/IO muscles. But that very fact is what makes the FDB/IO muscles suitable for voltage clamp experiments (able to space clamp the shorter fibers). Additionally, the voltage clamp preparation involves 20 minutes of dialyzing the intracellular solution to buffer Ca using EGTA to eliminate contraction during recordings. Although this allows us to record from damaged fibers, this will have a significant effect on free Ca concentrations in the cell, and will therefore have effects on the voltage-dependence and kinetics of the recorded current. There is evidence that the Ca channel current activation and inactivation properties have a dependence on intracellular Ca concentrations in cardiac muscle (Lee, Marban et al. 1985) and in skeletal muscle (Donaldson and Beam 1983). It has also been shown that the decay of slow calcium currents in frog muscle fibers is influenced by intracellular EGTA (Francini and Stefani 1989). Additionally, calcium currents have been shown to have a temperature dependence (Cota, Nicola Siri et al. 1983; Donaldson and Beam 1983).

Nifedipine as a Therapy for Patient Weakness

At first glance, one may think that nifedipine then provides a therapeutic option for myotonia congenita patients, specifically for their complaints of transient weakness. Unfortunately, this is not the case. Nifedipine acts on most L-Type Ca channels throughout the body, not only those in the skeletal muscle. At 10 μM doses, nifedipine would block the L-Type Ca channels of the heart and smooth muscle of the vasculature too much because they are more sensitive to the drug.

Nifedipine reduced the hanging behavior to 25% of ClC fibers only. This finding was perplexing as nifedipine significantly blocked the CaPIC under voltage clamp, yet did not completely eliminate the hanging behavior.

Pharmacologic studies always suffer from issues of drug dosing and delivery. To address this issue, future studies of hanging will be performed in mice with a mutation in the pore region of $Ca_V1.1$, eliminating ion passage through the main pore. I hypothesize that these mice will show no evidence of a CaPIC. Crossing these mice with the ClC mice should produce offspring that show no hanging behavior nor CaPIC. This finding would directly confirm the CaPIC role in the hanging behavior.

Differences between WT and ClC Hanging Behavior

While I do not know the mechanism underlying the differences in the hang state of WT muscle vs ClC muscle, there are some potential mechanisms to be explored in the future. This is of great interest as both muscles have genetically normal Ca channels and would be expected to behave similarly. This may be explained by some compensatory mechanism of the mutant muscle during development, where Ca channels are downregulated. Another potential explanation is a difference in K current passing through the BK channel. BK channels open in response to increases in intracellular Ca levels (Kim, Kim et al. 2014). If a CaPIC is activated, increasing intracellular Ca levels, it may activate a robust BK current response, strongly counteracting the hang state and repolarizing faster. Activation of large-conductance K channels have been shown to lead to membrane hyperpolarization (Latorre and Brauchi 2006).

Alternate Roles of the CaPIC

Another area of interest is the potential downstream effects of such a large Ca influx. Ca acts as a secondary messenger. This is a large flux of Ca as it is of large magnitude and stays open for very long (seconds). This rise in cytosolic Ca is very different than that experienced by the muscle fiber in response to a single AP. The depolarization during a single AP is known to activate $Ca_V1.1$. $Ca_V1.1$ is recognized to have a mechanical relationship with the RYR1. When $Ca_V1.1$ is activated, it opens the RYR allowing for Ca stores to be released from the sarcoplasmic reticulum. This, in turn, will lead to a contraction of the muscle fiber. This mechanism is what's responsible for excitation-contraction coupling (Cherednichenko, Hurne et al. 2004). The Ca is then resequestered and returned to the sarcoplasmic reticulum rapidly to prepare the stores for a following action potential.

The CaPIC is a previously unrecognized function of $Ca_V1.1$. As stated earlier, the CaPIC requires an elongated depolarization to activate. Physiologically, this would only occur with high-frequency firing of action potentials, which would lead to a depolarized average membrane potential. The only times a muscle fiber would reach a rapid enough firing frequency to achieve such a depolarized average potential is with maximal effort, as seen in weightlifting and progressive resistance exercise.

Keeping in mind Ca's role as a secondary messenger, I hypothesize that this CaPIC is involved in the muscle hypertrophy pathway. With further investigation, the CaPIC may prove to be a target for treatment against muscle-wasting disorders. Gain-of-function

mutants of L-Type Ca channels have previously been shown to have a bulky phenotype/body in C. elegans models (Lee, Lobel et al. 1997; Laine, Segor et al. 2014).

With these findings and confirmation of this hypothesis, I will have added to the field's view of the role of the L-Type Ca channel in skeletal muscle and its current's role in physiological pathways. This PIC may also be involved in Ca signaling and replenishment of Ca stores for the muscle fiber (Bannister and Beam 2013). This is in addition to $Ca_V1.1$'s known role as a voltage sensor to open the RYR to release Ca from SR stores (Tanabe, Beam et al. 1988).

Another physiological role of this CaPIC may be a response to depletion of Ca within the sarcoplasmic reticulum to allow Ca entry through the plasma membrane in order to refill SR stores. This mechanism has been described as SOCE or store-operated Ca entry (Cherednichenko, Hurne et al. 2004).
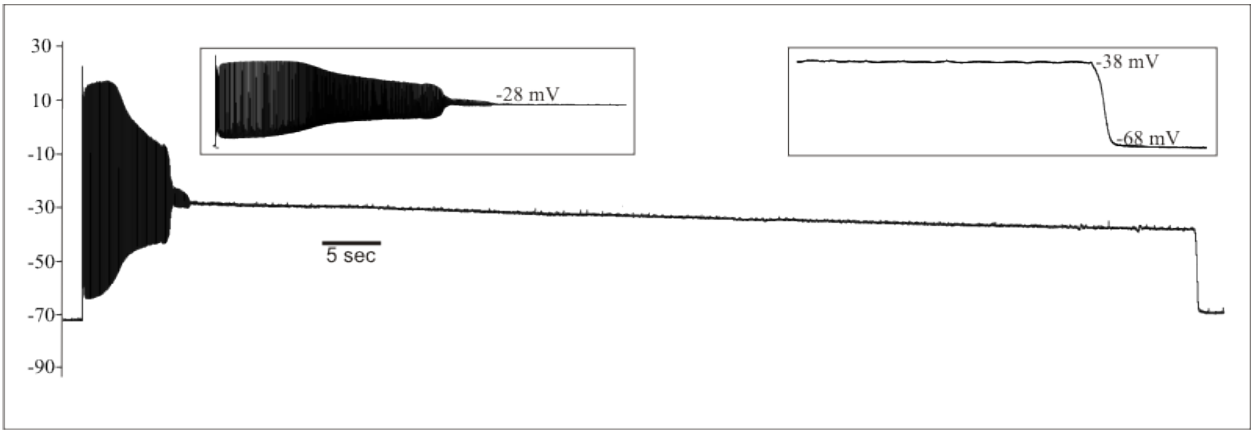
Figure 2.1: Myotonia leads into a hang state before returning to resting membrane potential

A run of myotonia, induced by a 200ms injection of depolarizing current, does not immediately return towards baseline after the last myotonic AP. The fiber spontaneously enters an extended period of depolarization and remains there for seconds. Over seconds, there is a slow repolarization. This is followed by a sudden, spontaneous repolarization towards resting membrane potential. This extended period of depolarization is referred to as the hang state.

The hang begins at **-26.4 ± 0.4 mV (n= 20 mice, 78 fibers)** and spontaneously repolarizes from **-38.9 ± 0.6 mV (n= 20 mice, 61 fibers)** to **-67.9 ± 0.9 mV (n= 20 mice, 51 fibers)**. Over seconds, the RMP repolarizes towards the RMP pre-myotonic run, presumably through the Na/K pump activity.
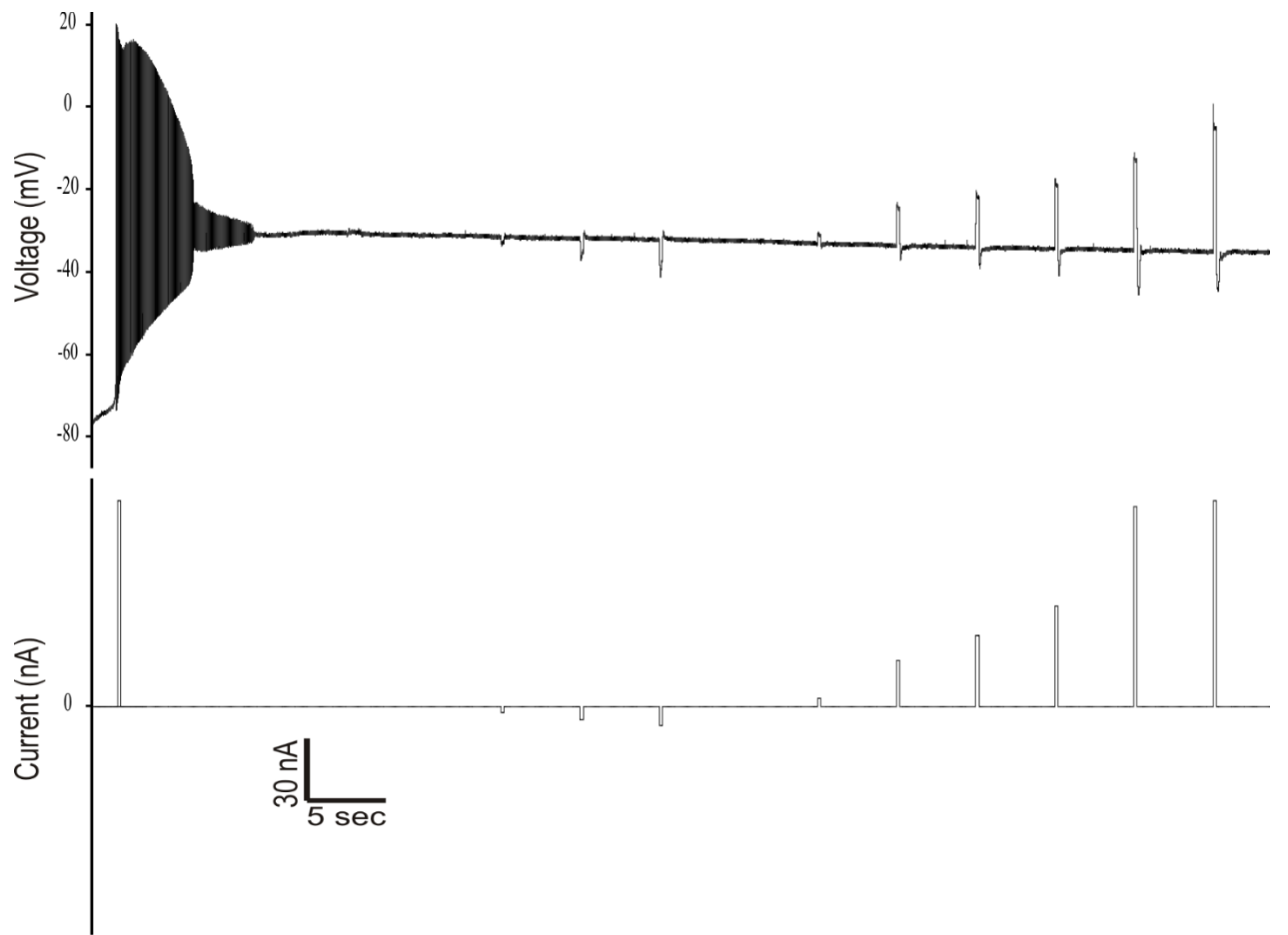
Figure 2.2: Inexcitability during hang periods

Shown is a myotonic run that leads into a hang state. During the hang state, depolarizing current is injected of varying amplitudes in an attempt to trigger action potentials. No action potentials can be triggered regardless of the current amplitude injected, demonstrating the inexcitability of the muscle fiber while in the hang state.
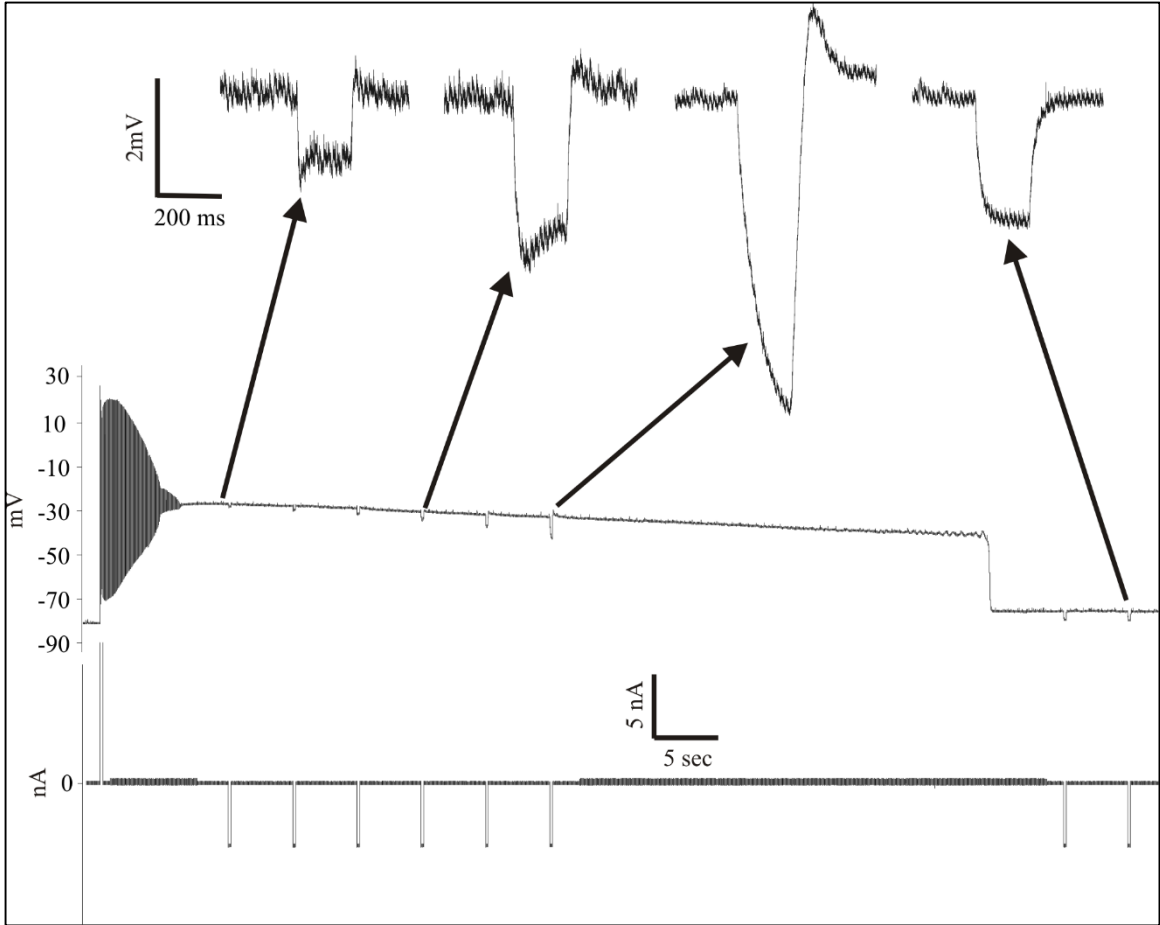
Figure 2.3: *Input Resistance during hang state is less than Input Resistance at RMP.*

Repolarization to RMP can be triggered by a hyperpolarizing current injection

Hyperpolarizing current injections were repeated throughout the slow repolarization of the hang state. All current injections were of the same amplitude and duration. Only when the hang state was repolarized enough was the current injection able to force repolarization from the hang state towards RMP. This shows the voltage-dependence of the sudden repolarization.

n= 4 mice, 13 fibers. A paired t-test revealed a significant difference in the input resistance ($p < .01$)
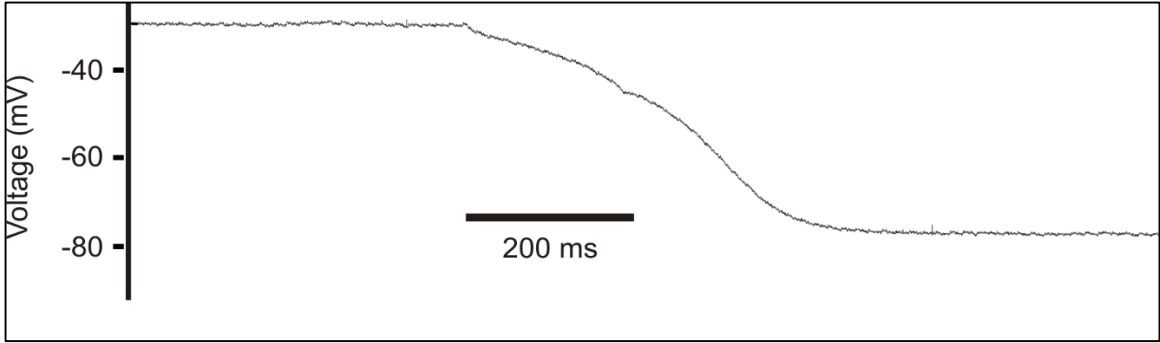
Figure 2.4: Induced recovery from hang state

Hang state can be triggered to repolarize to RMP with a current stimulus, demonstrating that the underlying current responsible for the hang is voltage-dependent.
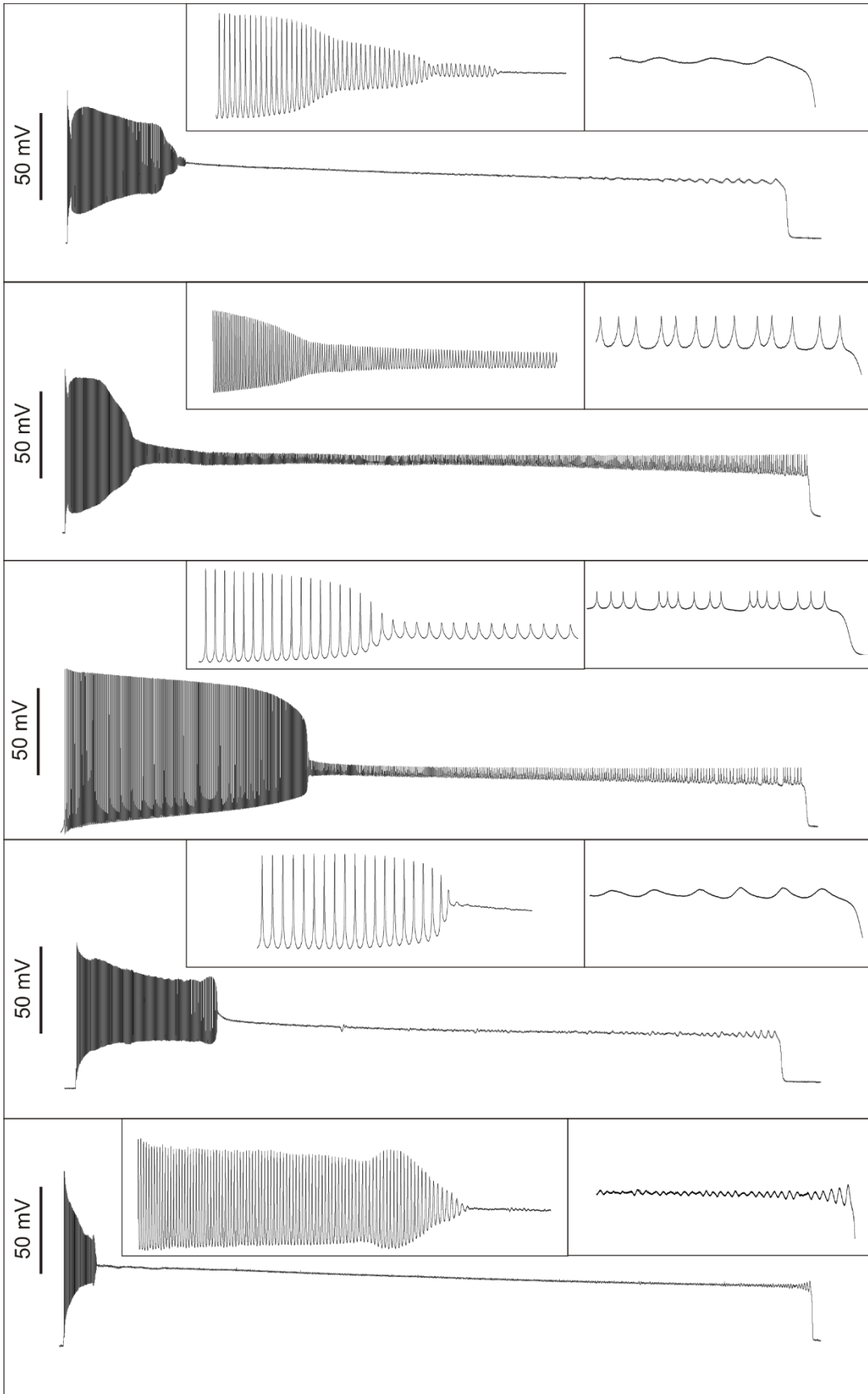
Figure 2.5: *Hang states present in different patterns*

Hang states from ClC muscle differ in pattern of depolarization and repolarization. The rate of depolarization that triggers the hang state is not conserved, with periods of slow depolarization and rapid depolarization.
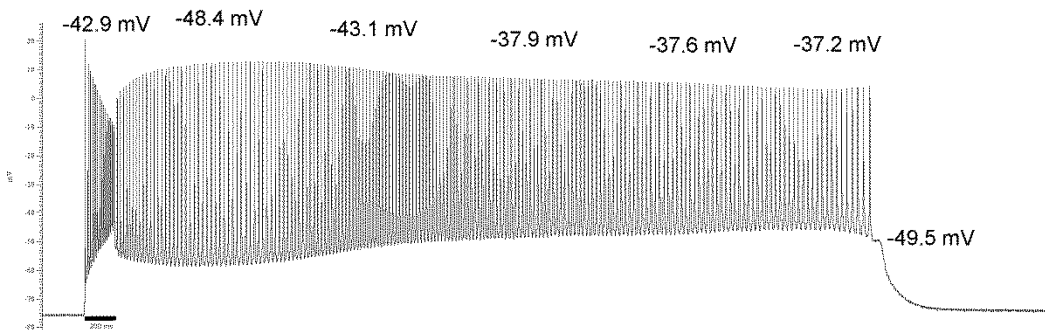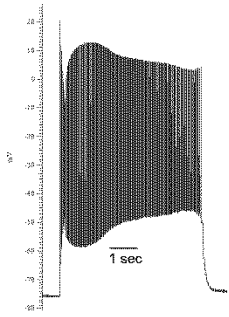
-42.9 mV   -48.4 mV   -43.1 mV   -37.9 mV   -37.6 mV   -37.2 mV

-49.5 mV

-41.1 mV   -45.0 mV   -39.0 mV   -35.4 mV   -34.0 mV

-29.9 mV

-24.3 mV
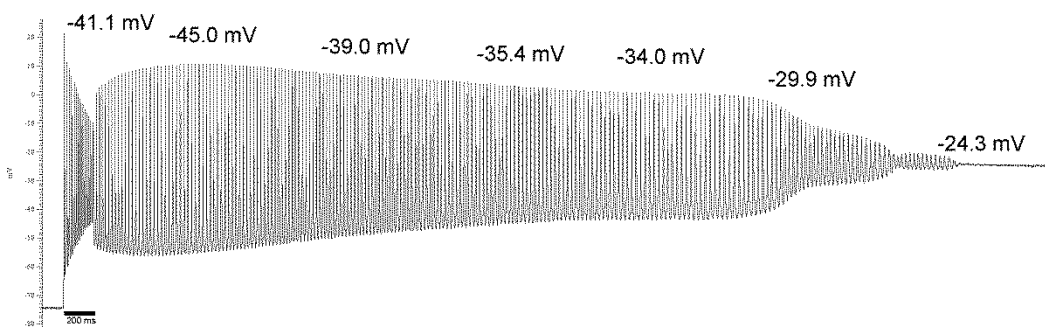
Figure 2.6: *Myotonic runs end in a hang state only if the average membrane potential is depolarized enough.*

Shown are two myotonic runs taken from the same fiber. Prior to stimulation by 200ms current injections, Above the myotonic run traces are average membrane potentials over a one second span.

The top myotonic run does not end in a hang state and reaches an average membrane potential of **-55.1 ± 1.5 mV** (n= 8 mice, 26 fibers). The bottom myotonic run, which results in a hang, reaches an average membrane potential of **-37.9 ± 1.2 mV** (n= 8 mice, 26 fibers) immediately prior to the hang.

Similar analyses (comparison of average membrane potentials of 2 myotonic runs in the same fiber) was done on 26 fibers from 8 mice. A paired t-test, comparing the average membrane potential of the last second of a myotonic run,was performed yielding a $p<.01$.
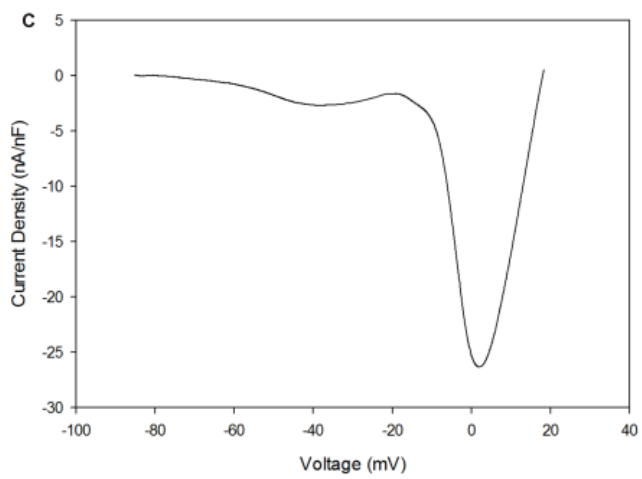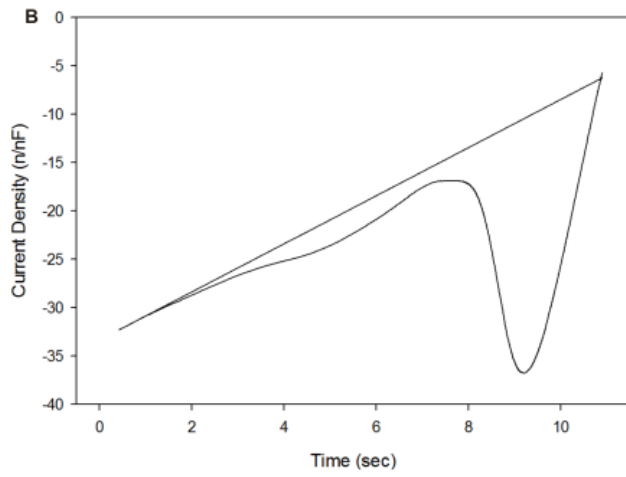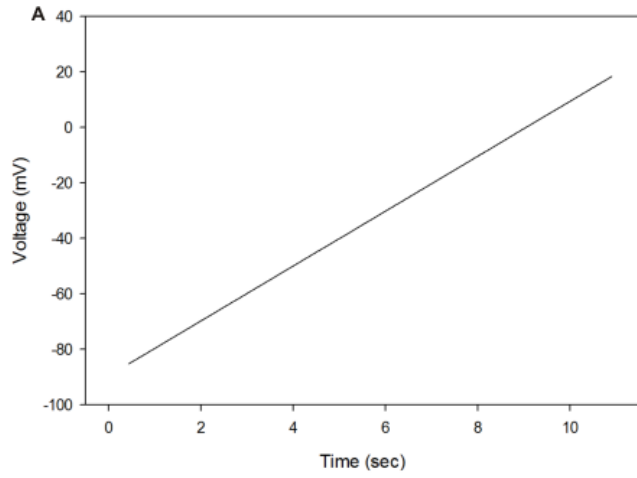
Figure 2.7: Ramp protocols showing another PIC that is larger and activates at a more depolarized potential than the NaPIC.

A representative ramp voltage clamp record from a CLCN1[adr-mto2J] fiber showing activation of two distinct PICs. From a holding potential of -85mV, the fiber is depolarized to +20 mV at a rate of 10mV/sec.

A PIC, in addition to the NaPIC, is seen to activate at **-18.3 ± 1.8 mV** and reach its maximum amplitude of **24.2 ± 3.4 nA/nF** at **-2.8 ± 1.5 mV** (n= 12 mice, 32 fibers)
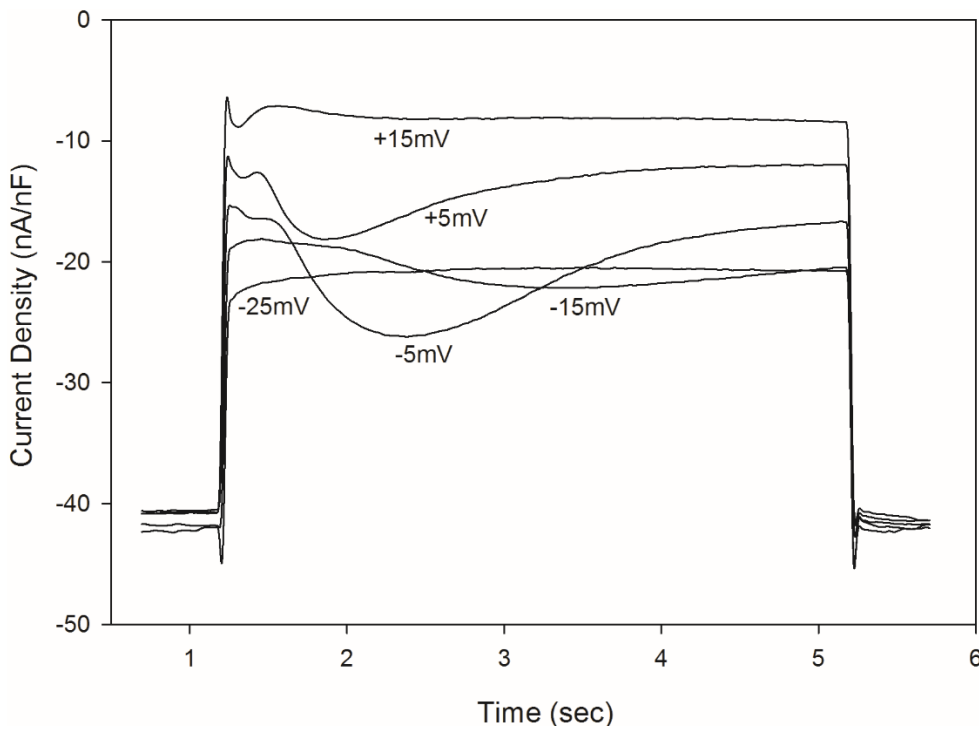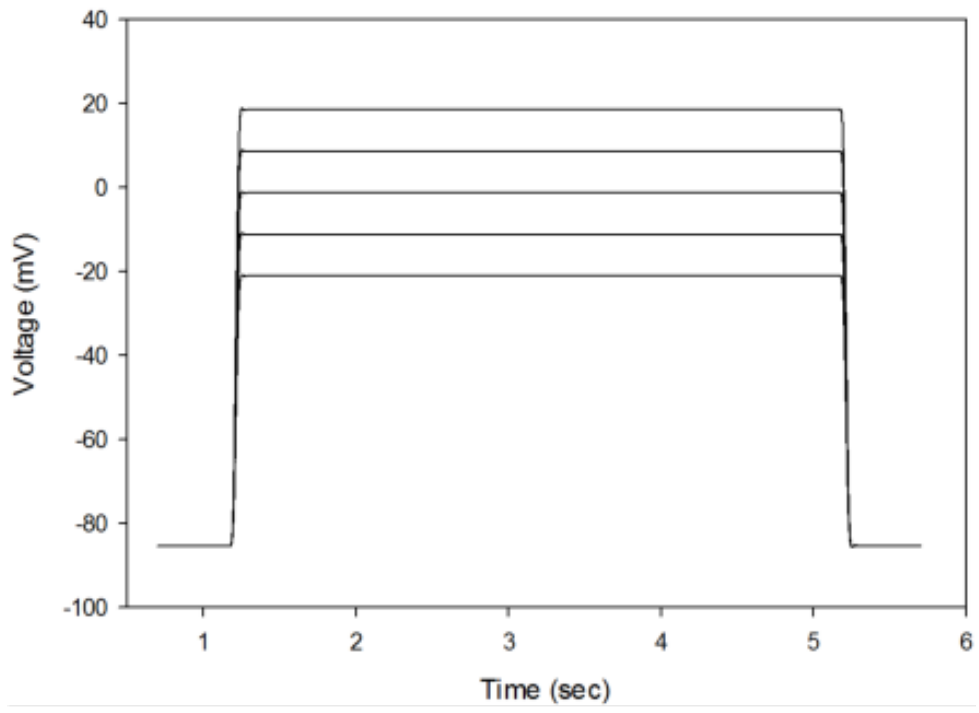
Fig 2.8: Rectangular protocols showing the CaPIC

A representative rectangular voltage clamp record from a CLCN1$^{adr-mto2J}$ fiber showing activation of a PIC. Voltage steps are taken from a holding potential of -85mV to -25, -15, -5, +5, and +15mV for 4 seconds.

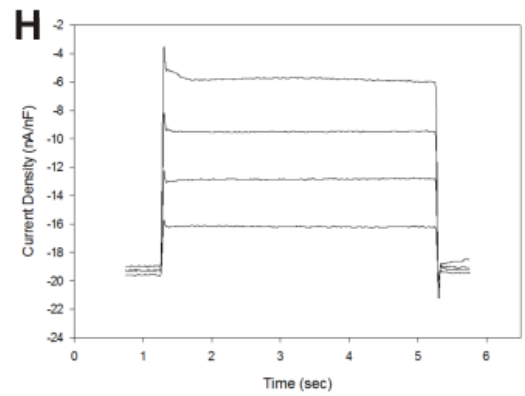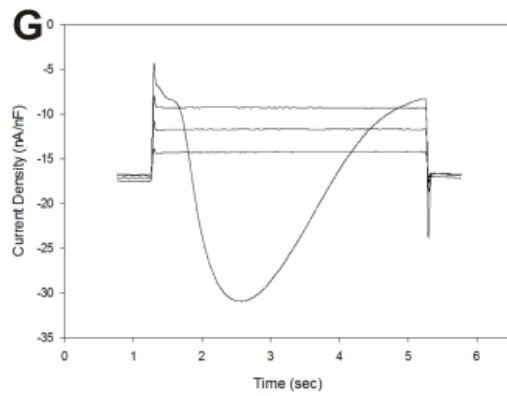Maximal PIC activation is seen during the -5mV step at 30.5 ± 5.4 nA/nF (n= 7 mice, 15 fibers).
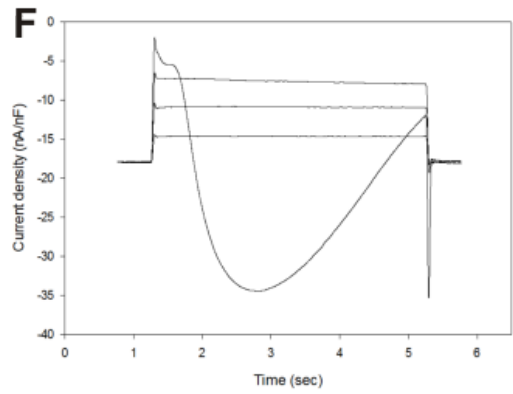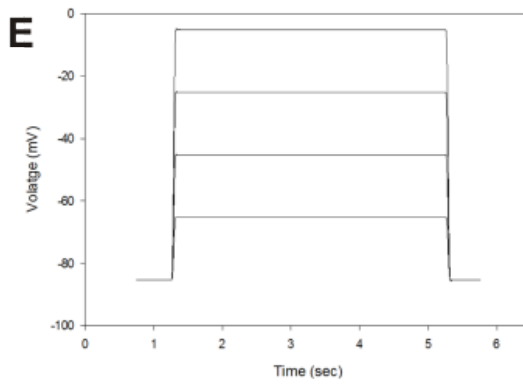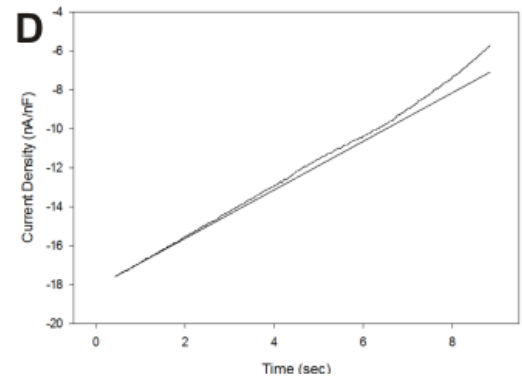
Fig 2.9: Nifedipine blocks the CaPIC

A single CLCN1$^{adr-mto2J}$ fiber is run through multiple voltage protocols with addition of drugs. This is a representative fiber.

A. Ramp voltage protocol used to identify CaPIC. From a holding potential of -85mV, the fiber is depolarized to 0mV at a rate of 10 mV/sec.

B. Current trace generated by voltage protocol. A fit line is drawn using the first 0.5 seconds of the raw trace.

C. Addition of 1 µM TTX blocks NaPIC

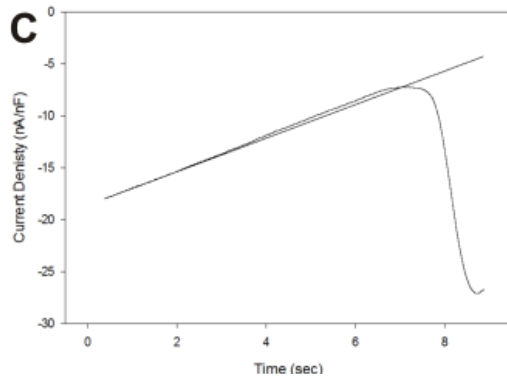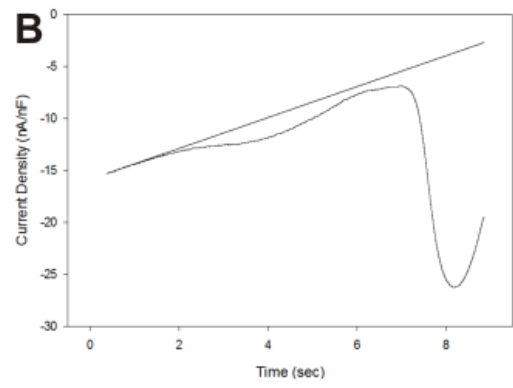D. Addition of 20 µM Nifedipine blocks CaPIC

E. Rectangular voltage protocol used to identify CaPIC. From a holding potential of -85mV, the fiber is depolarized to different potentials for 4 seconds.

F.   Current trace generated by voltage protocol. CaPIC is seen to activate at -5mV step.

G. Addition of 1 µM TTX blocks NaPIC

H. Addition of 20 µM Nifedipine blocks CaPIC

n = 3 mice, 9 fibers

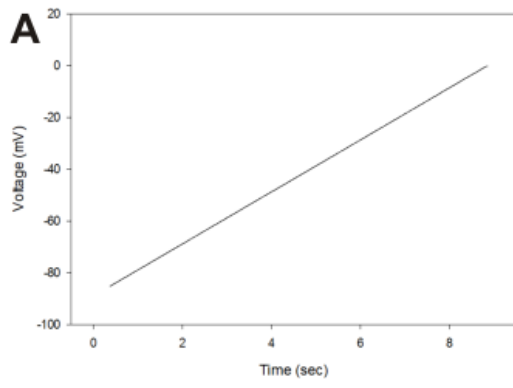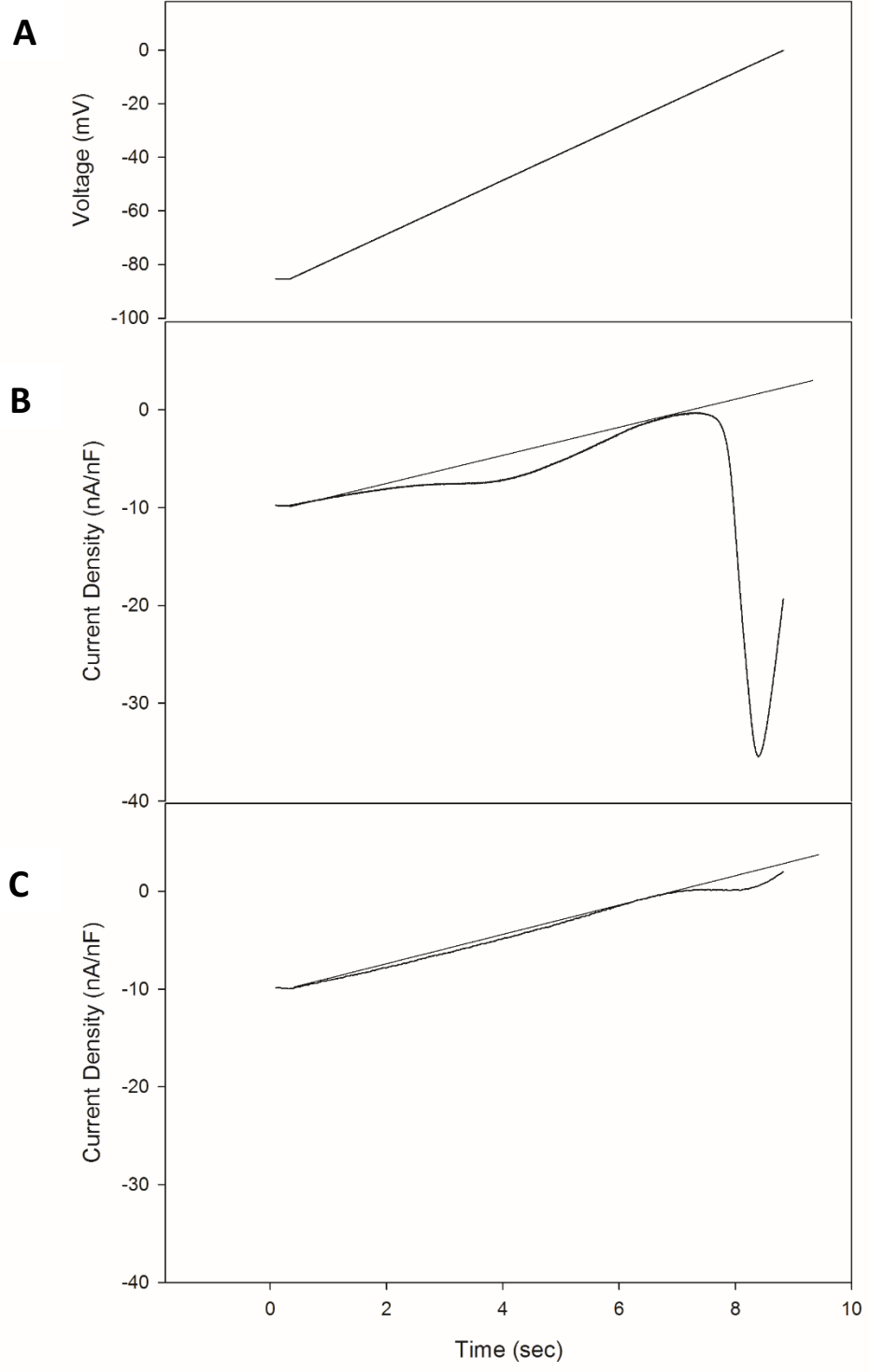***Fig 2.10: Verapamil blocks the CaPIC***

A single CLCN1$^{adr-mto2J}$ fiber is run through multiple voltage protocols with addition of drugs. This is a representative fiber.

A. Ramp voltage protocol used to identify CaPIC. From a holding potential of -85mV, the fiber is depolarized to +10mV at a rate of 10 mV/sec.

B. Current trace generated by voltage protocol. A fit line is drawn using the first 0.5 seconds of the raw trace.

C. Addition of 100 μM Verapamil largely blocks CaPIC

D. Rectangular voltage protocol used to identify CaPIC. From a holding potential of -85mV, the fiber is depolarized to different potentials for 4 seconds.

E. Current trace generated by voltage protocol. CaPIC is seen to activate at -5mV step.

F. Addition of 100μM Verapamil largely blocks CaPIC
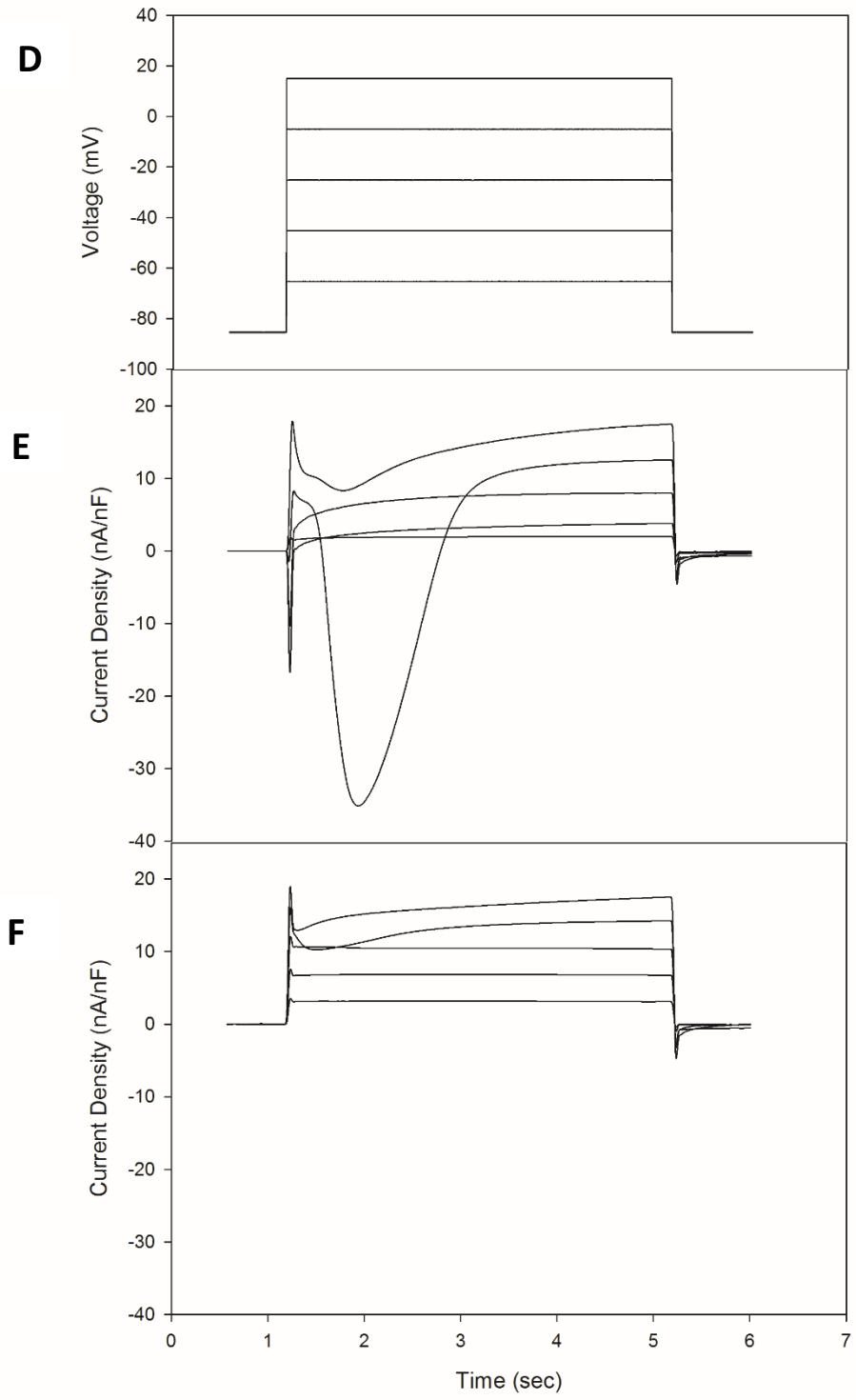
n = 3 mice, 12 fibers
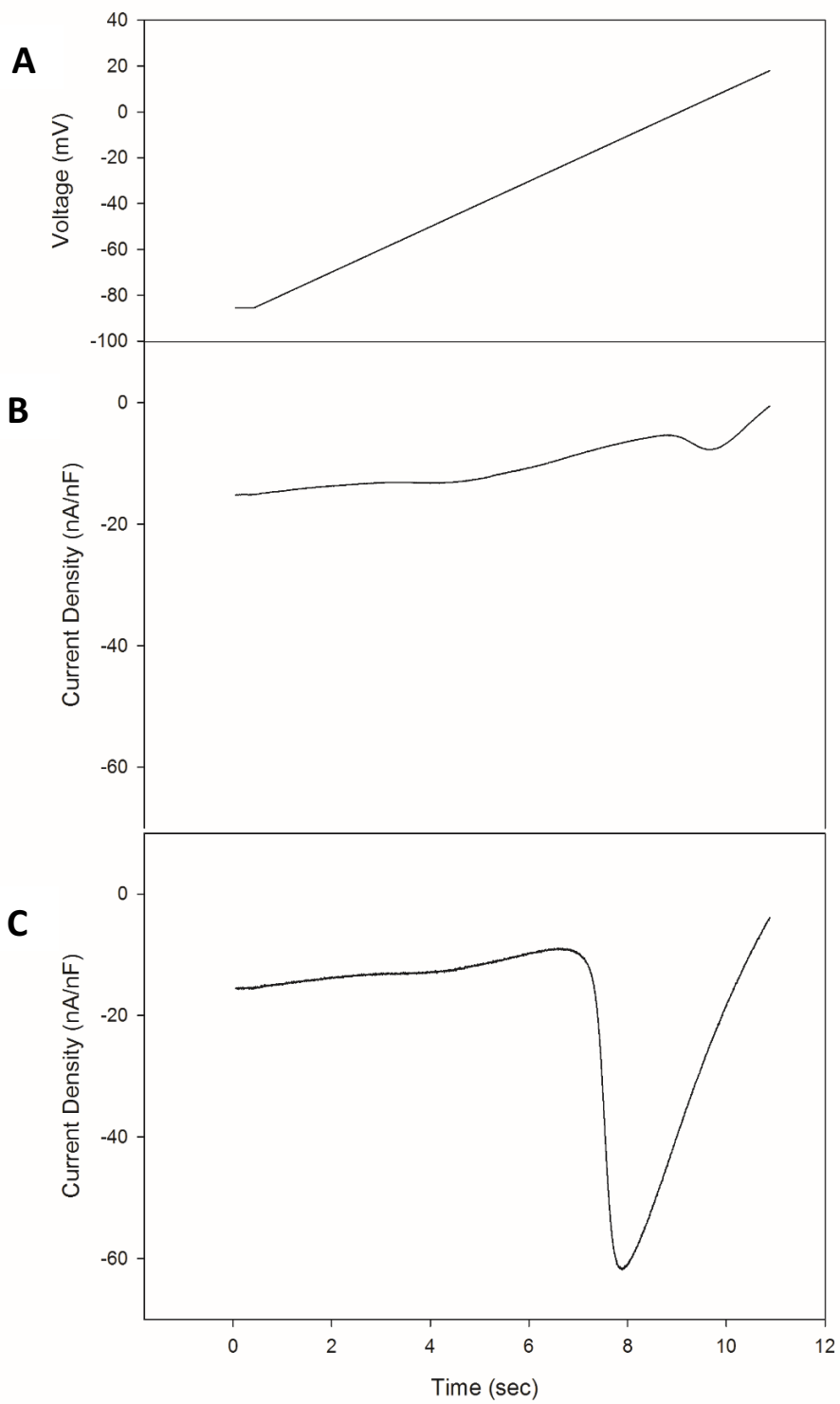
Fig 2.11: BayK enhances the CaPIC

A single CLCN1$^{adr-mto2J}$ fiber is run through multiple voltage protocols with addition of drugs. This is a representative fiber.

A. Ramp voltage protocol used to identify CaPIC. From a holding potential of -85mV, the fiber is depolarized to +20mV at a rate of 10 mV/sec.

B. Current trace generated by voltage protocol. A fit line is drawn using the first 0.5 seconds of the raw trace.

C. Addition of 20 µM BayK enhances CaPIC

n = 3 mice, 7 fibers
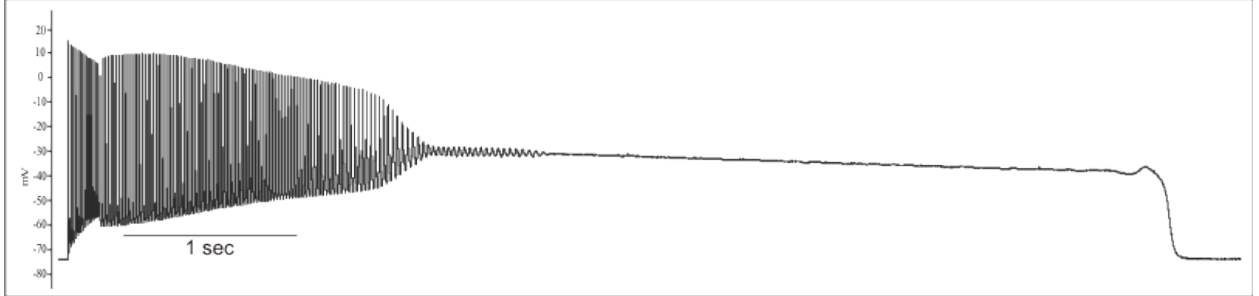
Fig 2.12: WT muscle made acutely myotonic exhibits similar hanging behavior

WT muscle treated with 9-AC is shown to exhibit hanging behavior after myotonic runs. The hang state of acutely myotonic WT muscle is briefer in duration than that of CLCN1$^{adr-mto2J}$ muscle and has a sharper repolarization slope before the sudden repolarization towards RMP.

Chapter VI: Conclusions & Future Directions

I have identified two distinct PICs in ClC muscle. The NaPIC, described in Specific Aim I, activates at subthreshold voltages and contributes to the afterdepolarization necessary for myotonic firing. The CaPIC, described in Specific Aim II, activates at more depolarized potentials and is responsible for the hang state, making the muscle fiber temporarily inexcitable. In this chapter, I discuss several topics that remain unanswered.

K^+ Contributions to Myotonia

I have previously described the role of K^+ buildup in the T-tubules as a major contributor to the depolarization required for the production of myotonia. I hypothesize that K^+ contributes to this depolarization in yet another way.

The NaPIC was measured in K^+-free solutions and K^+ channel blockers to be -1.4 ± 0.2 nA/nF and this portion of the overall PIC was shown to be TTX-sensitive. Figure 1.3B shows a significantly larger PIC when measured in physiological solutions. Switching from physiological solutions to K^+-free solutions reduced the maximal apparent PIC amplitude by ~90%. I hypothesize that the closing of K^+ channels is responsible for this discrepancy. Closing of an outward current, in a voltage clamp ramp protocol, would mimic the opening of an inward current. Further studies must be done to identify which specific channel is being closed to produce this apparent PIC and add to the depolarization required for myotonic firing. This also provides another avenue for therapeutic targeting. If we can pharmacologically inhibit the closing of this specific K

channel, it may decrease the maximal AfD amplitude so much so that myotonia is eliminated. This is demonstrated in Figure 3.1.

At first, this suggestion of treating myotonia with such a drug seems counterintuitive. If K buildup is involved in the depolarization required for myotonic firing, then the opening of K channels would be expected to allow for greater K buildup in the T-tubules and the worsening of myotonia. However, my findings with retigabine treatment, a KCNQ channel opener, showed the elimination of myotonia.

I hypothesize that the retigabine results, shown in Figure 1.2, were a result of the following series of events. Indeed, the opening of KCNQ channels exacerbates the depolarization caused by K buildup in the T-tubules. This is further supported by the localization of these channels to the T-tubular membrane. Even though there is a greater degree of K buildup and a more depolarized E_K than in an untreated ClC muscle, the fiber does not fire myotonic APs. The open K channel acts as a "voltage clamp" to the $E_K.$ The depolarization is enough to activate the NaPIC, which would lead to myotonia, but the open KCNQ channels counteract any further depolarization by PIC, thereby eliminating myotonia.

Interplay between NaPIC and CaPIC

Further investigation should be performed into identifying the cause of the depolarized average membrane potential triggering the hang. I hypothesize that the firing frequency during the myotonic run might be responsible. And I suggest that the maximal firing

frequency achieved during a myotonic run is directly proportional to the NaPIC amplitude.

A larger NaPIC amplitude will result in a faster subthreshold depolarization (AfD). A faster AfD would result in a higher firing frequency – a greater percentage of time spent in action potentials and less time spent at the RMP. When measuring an average membrane potential, it would be more depolarized, leading to the activation of CaPIC and entry into the hang state.

Another topic of interest is the effect of the hang on the NaPIC. I've described in the NaPIC chapter how the NaPIC is susceptible to slow inactivation (over seconds to minutes). This is evident in the warmup data showing that NaPIC is slow inactivated to the degree that it can no longer depolarize the fiber to AP threshold, so that there is no myotonia. I suggested that NaPIC slow inactivates over the course of a myotonic run, leading to the cessation of myotonic firing. Here, I suggest that the hanging behavior is another compensatory mechanism by the ClC muscle. By entering a hang state, the muscle fiber is completely inexcitable for the duration of the hang state – a temporary deficit. But this hang state provides a benefit to the fiber as well in its side effect of slow inactivating the NaPIC and normalizing the excitability of the fiber. In other words, the hang state induces the warmup phenomenon in the muscle so that the fiber is no longer myotonic (will cease firing once current injection is stopped). This can be seen in Figure 3.2, where I attempt to induce a myotonic run immediately after return from a hang state. The fiber reacts with no myotonia, as though it is warmed up.

The interplay of these PICs and the dependency of the hang state on a prior myotonic run gives us great insight for treatment options. Targeting the NaPIC helps the MC in two

ways – by eliminating myotonia and eliminating the possibility of a hang state. This may not hold true as myotonic firing is not the only way with which an average membrane potential can be depolarized enough to activate the CaPIC. Skeletal muscle can reach high frequencies upon maximal exertion, thereby producing a depolarized average membrane potentials. But targeting the NaPIC in addition to patient avoidance of maximal exertion should eliminate both major MC complaints.

Roles of PICs in MC Behaviors

In conclusion, the two identified PICs (NaPIC and CaPIC) play major roles in behaviors seen in MC muscle. This can be seen in Figure 3.2.

Activation of the NaPIC has been shown to be a necessary contributor to the AfD, responsible for myotonic firing. Decreasing the NaPIC amplitude has been shown to decrease the AfD to the point of eliminating myotonic firing altogether. The slow inactivation of the NaPIC is responsible for the spontaneous end of a myotonic run.

And activation of the CaPIC is responsible for entry into the hang state from a myotonic run. The slow activation of this PIC is responsible for the resolution of the hang state and the spontaneous return to RMP.

Implications for Other Diseases

Beyond myotonia congenita, our findings have implications for trinucleotide repeat disorders in which there are decreased currents through muscle ClC-1 channels. These disorders include myotonic dystrophies 1 and 2, Huntington's disease and spinal bulbar muscular atrophy (Cho and Tapscott 2007; Waters, Varuzhanyan et al. 2013; Oki, Halievski et al. 2015; Miranda, Wong et al. 2017). In myotonia congenita and the myotonic dystrophies, severe loss of ClC-1 currents produces the myotonic runs of involuntary APs we examined in this study. It is not yet known whether myotonia also occurs in Huntington's disease or spinal bulbar muscular atrophy. Analysis of muscle from mice at the end-stage of Huntington's disease revealed that the loss of chloride current is relatively severe such that it might trigger myotonia (Waters, Varuzhanyan et al. 2013; Miranda, Wong et al. 2017).

Identification of these PICs and their implications for MC behaviors provides novel therapeutic targets for MC as well as other non-dystrophic myotonias and alters the current standard of care.

K build up
in t tubules

Therapy 1

Depolarization

Therapy 2

Activation of
Na PIC

Closing of
K channels
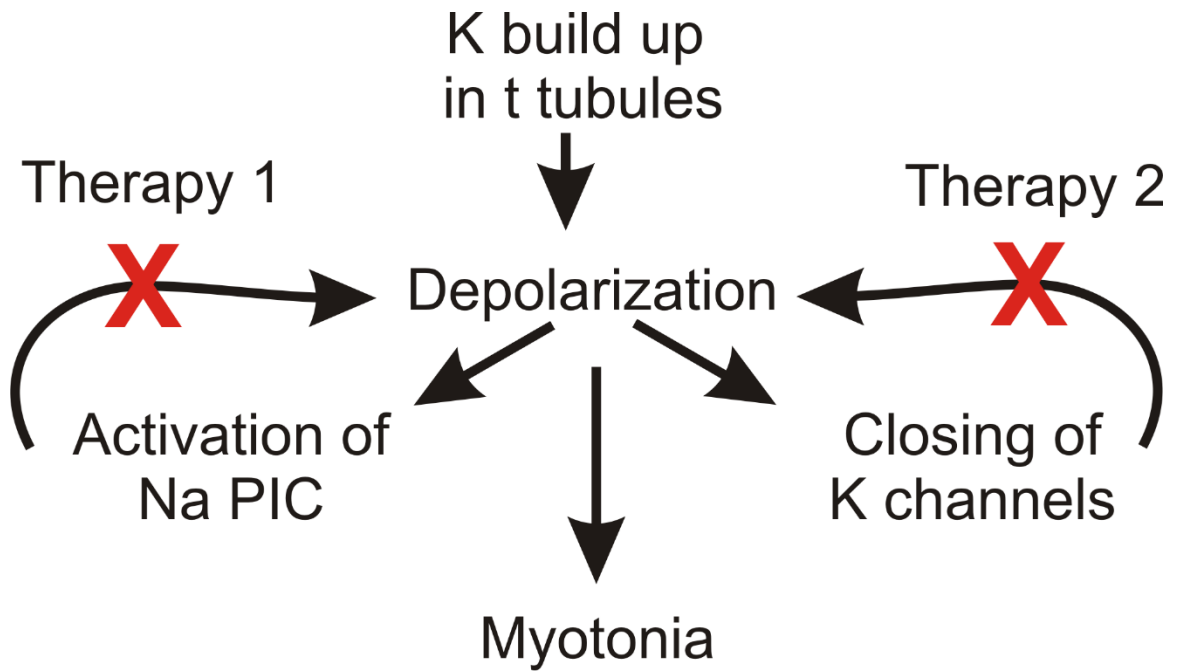
Myotonia

Fig 3.1: Contributors to depolarization required for myotonia

K buildup in the T-tubule system causes an initial depolarization, which activates the apparent PIC seen in physiological solutions. This apparent PIC can be accounted for by the activation of a NaPIC and the closing of an outward K current. Together, they depolarize the fiber enough for myotonic firing. This also provides two therapeutic targets.
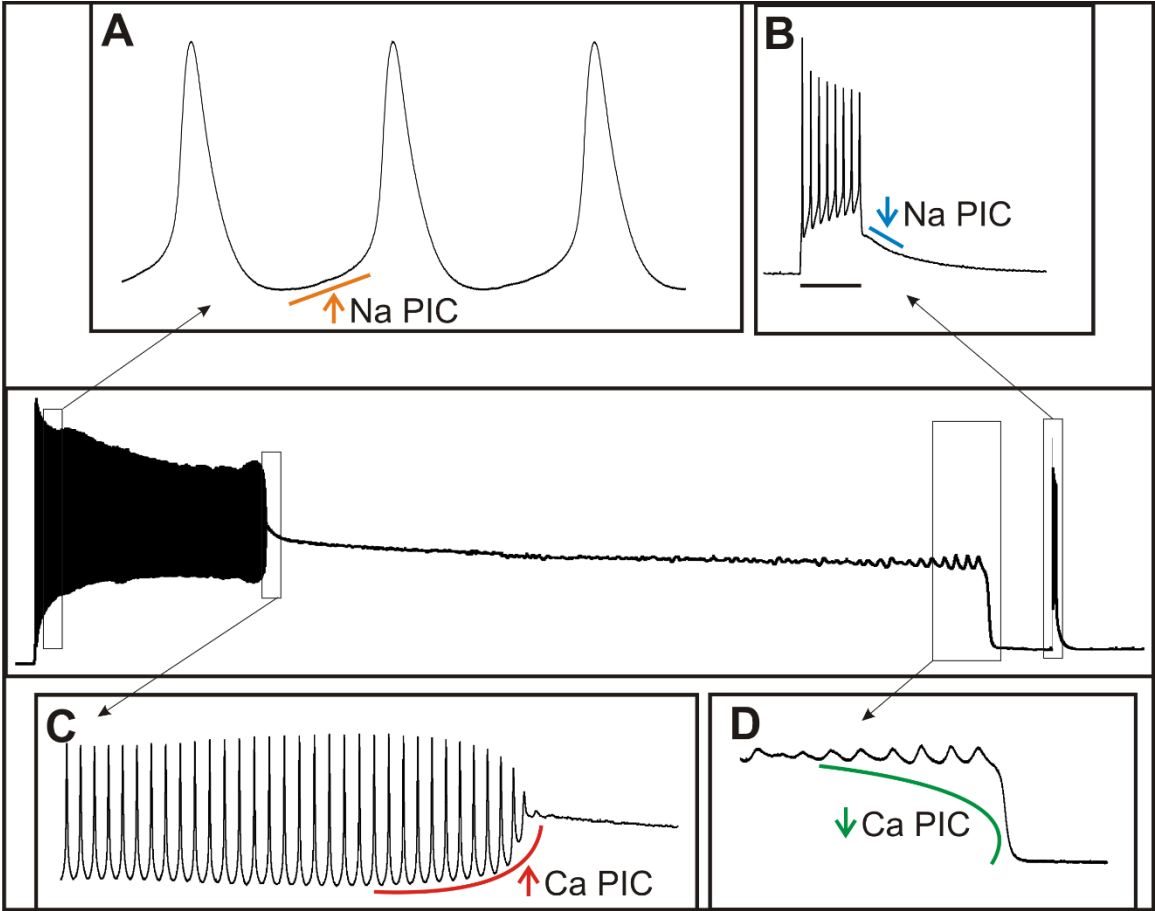
Fig 3.2: Role of PICs in MC Behaviors

(A) Activation of the NaPIC contributes to the AfD, a necessary contributor to the depolarization needed to fire myotonic APs. **(B)** The fiber is warmed up after a prolonged depolarization in the hang state. In response to a 200ms depolarizing current pulse, the fiber fires no myotonic action potentials. **(C)** In response to a depolarized average membrane potential, the CaPIC is activated and depolarizes the fiber into a hang state. **(D)** After minutes, of hanging, the CaPIC inactivates, allowing for the sudden repolarization towards RMP.

Chapter VII: References

Adelman, W. J., Jr. and Y. Palti (1969). "The effects of external potassium and long duration voltage conditioning on the amplitude of sodium currents in the giant axon of the squid, Loligo pealei." J Gen Physiol **54**(5): 589-606.

Adelman, W. J., Jr. and Y. Palti (1969). "The influence of external potassium on the inactivation of sodium currents in the giant axon of the squid, Loligo pealei." J Gen Physiol **53**(6): 685-703.

Adrian, R. H. and S. H. Bryant (1974). "On the repetitive discharge in myotonic muscle fibres." J Physiol **240**(2): 505-15.

Adrian, R. H. and M. W. Marshall (1976). "Action potentials reconstructed in normal and myotonic muscle fibres." J Physiol **258**(1): 125-43.

Al-Ghamdi, F., B. T. Darras, et al. (2017). "Spectrum of Nondystrophic Skeletal Muscle Channelopathies in Children." Pediatr Neurol.

Alaburda, A., J. F. Perrier, et al. (2002). "Mechanisms causing plateau potentials in spinal motoneurones." Adv Exp Med Biol **508**: 219-26.

Alagem, N., M. Dvir, et al. (2001). "Mechanism of Ba(2+) block of a mouse inwardly rectifying K+ channel: differential contribution by two discrete residues." J Physiol **534**(Pt. 2): 381-93.

Almers, W., P. R. Stanfield, et al. (1983). "Slow changes in currents through sodium channels in frog muscle membrane." J Physiol **339**: 253-71.

Alzheimer, C., P. C. Schwindt, et al. (1993). "Modal gating of Na+ channels as a mechanism of persistent Na+ current in pyramidal neurons from rat and cat sensorimotor cortex." J Neurosci **13**(2): 660-73.

Armstrong, C. M. (2006). "Na channel inactivation from open and closed states." Proc Natl Acad Sci U S A **103**(47): 17991-6.

Ashley, C. C. and E. B. Ridgway (1968). "Simultaneous recording of membrane potential, calcium transient and tension in single muscle fibers." Nature **219**(5159): 1168-9.

Balser, J. R., H. B. Nuss, et al. (1996). "Functional consequences of lidocaine binding to slow-inactivated sodium channels." J Gen Physiol **107**(5): 643-58.

Bannister, R. A. and K. G. Beam (2013). "Ca(V)1.1: The atypical prototypical voltage-gated Ca(2)(+) channel." Biochim Biophys Acta **1828**(7): 1587-97.

Bastian, J. and S. Nakajima (1974). "Action potential in the transverse tubules and its role in the activation of skeletal muscle." J Gen Physiol **63**(2): 257-78.

Beck, C. L., C. Fahlke, et al. (1996). "Molecular basis for decreased muscle chloride conductance in the myotonic goat." Proc Natl Acad Sci U S A **93**(20): 11248-52.

Birnberger, K. L., R. Rudel, et al. (1975). "Clinical and electrophysiological observations in patients with myotonic muscle disease and the therapeutic effect of N-propyl-ajmalin." J Neurol **210**(2): 99-110.

Brocard, C., V. Plantier, et al. (2016). "Cleavage of Na(+) channels by calpain increases persistent Na(+) current and promotes spasticity after spinal cord injury." Nat Med **22**(4): 404-11.

Burge, J. A. and M. G. Hanna (2012). "Novel insights into the pathomechanisms of skeletal muscle channelopathies." Curr Neurol Neurosci Rep **12**(1): 62-9.

Cannon, S. C. (2006). "Pathomechanisms in channelopathies of skeletal muscle and brain." Annu Rev Neurosci **29**: 387-415.

Cannon, S. C. (2010). "Voltage-sensor mutations in channelopathies of skeletal muscle." J Physiol **588**(Pt 11): 1887-95.

Cannon, S. C. (2015). "Channelopathies of skeletal muscle excitability." Compr Physiol **5**(2): 761-90.

Cannon, S. C., R. H. Brown, Jr., et al. (1993). "Theoretical reconstruction of myotonia and paralysis caused by incomplete inactivation of sodium channels." Biophys J **65**(1): 270-88.

Catterall, W. A. (2011). "Voltage-gated calcium channels." Cold Spring Harb Perspect Biol **3**(8): a003947.

Chandler, W. K. and H. Meves (1970). "Slow changes in membrane permeability and long-lasting action potentials in axons perfused with fluoride solutions." J Physiol **211**(3): 707-28.

Chen, M. F., R. Niggeweg, et al. (1997). "Chloride conductance in mouse muscle is subject to post-transcriptional compensation of the functional Cl- channel 1 gene dosage." J Physiol **504 (Pt 1)**: 75-81.

Cheong, A., A. M. Dedman, et al. (2001). "Expression and function of native potassium channel [K(V)alpha1] subunits in terminal arterioles of rabbit." J Physiol **534**(Pt 3): 691-700.

Cherednichenko, G., A. M. Hurne, et al. (2004). "Conformational activation of Ca2+ entry by depolarization of skeletal myotubes." Proc Natl Acad Sci U S A **101**(44): 15793-8.

Cho, D. H. and S. J. Tapscott (2007). "Myotonic dystrophy: emerging mechanisms for DM1 and DM2." Biochim Biophys Acta **1772**(2): 195-204.

Colding-Jorgensen, E. (2005). "[Electromyography and diagnosis of muscular diseases]." Ugeskr Laeger **167**(33): 3070; author reply 3070-2.

Colding-Jorgensen, E. (2005). "Phenotypic variability in myotonia congenita." Muscle Nerve **32**(1): 19-34.

Cota, G., L. Nicola Siri, et al. (1983). "Calcium-channel gating in frog skeletal muscle membrane: effect of temperature." J Physiol **338**: 395-412.

Courtney, K. R. (1981). "Comparative actions of mexiletine on sodium channels in nerve, skeletal and cardiac muscle." Eur J Pharmacol **74**(1): 9-18.

Desaphy, J. F., R. Carbonara, et al. (2014). "Preclinical evaluation of marketed sodium channel blockers in a rat model of myotonia discloses promising antimyotonic drugs." Exp Neurol **255**: 96-102.

Desaphy, J. F., G. Gramegna, et al. (2013). "Functional characterization of ClC-1 mutations from patients affected by recessive myotonia congenita presenting with different clinical phenotypes." Exp Neurol **248**: 530-40.

Desmedt, J. E. and K. Hainaut (1977). "Inhibition of the intracellular release of calcium by Dantrolene in barnacle giant muscle fibres." J Physiol **265**(2): 565-85.

Deymeer, F., S. Cakirkaya, et al. (1998). "Transient weakness and compound muscle action potential decrement in myotonia congenita." Muscle Nerve **21**(10): 1334-7.

Dolphin, A. C. (1996). "Facilitation of Ca2+ current in excitable cells." Trends Neurosci **19**(1): 35-43.

Donaldson, P. L. and K. G. Beam (1983). "Calcium currents in a fast-twitch skeletal muscle of the rat." J Gen Physiol **82**(4): 449-68.

Drost, G., J. H. Blok, et al. (2001). "Propagation disturbance of motor unit action potentials during transient paresis in generalized myotonia: a high-density surface EMG study." Brain **124**(Pt 2): 352-60.

Dutzler, R., E. B. Campbell, et al. (2002). "X-ray structure of a ClC chloride channel at 3.0 A reveals the molecular basis of anion selectivity." Nature **415**(6869): 287-94.

El-Bizri, N., K. M. Kahlig, et al. (2011). "Ranolazine block of human Nav1.4 sodium channels and paramyotonia congenita mutants." Channels **5**(2): 161-172.

Elbasiouny, S. M., D. J. Bennett, et al. (2005). "Simulation of dendritic CaV1.3 channels in cat lumbar motoneurons: spatial distribution." J Neurophysiol **94**(6): 3961-74.

Elbasiouny, S. M., D. J. Bennett, et al. (2006). "Simulation of Ca2+ persistent inward currents in spinal motoneurones: mode of activation and integration of synaptic inputs." J Physiol **570**(Pt 2): 355-74.

Fahlke, C., T. Knittle, et al. (1997). "Subunit stoichiometry of human muscle chloride channels." J Gen Physiol **109**(1): 93-104.

Ferradini, V., M. Cassone, et al. (2017). "Targeted Next Generation Sequencing in patients with Myotonia Congenita." Clin Chim Acta **470**: 1-7.

Fournier, E., M. Arzel, et al. (2004). "Electromyography guides toward subgroups of mutations in muscle channelopathies." Ann Neurol **56**(5): 650-61.

Fox, J. M. (1976). "Ultra-slow inactivation of the ionic currents through the membrane of myelinated nerve." Biochim Biophys Acta **426**(2): 232-44.

Francini, F. and E. Stefani (1989). "Decay of the slow calcium current in twitch muscle fibers of the frog is influenced by intracellular EGTA." J Gen Physiol **94**(5): 953-69.

Frank, G. B. (1958). "Inward movement of calcium as a link between electrical and mechanical events in contraction." Nature **182**(4652): 1800-1.

Fraser, J. A., C. L. Huang, et al. (2011). "Relationships between resting conductances, excitability, and t-system ionic homeostasis in skeletal muscle." J Gen Physiol **138**(1): 95-116.

Furman, R. E. and R. L. Barchi (1978). "The pathophysiology of myotonia produced by aromatic carboxylic acids." Ann Neurol **4**(4): 357-65.

Gage, P. W., G. D. Lamb, et al. (1989). "Transient and persistent sodium currents in normal and denervated mammalian skeletal muscle." J Physiol **418**: 427-39.

George, A. L., Jr. (2012). "Leaky channels make weak muscles." J Clin Invest **122**(12): 4333-6.

Gonzalez-Serratos, H. (1971). "Inward spread of activation in vertebrate muscle fibres." J Physiol **212**(3): 777-99.

Granit, R., D. Kernell, et al. (1963). "Quantitative Aspects of Repetitive Firing of Mammalian Motoneurones, Caused by Injected Currents." J Physiol **168**: 911-31.

Grunnet, M., D. Strobaek, et al. (2014). "Kv7 channels as targets for anti-epileptic and psychiatric drug-development." Eur J Pharmacol **726**: 133-7.

Gutmann, L. and L. H. Phillips, 2nd (1991). "Myotonia congenita." Semin Neurol **11**(3): 244-8.

Hadley, R. W. and J. R. Hume (1988). "Calcium channel antagonist properties of Bay K 8644 in single guinea pig ventricular cells." Circ Res **62**(1): 97-104.

Harvey, P. J., Y. Li, et al. (2006). "Persistent sodium currents and repetitive firing in motoneurons of the sacrocaudal spinal cord of adult rats." J Neurophysiol **96**(3): 1141-57.

Heatwole, C. R., J. M. Statland, et al. (2013). "The diagnosis and treatment of myotonic disorders." Muscle Nerve **47**(5): 632-48.

Heckman, C. J. and R. M. Enoka (2012). "Motor unit." Compr Physiol **2**(4): 2629-82.

Heckman, C. J., M. Johnson, et al. (2008). "Persistent inward currents in spinal motoneurons and their influence on human motoneuron firing patterns." Neuroscientist **14**(3): 264-75.

Heine, R., A. L. George, Jr., et al. (1994). "Proof of a non-functional muscle chloride channel in recessive myotonia congenita (Becker) by detection of a 4 base pair deletion." Hum Mol Genet **3**(7): 1123-8.

Hess, P., J. B. Lansman, et al. (1984). "Different modes of Ca channel gating behaviour favoured by dihydropyridine Ca agonists and antagonists." Nature **311**(5986): 538-44.

Hille, B. (1978). "Ionic channels in excitable membranes. Current problems and biophysical approaches." Biophys J **22**(2): 283-94.

Hodgkin, A. L. and P. Horowicz (1959). "The influence of potassium and chloride ions on the membrane potential of single muscle fibres." J Physiol **148**: 127-60.

Hoppe, K., F. Lehmann-Horn, et al. (2013). "In vitro muscle contracture investigations on the malignant hyperthermia like episodes in myotonia congenita." Acta Anaesthesiol Scand **57**(8): 1017-23.

Horlings, C. G., G. Drost, et al. (2009). "Trunk sway analysis to quantify the warm-up phenomenon in myotonia congenita patients." J Neurol Neurosurg Psychiatry **80**(2): 207-12.

Hoshi, T., W. N. Zagotta, et al. (1991). "Two types of inactivation in Shaker K+ channels: effects of alterations in the carboxy-terminal region." Neuron **7**(4): 547-56.

Hounsgaard, J., H. Hultborn, et al. (1988). "Bistability of alpha-motoneurones in the decerebrate cat and in the acute spinal cat after intravenous 5-hydroxytryptophan." J Physiol **405**: 345-67.

Hounsgaard, J. and O. Kiehn (1985). "Ca++ dependent bistability induced by serotonin in spinal motoneurons." Exp Brain Res **57**(2): 422-5.

Hounsgaard, J. and O. Kiehn (1989). "Serotonin-induced bistability of turtle motoneurones caused by a nifedipine-sensitive calcium plateau potential." J Physiol **414**: 265-82.

Hounsgaard, J. and O. Kiehn (1993). "Calcium spikes and calcium plateaux evoked by differential polarization in dendrites of turtle motoneurones in vitro." J Physiol **468**: 245-59.

Hsiao, C. F., C. A. Del Negro, et al. (1998). "Ionic basis for serotonin-induced bistable membrane properties in guinea pig trigeminal motoneurons." J Neurophysiol **79**(6): 2847-56.

Huxley, H. E. (1958). "The contraction of muscle." Sci Am **199**(5): 67-72 passim.

Iannotti, F. A., E. Panza, et al. (2010). "Expression, localization, and pharmacological role of Kv7 potassium channels in skeletal muscle proliferation, differentiation, and survival after myotoxic insults." J Pharmacol Exp Ther **332**(3): 811-20.

Jorquera, G., F. Altamirano, et al. (2013). "Cav1.1 controls frequency-dependent events regulating adult skeletal muscle plasticity." J Cell Sci **126**(Pt 5): 1189-98.

Jurkat-Rott, K. and F. Lehmann-Horn (2005). "Muscle channelopathies and critical points in functional and genetic studies." J Clin Invest **115**(8): 2000-9.

Kernell, D. (1965). "Synaptic Influence on the Repetitive Activity Elicited in Cat Lumbosacral Motoneurones by Long-Lasting Injected Currents." Acta Physiol Scand **63**: 409-10.

Khodorov, B. I. (1981). "Sodium inactivation and drug-induced immobilization of the gating charge in nerve membrane." Prog Biophys Mol Biol **37**(2): 49-89.

Khodorov, B. I., E. G. Vornovitskii, et al. (1974). "[Possible role of slow sodium-calcium channels in the mechanism of changes in the electrical and mechanical activity of guinea pig myocardial cells under local anaphylaxis (isoptin effects)]." Biull Eksp Biol Med **78**(7): 24-8.

Khodorov, B. I., E. G. Vornovitskii, et al. (1976). "[Mechanism of excitation and contraction uncoupling in frog and guinea pig myocardial fibers during block of slow sodium-calcium channels by compound D-600]." Biofizika **21**(6): 1024-30.

Kim, J. B., S. J. Kim, et al. (2014). "The large-conductance calcium-activated potassium channel holds the key to the conundrum of familial hypokalemic periodic paralysis." Korean J Pediatr **57**(10): 445-50.

Klocke, R., K. Steinmeyer, et al. (1994). "Role of innervation, excitability, and myogenic factors in the expression of the muscular chloride channel ClC-1. A study on normal and myotonic muscle." J Biol Chem **269**(44): 27635-9.

Koch, M. C., K. Steinmeyer, et al. (1992). "The skeletal muscle chloride channel in dominant and recessive human myotonia." <u>Science</u> **257**(5071): 797-800.

Kubisch, C., T. Schmidt-Rose, et al. (1998). "ClC-1 chloride channel mutations in myotonia congenita: variable penetrance of mutations shifting the voltage dependence." <u>Hum Mol Genet</u> **7**(11): 1753-60.

Kuo, J. J., R. H. Lee, et al. (2003). "Active dendritic integration of inhibitory synaptic inputs in vivo." <u>J Neurophysiol</u> **90**(6): 3617-24.

Kwieciński, H., B. Ryniewicz, et al. (1992). "Treatment of myotonia with antiarrhythmic drugs." <u>Acta Neurologica Scandinavica</u> **86**(4): 371-375.

Lacomis, D., J. T. Gonzales, et al. (1999). "Fluctuating clinical myotonia and weakness from Thomsen's disease occurring only during pregnancies." <u>Clin Neurol Neurosurg</u> **101**(2): 133-6.

Laine, V., J. R. Segor, et al. (2014). "Hyperactivation of L-type voltage-gated Ca2+ channels in Caenorhabditis elegans striated muscle can result from point mutations in the IS6 or the IIIS4 segment of the alpha1 subunit." <u>J Exp Biol</u> **217**(Pt 21): 3805-14.

Lamb, G. D., R. M. Murphy, et al. (2011). "On the localization of ClC-1 in skeletal muscle fibers." <u>J Gen Physiol</u> **137**(3): 327-9; author reply 331-3.

Lampl, I., P. Schwindt, et al. (1998). "Reduction of cortical pyramidal neuron excitability by the action of phenytoin on persistent Na+ current." <u>J Pharmacol Exp Ther</u> **284**(1): 228-37.

Lanari, A. (1946). "The mechanism of myotonic contraction." <u>Science</u> **104**(2697): 221.

Large, C. H., D. M. Sokal, et al. (2012). "The spectrum of anticonvulsant efficacy of retigabine (ezogabine) in animal models: implications for clinical use." <u>Epilepsia</u> **53**(3): 425-36.

Latorre, R. and S. Brauchi (2006). "Large conductance Ca2+-activated K+ (BK) channel: activation by Ca2+ and voltage." <u>Biol Res</u> **39**(3): 385-401.

Lee, K. S., E. Marban, et al. (1985). "Inactivation of calcium channels in mammalian heart cells: joint dependence on membrane potential and intracellular calcium." <u>J Physiol</u> **364**: 395-411.

Lee, R. H. and C. J. Heckman (1998). "Bistability in spinal motoneurons in vivo: systematic variations in persistent inward currents." <u>J Neurophysiol</u> **80**(2): 583-93.

Lee, R. H. and C. J. Heckman (2000). "Adjustable amplification of synaptic input in the dendrites of spinal motoneurons in vivo." <u>J Neurosci</u> **20**(17): 6734-40.

Lee, R. H. and C. J. Heckman (2001). "Essential role of a fast persistent inward current in action potential initiation and control of rhythmic firing." <u>J Neurophysiol</u> **85**(1): 472-5.

Lee, R. Y., L. Lobel, et al. (1997). "Mutations in the alpha1 subunit of an L-type voltage-activated Ca2+ channel cause myotonia in Caenorhabditis elegans." <u>EMBO J</u> **16**(20): 6066-76.

Lehmann-Horn, F., K. Jurkat-Rott, et al. (2008). "Diagnostics and therapy of muscle channelopathies--Guidelines of the Ulm Muscle Centre." <u>Acta Myol</u> **27**: 98-113.

Li, X. and D. J. Bennett (2007). "Apamin-sensitive calcium-activated potassium currents (SK) are activated by persistent calcium currents in rat motoneurons." <u>J Neurophysiol</u> **97**(5): 3314-30.

Li, Y. and D. J. Bennett (2003). "Persistent sodium and calcium currents cause plateau potentials in motoneurons of chronic spinal rats." <u>J Neurophysiol</u> **90**(2): 857-69.

Lipicky, R. J. and S. H. Bryant (1966). "Sodium, potassium, and chloride fluxes in intercostal muscle from normal goats and goats with hereditary myotonia." <u>J Gen Physiol</u> **50**(1): 89-111.

Lipicky, R. J., S. H. Bryant, et al. (1971). "Cable parameters, sodium, potassium, chloride, and water content, and potassium efflux in isolated external intercostal muscle of normal volunteers and patients with myotonia congenita." <u>J Clin Invest</u> **50**(10): 2091-103.

Lipicky, R. J., S. H. Bryant, et al. (1971). "Cable parameters, sodium, potassium, chloride, and water content, and potassium efflux in isolated external intercostal muscle of normal volunteers and patients with myotonia congenita." Journal of Clinical Investigation **50**(10): 2091-103.

Lossin, C. (2013). "Nav 1.4 slow-inactivation: is it a player in the warm-up phenomenon of myotonic disorders?" Muscle Nerve **47**(4): 483-7.

Lossin, C. and A. L. George, Jr. (2008). "Myotonia congenita." Adv Genet **63**: 25-55.

Lueck, J. D., C. Lungu, et al. (2007). "Chloride channelopathy in myotonic dystrophy resulting from loss of posttranscriptional regulation for CLCN1." Am J Physiol Cell Physiol **292**(4): C1291-7.

Lueck, J. D., A. E. Rossi, et al. (2010). "Sarcolemmal-restricted localization of functional ClC-1 channels in mouse skeletal muscle." J Gen Physiol **136**(6): 597-613.

Matthews, E., D. Fialho, et al. (2010). "The non-dystrophic myotonias: molecular pathogenesis, diagnosis and treatment." Brain **133**(Pt 1): 9-22.

Miranda, D. R., M. Wong, et al. (2017). "Progressive Cl- channel defects reveal disrupted skeletal muscle maturation in R6/2 Huntington's mice." J Gen Physiol **149**(1): 55-74.

Novak, K. R., P. Nardelli, et al. (2009). "Inactivation of sodium channels underlies reversible neuropathy during critical illness in rats." J Clin Invest **119**(5): 1150-8.

Novak, K. R., J. Norman, et al. (2015). "Sodium channel slow inactivation as a therapeutic target for myotonia congenita." Ann Neurol **77**(2): 320-32.

Oki, K., K. Halievski, et al. (2015). "Contractile dysfunction in muscle may underlie androgen-dependent motor dysfunction in spinal bulbar muscular atrophy." J Appl Physiol (1985) **118**(7): 941-52.

Palade, P. T. and R. L. Barchi (1977). "Characteristics of the chloride conductance in muscle fibers of the rat diaphragm." J Gen Physiol **69**(3): 325-42.

Palade, P. T. and R. L. Barchi (1977). "On the inhibition of muscle membrane chloride conductance by aromatic carboxylic acids." J Gen Physiol **69**(6): 879-96.

Patlak, J. B. and M. Ortiz (1986). "Two modes of gating during late Na+ channel currents in frog sartorius muscle." J Gen Physiol **87**(2): 305-26.

Patlak, J. B., M. Ortiz, et al. (1986). "Opentime heterogeneity during bursting of sodium channels in frog skeletal muscle." Biophys J **49**(3): 773-7.

Peachey, L. D. (1975). Structure and Function of the T-System of Vertebrate Skeletal Muscle. The Nervous System. D. B. Tower. New York, Raven Press. **1:** 81-89.

Perrier, J. F., A. Alaburda, et al. (2002). "Spinal plasticity mediated by postsynaptic L-type Ca2+ channels." Brain Res Brain Res Rev **40**(1-3): 223-9.

Perrier, J. F., S. Mejia-Gervacio, et al. (2000). "Facilitation of plateau potentials in turtle motoneurones by a pathway dependent on calcium and calmodulin." J Physiol **528 Pt 1**: 107-13.

Podsiadlo, D. and S. Richardson (1991). "The timed "Up & Go": a test of basic functional mobility for frail elderly persons." J Am Geriatr Soc **39**(2): 142-8.

Powers, R. K., P. Nardelli, et al. (2008). "Estimation of the contribution of intrinsic currents to motoneuron firing based on paired motoneuron discharge records in the decerebrate cat." J Neurophysiol **100**(1): 292-303.

Pusch, M. (2002). "Myotonia caused by mutations in the muscle chloride channel gene CLCN1." Hum Mutat **19**(4): 423-34.

Pusch, M., K. Steinmeyer, et al. (1994). "Low single channel conductance of the major skeletal muscle chloride channel, ClC-1." Biophys J **66**(1): 149-52.

Rhodes, T. H., C. H. Vite, et al. (1999). "A missense mutation in canine C1C-1 causes recessive myotonia congenita in the dog." FEBS Lett **456**(1): 54-8.

Rich, M. M. (2006). "The control of neuromuscular transmission in health and disease." Neuroscientist **12**(2): 134-42.

Rich, M. M. and M. J. Pinter (2003). "Crucial role of sodium channel fast inactivation in muscle fibre inexcitability in a rat model of critical illness myopathy." J Physiol **547**(Pt 2): 555-66.

Ricker, K., A. Haass, et al. (1978). "Transient muscular weakness in severe recessive myotonia congenita. Improvement of isometric muscle force by drugs relieving myotomic stiffness." J Neurol **218**(4): 253-62.

Ricker, K., H. M. Meinch, et al. (1973). "[Neurophysiological studies on the temporary paresis in myotonia congenita and dystrophia myotonica]." Z Neurol **204**(2): 135-48.

Ricker, K. and H. M. Meinck (1972). "Muscular paralysis in myotonia congenita." Eur Neurol **7**(4): 221-7.

Rudel, R., K. Ricker, et al. (1988). "Transient weakness and altered membrane characteristic in recessive generalized myotonia (Becker)." Muscle Nerve **11**(3): 202-11.

Rychkov, G. Y., M. Pusch, et al. (1996). "Concentration and pH dependence of skeletal muscle chloride channel ClC-1." J Physiol **497 (Pt 2)**: 423-35.

Sandow, A. (1965). "Excitation-contraction coupling in skeletal muscle." Pharmacol Rev **17**(3): 265-320.

Saviane, C., F. Conti, et al. (1999). "The muscle chloride channel ClC-1 has a double-barreled appearance that is differentially affected in dominant and recessive myotonia." J Gen Physiol **113**(3): 457-68.

Schoser, B. G., C. Schneider-Gold, et al. (2004). "Muscle pathology in 57 patients with myotonic dystrophy type 2." Muscle Nerve **29**(2): 275-81.

Schwindt, P. and W. E. Crill (1977). "A persistent negative resistance in cat lumbar motoneurons." Brain Res **120**(1): 173-8.

Schwindt, P. C. and W. E. Crill (1980). "Properties of a persistent inward current in normal and TEA-injected motoneurons." J Neurophysiol **43**(6): 1700-24.

Schwindt, P. C. and W. E. Crill (1982). "Factors influencing motoneuron rhythmic firing: results from a voltage-clamp study." J Neurophysiol **48**(4): 875-90.

Sherman, S. J. and W. A. Catterall (1985). "The developmental regulation of TTX-sensitive sodium channels in rat skeletal muscle in vivo and in vitro." Soc Gen Physiol Ser **39**: 237-63.

Skov, M., F. V. De Paoli, et al. (2015). "Extracellular magnesium and calcium reduce myotonia in isolated ClC-1 chloride channel-inhibited human muscle." Muscle Nerve **51**(1): 65-71.

Skov, M., A. Riisager, et al. (2013). "Extracellular magnesium and calcium reduce myotonia in ClC-1 inhibited rat muscle." Neuromuscul Disord **23**(6): 489-502.

Standen, N. B. and P. R. Stanfield (1980). "Rubidium block and rubidium permeability of the inward rectifier of frog skeletal muscle fibres." J Physiol **304**: 415-35.

Statland, J. M. and R. J. Barohn (2013). "Muscle channelopathies: the nondystrophic myotonias and periodic paralyses." Continuum (Minneap Minn) **19**(6 Muscle Disease): 1598-614.

Statland, J. M., B. N. Bundy, et al. (2012). "Mexiletine for symptoms and signs of myotonia in nondystrophic myotonia: A randomized controlled trial." JAMA **308**(13): 1357-1365.

Statland, J. M., B. N. Bundy, et al. (2012). "Mexiletine for symptoms and signs of myotonia in nondystrophic myotonia: a randomized controlled trial." JAMA **308**(13): 1357-65.

Steinmeyer, K., R. Klocke, et al. (1991). "Inactivation of muscle chloride channel by transposon insertion in myotonic mice." Nature **354**(6351): 304-8.

Steinmeyer, K., C. Lorenz, et al. (1994). "Multimeric structure of ClC-1 chloride channel revealed by mutations in dominant myotonia congenita (Thomsen)." EMBO J **13**(4): 737-43.

Steinmeyer, K., C. Ortland, et al. (1991). "Primary structure and functional expression of a developmentally regulated skeletal muscle chloride channel." Nature **354**(6351): 301-4.

Strickholm, A. (1974). "Intracellular generated potentials during excitation-contraction coupling in muscle." J Neurobiol **5**(2): 161-87.

Striessnig, J., H. J. Bolz, et al. (2010). "Channelopathies in Cav1.1, Cav1.3, and Cav1.4 voltage-gated L-type Ca2+ channels." Pflugers Arch **460**(2): 361-74.

Struyk, A. F. and S. C. Cannon (2008). "Paradoxical depolarization of BA2+- treated muscle exposed to low extracellular K+: insights into resting potential abnormalities in hypokalemic paralysis." Muscle Nerve **37**(3): 326-37.

Su, T. R., W. S. Zei, et al. (2012). "The Effects of the KCNQ Openers Retigabine and Flupirtine on Myotonia in Mammalian Skeletal Muscle Induced by a Chloride Channel Blocker." Evid Based Complement Alternat Med **2012**: 803082.

Suarez-Isla, B. A., C. Orozco, et al. (1986). "Single calcium channels in native sarcoplasmic reticulum membranes from skeletal muscle." Proc Natl Acad Sci U S A **83**(20): 7741-5.

Svirskis, G. and J. Hounsgaard (1997). "Depolarization-induced facilitation of a plateau-generating current in ventral horn neurons in the turtle spinal cord." J Neurophysiol **78**(3): 1740-2.

Tanabe, T., K. G. Beam, et al. (1988). "Restoration of excitation-contraction coupling and slow calcium current in dysgenic muscle by dihydropyridine receptor complementary DNA." Nature **336**(6195): 134-9.

Theiss, R. D., J. J. Kuo, et al. (2007). "Persistent inward currents in rat ventral horn neurones." J Physiol **580**(Pt. 2): 507-22.

Townsend, C. and R. Horn (1997). "Effect of alkali metal cations on slow inactivation of cardiac Na+ channels." J Gen Physiol **110**(1): 23-33.

Trip, J., G. Drost, et al. (2006). "Drug treatment for myotonia." Cochrane Database Syst Rev(1): CD004762.

Trivedi, J. R., B. Bundy, et al. (2013). "Non-dystrophic myotonia: prospective study of objective and patient reported outcomes." Brain **136**(Pt 7): 2189-200.

Trivedi, J. R., S. C. Cannon, et al. (2014). "Nondystrophic myotonia: challenges and future directions." Exp Neurol **253**: 28-30.

Tseng, P. Y., B. Bennetts, et al. (2007). "Cytoplasmic ATP inhibition of CLC-1 is enhanced by low pH." J Gen Physiol **130**(2): 217-21.

Van Beekvelt, M. C., G. Drost, et al. (2006). "Na+-K+-ATPase is not involved in the warming-up phenomenon in generalized myotonia." Muscle Nerve **33**(4): 514-23.

Wagenknecht, T., R. Grassucci, et al. (1989). "Three-dimensional architecture of the calcium channel/foot structure of sarcoplasmic reticulum." Nature **338**(6211): 167-70.

Wallinga, W., S. L. Meijer, et al. (1999). "Modelling action potentials and membrane currents of mammalian skeletal muscle fibres in coherence with potassium concentration changes in the T-tubular system." Eur Biophys J **28**(4): 317-29.

Waters, C. W., G. Varuzhanyan, et al. (2013). "Huntington disease skeletal muscle is hyperexcitable owing to chloride and potassium channel dysfunction." Proc Natl Acad Sci U S A **110**(22): 9160-5.

Wu, F., W. Mi, et al. (2012). "A calcium channel mutant mouse model of hypokalemic periodic paralysis." J Clin Invest **122**(12): 4580-91.

Yan, H., C. Wang, et al. (2017). "Calmodulin limits pathogenic Na+ channel persistent current." J Gen Physiol **149**(2): 277-293.

Yang, J. S., J. T. Sladky, et al. (1991). "TTX-sensitive and TTX-insensitive sodium channel mRNA transcripts are independently regulated in adult skeletal muscle after denervation." Neuron **7**(3): 421-7.

Zeng, J., R. K. Powers, et al. (2005). "Contribution of persistent sodium currents to spike-frequency adaptation in rat hypoglossal motoneurons." J Neurophysiol **93**(2): 1035-41.

Appendix

Abbreviations

9-AC   9 - Anthracenecarboxylic acid

AfD   Afterdepolarization

AP   Action potential

CaPIC   Calcium persistent inward current

dV/dt   Rate of rise of action potential

EMG   Electromyograph

MC   Myotonia Congenita

NaPIC   Sodium persistent inward current

NMJ   Neuromuscular junction

PIC   Persistent inward current

RMP   Resting membrane potential

SR   Sarcoplasmic reticulum

T-tubule   Transverse-tubule

TTX   Tetrodotoxin

WT   Wild-Type